RESVERATROL AS A NOVEL THERAPEUTIC AGENT FOR TREATING DUCHENNE MUSCULAR DYSTROPHY

Matthew Burt

Cellular and Molecular Medicine

Faculty of Medicine

University of Ottawa

Abstract

Duchenne Muscular Dystrophy (DMD) is an x-linked neuromuscular disease that is caused by an absence of dystrophin protein, rendering skeletal muscle more susceptible to contraction-induced damage. One therapeutic strategy focuses on increasing the expression of endogenous utrophin A, a dystrophin homologue. Interestingly, slow muscle is more resistant to the dystrophic pathology and has increased utrophin A expression (Webster 1998; Gramolini 2001b). These observations led researchers to explore the therapeutic potential of stimulating the slow, oxidative myogenic program (SOMP) in the *mdx* context. Beneficial adaptations were seen with pharmacological activation of PPARδ and AMPK. We treated *mdx* mice with resveratrol (~100mg/kg/day), a putative SIRT1 activator, for 6-7 weeks and evaluated the activity of phenotypic modifiers that are known to influence the SOMP. SIRT1 activity and protein levels increased significantly, as well as downstream PGC-1α activity. There was evidence of a fibre type conversion as the treated mice had a higher proportion of the slow myosin heavy chain isoforms in both the EDL and Soleus skeletal muscles. Utrophin A protein levels showed modest, but consistent increases with resveratrol treatment. Finally, histological analysis revealed improvements in central nucleation and fibre size variability. These findings were promising, but raised the question of whether modifying the treatment regimen may result in greater therapeutic benefits. Surprisingly, we discovered that an elevated dose of 500mg/kg/day was ineffective in its promotion of the SOMP. SIRT1 was not activated and there was no change in utrophin A levels with resveratrol treatment. Taken together, this study demonstrates that resveratrol has the ability to promote the SOMP through SIRT1 and PGC-1α activation. It also

highlights the importance of selecting an appropriate dose of resveratrol to maximize its effectiveness.

Acknowledgements

First, I would like to thank my supervisor, Dr. Bernard Jasmin. I had originally planned on doing my M.Sc. at Queen's University, but due to unforeseen circumstances I was unable to continue my studies there. Dr. Jasmin accepted me on short notice and has always had my best interests at heart. I have learned a tremendous amount from discussions that we have shared and from the way that he carries himself on a daily basis.

I would also like to thank all members of the Jasmin lab, past and present, for their encouragement and helpful discussions. A big shout out goes to Vlad Ljubicic for showing me the ropes and being a great mentor, both inside and outside the lab. John, you definitely made the transition to life in the lab easy and taught me how to take full advantage of department socials. I would also like to thank my good friends and lab mates, Lucas, Tara and Aymeric for listening to my riddles and sharing some laughs. Thanks to Guy, Adel, Adele, Aatika, and Hasanen for all of their help.

I also appreciate all of the constructive feedback and assistance provided by my thesis advisory committee, comprising Dr. Jean-Marc Renaud and Dr. Bob Korneluk.

Finally, I would like to thank my entire family for always supporting me and motivating me. Mom and dad, I couldn't have done it without you. Also, to Andrew and Justin who have always been excellent role models.

Table of Contents

List of Figures

Glossary

AAV- adeno-associated viral
ACh- aceylcholine
AChE- acetylcholinesterase
AChR- acetylcholine receptor
AICAR- 5-amino-4-imidazolecarboxamide riboside
AO- antisense oligonucleotide
ARE- AU-rich element
AUBP- AU-rich element-binding poteins
BMD- Becker muscular dystrophy
Ca^{2+}- calcium
CaM- calmodulin
CaMBP- CaM-binding peptide
COX- cytochrome c oxidase
CS- citrate synthase
CSA- cross-sectional area
CsA- cyclosporine
DAPC- dystrophin-associated protein complex
DHPR- dihydropyridine receptor
DMD- Duchenne muscular dystrophy
ECM- extracellular matrix
ECM- extracellular matrix
EDL- extensor digitorum longus
FOXO- forkhead box class O
GAPB- GA binding protein
GLUT4- glucose transporter type 4
GRMD- golden retriever muscular dystrophy
IGF-1- insulin growth factor-1
IGF-I- insulin growth factor
IgM- immunoglobin M
IP- immunoprecipitation
K- potassium
Mb- myoglobin
mdx- X-linked muscular dystrophy
MHC – myosin heavy chain
Na- sodium
NBD- NEMO-binding domain
NFAT- nuclear factor of activated T cells
NF-κB- nuclear factor kappa-light-chain-enhancer of activated B cells

NMJ- neuromuscular junction
NO- nitric oxide
NOS- nitric oxide synthase
PGC-1α- peroxisome proliferator-activated receptor ϒ coactivator 1α
PPAR- peroxisome proliferator-activated receptor
PPRE- PPAR- response element
RSV- resveratrol
RT-PCR- reverse transcription polymerase reaction
RyR- ryanodine receptor
SDH- succinate dehydrogenase
SIRT- sirtuin (silent mating type information regulation 2 homolog)
SOL- soleus
SOMP- slow oxidative myogenic program
SR- sarcoplasmic reticulum
TA- tibialis anterior
TCA- tricarboxylic acid cycle
TGFβ- transforming growth factor-β
TNF-α- tumor necrosis factor a
α-DB- α-dystrobrevin
α-syn- α-syntrophin
β-DG- β-dystroglycan

1: Introduction

1.1 Duchenne muscular dystrophy (DMD)

Duchenne Muscular dystrophy (DMD) is an X-linked, neuromuscular disease that occurs in approximately 1 out of every 3500 live male births, making it the most common lethal, genetic paediatric disorder (Moser 1984; Emery 1991; Anderson 1992). Although the disease is present from birth, the affected patient usually does not display symptoms until three to five years of age. Initial complaints often include leg weaknesses, which inevitably lead to loss of ambulation by 12 years of age (Anderson 1992). The progressive loss of muscle continues throughout adulthood with the proximal muscles affected first, followed by the more distal muscles, with respiratory failure and death often occurring in the early twenties (Jennekens 1991; Anderson 1992).

DMD is caused by mutations in the DMD/dystrophin gene, one of the largest known genes in humans. Located on chromosome Xp21, the dystrophin gene spans approximately 2.4 megabases and consists of 79 exons (Blake 2002; Yiu 2008). Due to the presence of three independent promoters, the dystrophin gene can be transcribed into three full-length isoforms, with a spliced transcript size of 14 kb, distinguishable only by their unique amino-terminal sequences (Ahn 1993; Muntoni 2003). The complexity of dystrophin is exacerbated by the presence of internal promoters that give rise to truncated isoforms of dystrophin: Dp260, Dp140, Dp16, Dp71 (Feener 1989; Byers 1993; D'Souza 1995) (**Figure 1.1**). Full length dystrophin is restricted to the brain, as well as skeletal and cardiac muscles, whereas the truncated isoforms are absent from adult muscle, but can be found in the brain, retina, lungs, kidney, and liver (Byers 1993; Gramolini 1998). The severity of the pathology is

A)

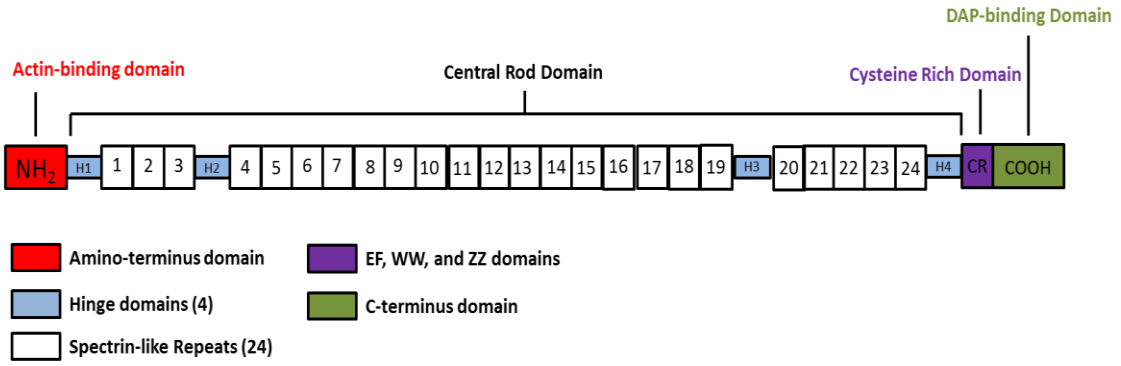

B)

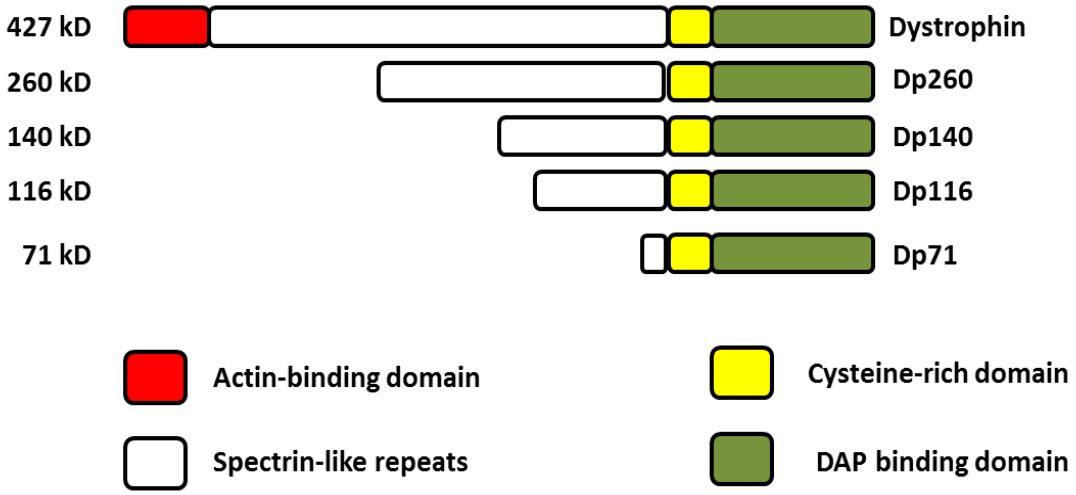

Figure 1.1 – Schematic representation of dystrophin isoforms

A) Structural illustration of dystrophin protein with its different functional domains. The amino-terminus domain binds to actin and the C-terminus domain binds to the DAPC, providing a structural link at the sarcolemma B) Different isoforms of dystrophin, named thus due to their different molecular weights. Dp, dystrophin protein; kD, kiloDalton.

influenced by the nature of the mutation (Coffey 1992; Bushby 2010). Certain mutations that result in a maintained open reading frame and consequent production of a truncated but partly functional protein are characteristic of Becker muscular dystrophy (BMD), a milder form of disease (Monaco 1988; Bushby 2010). However, in patients with DMD, the open reading frame of the dystrophin gene is disrupted by deletions (~65%), duplications (~10%), point mutations (~25%), or other smaller rearrangements that lead to an absence of functional dystrophin (De la Porte 1987; Hoffman 1987; Morris 1993). Common indicators of the DMD pathology are elevated levels of serum creatine kinase, centrally nucleated myofibres, high variability in muscle fibre size/diameter, and an accumulation of necrotic myofibres (Emery 1977; Anderson 1992; Yiu 2008).

Dystrophin is the 427 kDa protein that is the product of the gene defective in DMD (Ahn 1993; Ervasti 2007). In normal human muscle fibres, dystrophin is located on the cytoplasmic face of the sarcolemma, as well as along the troughs of the neuromuscular junction (Blake 2002; Jasmin 2002; Ervasti 2007). Dystrophin is comprised of four major domains: N-terminal domain, central rod domain, cysteine-rich domain and the C-terminal domain (Ervasti 2007) (**Figure 1.1**). The amino terminal contains a functional actin binding domain, which is responsible for anchoring dystrophin to cytoskeletal filamentous ϒ-actin (Straub 1992; Matsumura 1994; Lapidos 2004). The central rod domain helps maintain flexibility of the sarcolemma, through its combination of spectrin-like repeats and four hinge regions (Anderson 1992; Grum 1999). This central rod domain was initially considered to be of low importance for overall dystrophin function, but recent evidence demonstrates that destabilizing a single repeat (repeat 23) can contribute to a severe DMD phenotype (Legardinier 2009). The cysteine-rich domain of dystrophin interacts with a membrane

protein, called β-dystroglycan (β-DG), while the C-terminus is involved in binding α-dystrobrevin (α-DB) and α-syntrophin (α-syn) (Straub 1992; Matsumura 1994; Lapidos 2004). This trans-membranous structure, which provides a link between the extracellular matrix and the underlying filamentous actin network, is referred to as the dystrophin-associated protein complex (DAPC) (Matsumura 1994; Lapidos 2004; Chakkalakal 2006) (**Figure 1.2**).

Proper assembly of the DAPC requires the presence of a functional dystrophin protein (Ervasti 1990). Its absence impairs recruitment of other members of the DAPC to the sarcolemma and creates a pathophysiological cascade with numerous adverse downstream events. One of the most significant is the loss of this structural linkage, leading to instability of the sarcolemma (Lapidos 2004; Chakkalakal 2006). Consequently, the threshold for contraction-induced muscle damage is lower, resulting in repetitive cycles of degeneration and regeneration (Weller 1990; Cohn 2000; Rando 2001). The overloading of the muscle's regenerative capacity inevitably leads to muscle necrosis/wasting and replacement with fibrous and adipose tissues (Petrof 1993). This sarcolemmal instability also leaves muscle cells more susceptible to calcium accumulation through the leaky membranes (Alderton 2000). This is problematic because calcium regulates a number of signaling events involved in proteolysis (Alderton 2000).

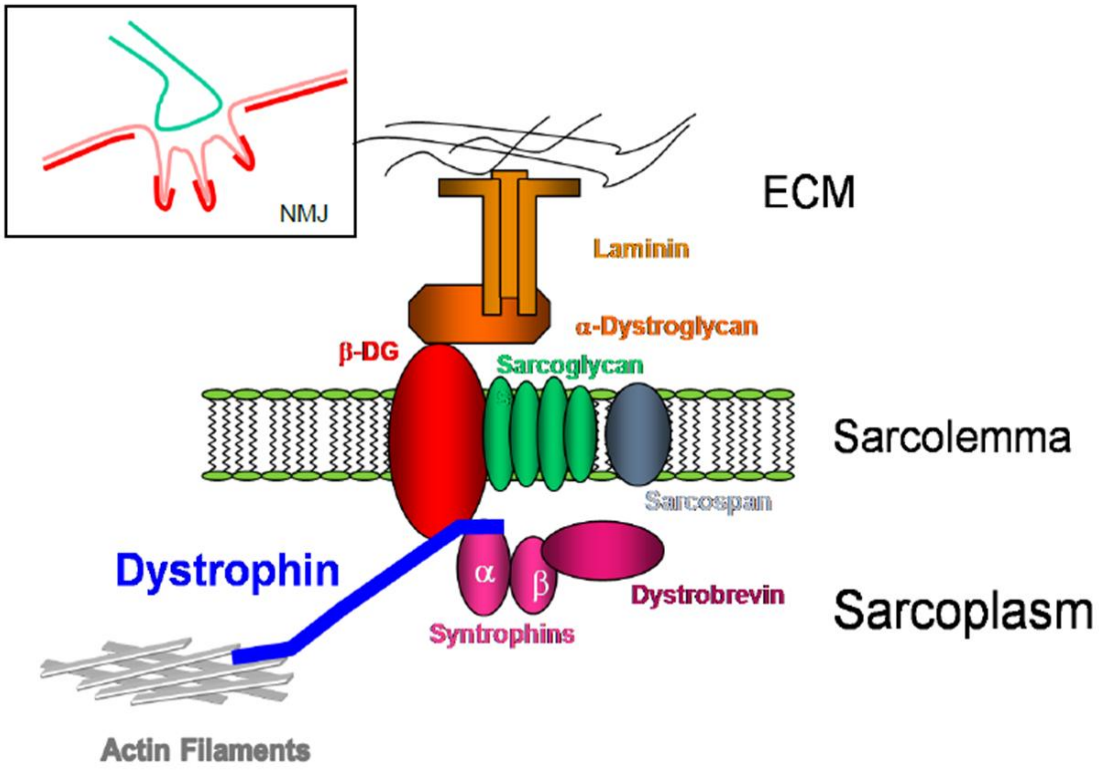

Figure 1.2 – Dystrophin and its interaction with members of the dystrophin-associated protein complex (DAPC) in healthy adult skeletal muscle fibres

Dystrophin provides a structural link between intracellular actin and the extracellular matrix through its association with the DAPC. This protects the muscle from contraction-induced damage. It also helps recruit other members of this complex, including β-DG. Localization of dystrophin in healthy adult skeletal muscle is shown. It can be found along the sarcolemma and troughs of the neuromuscular junction.

1.2 Animal models for DMD

In order to characterize the disease, as well as test the efficacy of different treatment options, several animal models for DMD have been developed. These include canine models (Kornegay 2012), fish models (Chambers 2001), drosophila (Mosqueira 2010), *C. Elegans* (Wells 2005), and mouse models (De Luca 2012). The two models that are most well-studied and translatable to humans are the Golden Retriever Muscular Dystrophy (GRMD) dog and the *mdx* mouse. The GRMD species carries a splice site point mutation with skipping of exon 7, which results in a premature termination of the dystrophin transcript within its N-terminal domain (Kornegay 2012). This model is a good representative of the human disease in terms of the severity of the pathology. GRMD dogs exhibit stunted growth, a more stilted gait, muscle atrophy, problems with bone development in the form of lordosis, and cardiomyopathy (Kornegay 2012). They also demonstrate the characteristic cycles of muscle degeneration and regeneration, eventually leading to muscle wasting/necrosis (Kornegay 2012). Much like humans with DMD, the GRMD dogs have significantly shorter lifespans, often due to respiratory or cardiac complications (Kornegay 2012). Although, this model carries critical similarities to the human pathology, the cost of maintaining and treating these animals is often prohibitive. This is one of the main reasons why mice are used as suitable models for the disease.

The most commonly used mouse strain is the C57Bl/10ScSn (*mdx*) mouse (Bulfield 1984). The *mdx* mouse is dystrophin-deficient, due to a naturally occurring point mutation in exon 23 of the dystrophin gene. This results in a premature transcriptional stop codon, leading to the absence of functional dystrophin (Bulfield 1984). Despite being a genetic and biochemical homologue of the disease, *mdx* mice exhibit a somewhat milder phenotype,

resulting in an almost normal lifespan (Collins 2003). The characteristic pathology of the disease, including the presence of necrotic foci, centrally nucleated myofibres and elevated levels of creatine kinase, is most evident between two and eight weeks of age. Furthermore, different muscles seem to be affected more severely than others. For example, the gastrocnemius and diaphragm are severely affected, whereas the masseter is relatively unchanged when compared to wild-type mice (Collins 2003). Although the *mdx* model is not a perfect representation of the human disease, it still provides a valuable tool to study potential treatment options for patients with DMD.

1.3 Treatment of DMD

In 1974, Drachman and colleagues were the first to use steroids in a clinical study of patients with DMD. After treating almost thirty patients with prednisone, it was discovered that corticosteroids yielded beneficial outcomes with respect to motor power and muscular activities, such as the ability to rise from a chair and climb stairs (Drachman 1974). As time progressed, steroids, including deflazacort and predisone, became the primary therapeutic treatment for patients with DMD, due to their ability to improve muscle strength and function (Fenichel 1991; Angelini 1994). To this day, there is no cure for the disease and glucocorticoids are the only clinically-vetted therapeutic available that prolongs ambulation and slows the decline in skeletal muscle, cardiac, and pulmonary functions (Bushby 2010; McMillan 2010). However, treatment remains symptomatic and administration of these drugs can lead to several unwanted side effects, including weight gain (Bonifati 2000), impairments in bone mineral density leading to vertebral fractures (Bothwell 2003), cataracts, hypertension (Angelini 2012) and behavioural disorders (Pichavant 2011).

Due to these shortcomings, multiple approaches to treat DMD are currently under investigation. These are generally divided into three sub-categories: cell-based therapy, gene-based therapy, and pharmacological approaches.

1.3.1 Cell-based therapy

In healthy individuals, damaged muscles are physiologically repaired by proliferation and fusion with satellite cells. However, in DMD patients, the repaired myofibres still lack dystrophin, leaving them susceptible to further contraction-induced damage (Meregalli 2012). Eventually, the regenerative capacity is exhausted and this repair mechanism is completely lost (Palmieri 2010; Meregalli 2012). This led researchers to experiment with cell-based therapy, which is built around the idea of transplanting healthy skeletal muscle precursor cells or stem cells into dystrophic muscle tissue. Partridge and colleagues were the first to put this theory into practice in 1989. This research group fused healthy myoblasts with regenerating *mdx* muscle fibres and were able to render many of these myofibres dystrophin-positive (Partridge 1989). However, early clinical trials implementing this strategy produced weak results with very little evidence of an increase in dystrophin-positive fibres from donor origin (Tremblay 1993). Over the years, myoblast transplantation methods have been met with a variety of problems, including harsh immune responses (Hong 2002), problems with delivery and migration (Meregalli 2012), and poor cell survival (Mouly 2005). Some of these issues can be circumvented though the use of stem cells, which are capable of self-renewal and differentiation (Peault 2007; Meregalli 2010). Furthermore, certain types of stem cells, namely those derived from bone marrow, have the ability to circulate and reach all muscles, facilitating systemic delivery (Grounds 2007). To date, stem-cell therapy has been used with success in models of muscular dystrophy. For example,

endothelial-derived stem cells, called mesoangioblasts, have been delivered intra-arterially to α-sarcoglycan-null mice (a model for limb-girdle muscular dystrophy), resulting in significant functional improvements of the dystrophic phenotype (Sampaolesi 2003). More recently, mesenchymal stem cells were injected in the diaphragm of *mdx* mice, causing beneficial changes in muscle remodelling (Lessa 2012). Furthermore, the systemic delivery of adherent stem cells to dystrophic dogs has resulted in increased myofibre regeneration, dystrophin expression, and satellite cell replenishment (Rouger 2011). More work is needed to push these practices to the clinical setting but this area of research shows great promise.

1.3.2 Gene-based therapy

One primary area of gene-based therapy in DMD involves the introduction of a functional copy of the DMD gene in an attempt to restore muscle function and sarcolemmal integrity (Pichavant 2011). An advantage of this method is that it is not dependent on any particular mutation in the patient's gene (Goyenvalle 2011). However, identifying safe and effective delivery methods has proved challenging. For example, one difficulty is that the size of full-length dystrophin is often incongruent with the carrying capacity of viral-type vehicles. To circumvent this problem, researchers have developed functional dystrophin genes, called "mini-" and "micro-" dystrophin, with internally deleted regions (Sakamoto 2002). These truncated versions of DMD have proven effective in ameliorating the dystrophic pathology in *mdx* mice (Wang 2000; Sakamoto 2002).

There are three main types of viral vectors that are under investigation in the DMD context: lentiviral vectors, adenoviral, and adeno-associated viral (AAV) (Pichavant 2011). Lentiviral vectors are categorized as a class of retroviral vectors that are capable of integrating into the genomes of quiescent and non-quiescent cells (Kafri 1997; Kimura

2010). These vectors have low immunogenicity and have a fairly large carrying capacity (~9kb) (Kafri 1997). However, they fail to attain widespread transduction of muscle tissues in vivo. Thus, the efficiency of this method is too low to carry therapeutic value at this time (Kafri 1997; Kimura 2010; Pichavant 2011).

Adenoviral vectors, on the other hand, do not integrate into the host genome and exist as independent episomes, following infection (Goyenvalle 2011). They also have a large carrying capacity (~30kb) and demonstrate excellent transduction levels in regenerating or immature muscle tissue (Goyenvalle 2011). However, this method has the potential to trigger an immune response that has proved fatal in the past, prohibiting its transition to clinical trials for patients with DMD (Brunetti-Pierri 2004). The AAV vector is the most efficient for local or systemic delivery to the skeletal muscle and heart, but its packing capacity can only accommodate truncated forms of the dystrophin transgene (Pichavant 2011). Despite this fact, the vector has been used in the *mdx* model, demonstrating an ability to significantly elevate levels of dystrophin (Wang 2000). This success led to the initiation of a clinical trial, using an AAV vector encoding for a functional micro-dystrophin (Bowles 2012). Although the trials were safe, the virus was met with an immune response, which prevented any significant changes with respect to dystrophin. Perhaps this T-cell response could be resolved with transient immune suppression, but this carries risks as well.

Another gene-based therapy, which combines elements of drug-based therapy, involves exon skipping with the use of antisense oligonucleotides (AOs) as a means to restore the production of functional dystrophin (Foster 2012). AO's are single-stranded DNA or RNA molecules that target a complementary sequence of nucleotides. Through this exclusion of targeted frame-shift exons, these AO's can restore the reading frame of the dystrophin gene and synthesize truncated, but functional, BMD-like dystrophin protein

(Foster 2012). This method of AO-induced exon skipping to produce a functional dystrophin protein was first used by Dunckley and colleagues in 1996, and later by several researchers in animal models of DMD (Mann 2002; McClorey 2006). Promising results from these studies, paved the way for clinical trials, which began in 2007. By skipping exon 51 with local injection of AO's, the open reading frame was restored and functional dystrophin expression was observed in patients with DMD (van Deutekom 2007; Kinali 2009). These AO's showed no adverse effects, but functional improvements and increases in dystrophin-positive fibres were modest (Foster 2012). One of the main issues with AO-induced transcript editing is delivery of the AO's. If administered systemically, in the hope of reaching whole-body musculature, the majority of the AO's are taken up and cleared by the liver and kidney (Foster 2012). Additionally, due to the fact that AO's act on the transcript, rather than the gene itself, their effects are ephemeral. Thus, a continual delivery of AO's is required to maintain a significant therapeutic effect (Foster 2012).

1.3.3 Pharmacological Approaches

Pharmacological therapies encompass the use of small molecules or pharmacological agents in an effort to ameliorate the primary and secondary pathological features of DMD. As discussed earlier, glucocorticoids are the only therapeutic option that is in common use among patients with DMD, but alternatives are currently under investigation. Some of these drugs aim to target the disease at the RNA level by correcting mutations in the dystrophin gene. More specifically, they purpose to fix mutations that result in the formation of a premature stop codon within the coding sequence of dystrophin (Barton-Davis 1999; Chakkalakal 2005). Researchers have discovered that several antibiotics, such as gentamicin, can suppress the stop codons, and replace them with alternative amino acids (Barton-Davis

1999; Chakkalakal 2005). This method of stop codon read-through has been implemented with success in *mdx* mice, leading to increased expression of dystrophin, improved sarcolemmal stability and resistance to force drop following eccentric contractions (Barton-Davis 1999).

These positive results sparked a transition to clinical trials, where DMD patients were treated with gentamicin for six months (Malik 2010). Modest increases in dystrophin and subtle improvements in muscle strength were encouraging, but the drawbacks of intravenous administration, led researchers to explore other possibilities. More recently, Ataluren (formerly known as PTC 124) was developed as an orally administered read-through agent for stop-codon mutations (Welch 2007). Favourable results in *mdx* mice pushed the drug to clinical trials, where preliminary tests revealed only modest improvements in the 6-minute walking test (Malik 2012; http://www.clinicaltrials. gov/ct2/results?). Trials are ongoing and determination of an optimum dose for the drug is of utmost importance.

Instead of increasing dystrophin or correcting mutations in dystrophin, other strategies have focused on trying to treat the consequences of the dystrophic process (Malik 2012). For example, increasing muscle size and strength through inhibition of the myostatin pathway, has been explored in the context of DMD (Bogdanovich 2002). Myostatin is a protein that inhibits muscle differentiation and growth, so researchers have attempted to arrest its function to improve muscle growth. Bogdanovich and colleagues set up a myostatin blockade in *mdx* mice, which led to an increase in muscle mass/size/strength, and a reduction in skeletal muscle degeneration and serum creatine kinase levels (Bogdanovich 2002). Clinical trials, using myostatin inhibitors in patients with DMD, are still in the early stages and no conclusive findings have been reported.

Activation of insulin-like growth factor-1 (IGF-1) is viewed as another way of potentially increasing muscle mass and strength in patients with DMD. Its overexpression in *mdx* mice has already proved effective at increasing muscle mass of the extensor digitorum longus (EDL) and diaphragm muscle, and reducing necrosis and fibrosis (Barton 2002; Shaylakadze 2004). There are obvious issues with these strategies. Although, muscle function and strength may improve, this effect is transient as the muscles still lack dystrophin. However, increases in muscle functionality will undoubtedly improve the quality of life for patients with DMD.

Aside from a drastic reduction in muscle strength and functionality, fibrosis and inflammation are other major consequences of the dystrophic pathology (Malik 2012). Several pre-clinical anti-fibrotic therapies focus on inhibiting cytokine signaling from the transforming growth factor (TGF)-β pathway. These pharmaceuticals include losartan (Cohn 2007), pirfenidone (Gosselin 2007), halofuginone (Huebner 2008) and Suramin (Taniguti 2011) and they have been successful at diminishing fibrosis in pre-clinical trials. Inflammation is also abnormally high in patients with DMD and this is partly due to chronic activation of the NF-kB signaling pathway (Acharyya 2007). Researchers have attempted to block this pathway through the use of inhibitors, including NEMO-binding domain (NBD) peptide (Delfin 2011; Peterson 2011). In pre-clinical trials, the NBD peptide has reduced skeletal muscle damage and improved muscle function in *mdx* mice (Delfin 2011; Peterson 2011).

Alternative therapeutic strategies disregard attempting to manipulate levels of functional dystrophin and shift away from a focus on specific secondary pathological features. Instead, through a combination of pharmaceuticals, gene- and cell-therapy,

researchers aim to functionally compensate for the lack of dystrophin by increasing endogenous levels of utrophin A protein.

1.3.4 Utrophin A upregulation

Many years ago, a gene was identified that encodes a large cytoskeletal protein with extensive sequence identity to dystrophin (Love 1989; Jasmin 1990; Khurana 1990). This gene, named utrophin, is located on chromosome 6q24, and is approximately 1 Mb in length, containing 74 exons (Pearce 1993). Originally named dystrophin-related-protein, utrophin was named thus due to its ubiquitous nature of expression. High levels of utrophin have been observed in most tissues, including heart, lungs, skeletal and smooth muscle, kidney, liver, nervous system and vascular endothelial cells (Khurana 1990). Like dystrophin, utrophin has multiple promoters, A and B, which encode for two full-length isoforms: utrophin A and utrophin B (Blake 2002). These proteins carry a molecular mass of approximately 395 kDa, but differ in their localization (Blake 2002).Utrophin A is typically expressed in peripheral nerves, vascular smooth muscle and at the crests of NMJ's of skeletal muscle, whereas utrophin B is mostly found in vascular endothelial cells (Burton 1999). Expression levels of utrophin A in skeletal muscle change during development and regeneration. In mature muscle fibres, utrophin A is largely limited to the cytoplasmic face of the neuromuscular junction and myotendinous junctions (Tinsley 1998; Blake 2002; Jasmin 2002) (**Figure 1.3**). In developing and regenerating muscle, it can be found along the length of the sarcolemma.

The primary structure of utrophin is similar to dystrophin throughout its full length, particularly the NH_2 and the COOH termini, where the actin binding domains and the dystrophin-associated glycoprotein binding domains have 85% and 88% similarity,

respectively (Pearce 1993; Fisher 2001; Blake 2002) (**Figure 1.3**). This level of similarity translates to relatively analogous functions (Winder 1995; Muthu 2012). The central rod domain of utrophin is the least conserved region, sharing approximately 35% of its sequence identity with dystrophin (Winder 1995; Muthu 2012). It consists of twenty-two spectrin repeats (24 for dystrophin), interspersed with two hinge regions (Muthu 2012). Despite this seemingly large deviation in sequence similarity, the function of this domain in both proteins is almost identical - the combination of spectrin repeats and hinge regions acts as spring units by undergoing force-induced folding to provide membrane flexibility (Muthu 2012).

The structural similarity between the two proteins grants utrophin the potential to compensate for a lack of dystrophin in patients suffering from DMD. Importantly, muscle fibres from DMD patients express utrophin endogenously, eliminating any concerns about immunogenicity. In fact, utrophin A expression is up-regulated in the skeletal muscle of DMD patients (Mizuno 1993; Kleopa 2006) and *mdx* mice (De la Porte 1999), presumably as a compensatory mechanism. Several studies, using *mdx* mice, have shown that by increasing utrophin A through transgenic methods, the dystrophic pathology is almost completely prevented (Tinsley 1996; Tinsley 1998; Gilbert 1999; Fisher 2001). Other methods have emerged since, including adenoviral utrophin A gene transfer (Deol 2007; Odom 2008; Lin 2012), protein therapy (Sonnemann 2009; Amenta 2011; Call 2011), and pharmacological interventions (Chaubourt 1999; Tinsley 2011).

A)

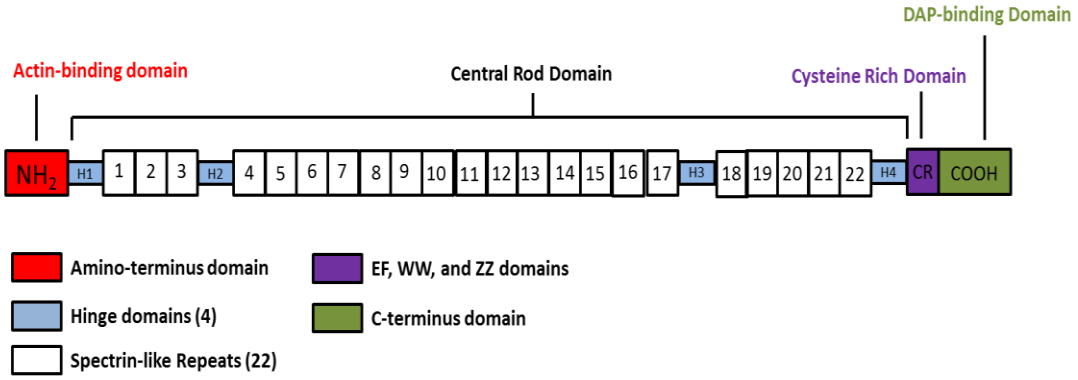

B)

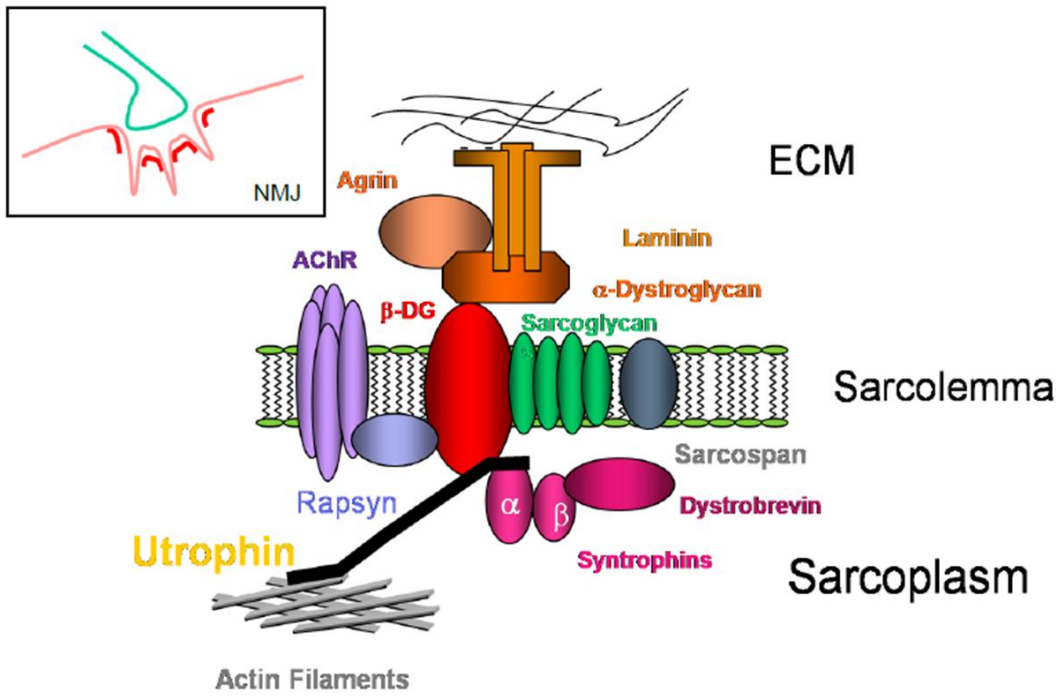

Figure 1.3 - Utrophin A and its interaction with members of the dystrophin-associated protein complex (DAPC) in healthy adult skeletal muscle fibres

A) Structural illustration of utrophin A protein with its different functional domains. B) Utrophin A provides a structural link between intracellular actin and the extracellular matrix through its association with the DAPC. This protects the muscle from contraction-induced damage. It also helps recruit other members of this complex, including β-DG. Localization of utrophin A in healthy adult skeletal muscle is shown. It can be found at the crests of the neuromuscular junction.

AAV vectors, harboring full-length or micro-utrophin transgenes, have been used to treat adult *mdx* and dystrophin (-/-) / utrophin (-/-) double knockout mice, respectively (Deol 2007; Odom 2008). This has resulted in localization of utrophin A to the sarcolemma, as well as restoration of the DAPC and improvements in the pathophysiological abnormalities associated with these mouse models (Deol 2007; Odom 2008). One problem with this method is that utrophin A expression does not persist indefinitely, suggesting that multiple injections may be necessary to maintain these elevated levels of utrophin A (Deol 2007).

Protein therapy involves delivery of proteins that would otherwise be absent within the muscle cells of DMD patients. Administration of recombinant full-length utrophin or DeltaR4-21 "micro" utrophin and recombinant biglycan are examples of protein therapeutic strategies designed for the DMD context (Sonnemann 2009; Call 2011; Amenta 2011). TAT-mediated utrophin protein delivery to *mdx* mice resulted in a successful reduction in serum levels of creatine kinase, centrally nucleated fibres, and percentage of force drop following eccentric contractions (Sonnemann 2009; Call 2011). Biglycan is an extracellular matrix protein that binds members of the DAPC, including α-dystroglycan and the sarcoglycans (Amenta 2011). Systemically delivered recombinant human biglycan enhances the presence of utrophin A at the sarcolemma, ameliorates the dystrophic pathology, and improves muscle function (Amenta 2011).

Pharmacological interventions are also being implemented in an effort to stimulate utrophin expression. Chaubourt and colleagues experimented with using L-arginine as a means of achieving this goal. L-arginine is a precursor, necessary for NOS-induced NO synthesis (Chaubourt 1999). NOS and utrophin A share similar patterns of localization in

adults muscle, suggesting that NO helps utrophin A maintenance (Karpati 1993). Chaubourt and colleagues discovered that L-arginine treatment leads to increased levels of utrophin A and rearrangement to the sarcolemma in wild-type and *mdx* mice (Chaubourt 1999). Follow-up studies demonstrated that L-arginine treatment in *mdx* mice reduces necrosis and creatine kinase levels, relocalizes beta-dystroglycan and utrophin A to the membrane, increases isometric tension in the diaphragm, and reduces the immune response (Voisin 2005; Archer 2006; Hnia 2008). Recently, a high-throughput transcription screen has identified a novel drug, called SMTC1100, which increases utrophin A mRNA and protein significantly in skeletal muscle (Tinsley 2011). This drug is currently proceeding to phase II trials due to pre-clinical success.

One of the primary challenges for utrophin-based therapy is to stimulate utrophin A expression at high levels along the entire length of the sarcolemma, including synaptic and extrasynaptic compartments of muscle fibres. Several factors are involved in regulating utrophin A expression, including those involved in the development of the neuromuscular junction and muscle fibre type. Studying the mechanisms involved in these processes is critical to find targets that can be used to influence utrophin A expression and localization.

1.4 Utrophin A regulation

1.4.1 Neuromuscular junction (NMJ)

Utrophin A is primarily expressed at the NMJ of adult skeletal muscle fibres. Understanding the role of the nerve and its surrounding factors is important for manipulating utrophin A expression. The Jasmin lab was the first to reveal the importance of neuronal cues that regulate utrophin A expression and localization at the NMJ (Gramolini 1997a). They

showed that utrophin A mRNAs selectively accumulate within the post-synaptic sarcoplasm of adults skeletal muscle fibres, and that nerve-derived factors regulate locally the transcriptional activation of utrophin A (Gramolini 1997a-b). They also suggest that, given the necessary neuronal cues, extra-synaptic regions have the capability to express utrophin A (Gramolini 1997a-b). Agrin was identified as one such neuronal cue, as it triggered utrophin A expression in cultured muscle cells via transcriptional activation (Gramolini 1998).

The nerve-derived trophic factor, heregulin, was also tested for its ability to stimulate utrophin A expression via a transcriptional mechanism. Gramolini and colleagues demonstrated that heregulin induces utrophin A transcription through GA binding protein (GABP)'s interaction with a conserved N-Box motif, located within the utrophin A promoter (Gramolini 1999). Khurana and colleagues confirmed this finding, cementing a role for the heregulin signaling pathway in utrophin A regulation (Khurana 1999). Stimulating this pathway in *mdx* mice has been studied more recently, where researchers found significant increases in utrophin A expression, as well as improvements in muscle functionality, evidenced by resistance to eccentric contraction-mediated damage (Krag 2004). These studies highlight the importance of transcriptional regulation of utrophin A in its localisation at the NMJ. Other factors also affect utrophin A regulation at the transcriptional and post-transcriptional level, including skeletal muscle fibre type.

1.4.2 Slow vs. fast muscle

Mammalian skeletal muscle is composed of different fibre types, which have historically been generalized into two main groups: slow-twitch and fast-twitch. Slow-twitch muscles are characterized as rich in myoglobin and oxidative enzymes, resistant to fatigue,

and red in appearance. Their fast-twitch counterparts rely on glycolytic metabolism, making them well-suited for phasic activity and are white in appearance (Schiaffino 2011). In recent years, this two-tiered classification system has been replaced with one which recognizes four major skeletal muscle fibre types: type I (slow oxidative, MHC7), IIa (fast oxidative, MHC2), IIx (fast glycolytic, MHC1), and IIb (very fast glycolytic, MHC4) (Schiaffino 2011). In addition to myosin composition and energy metabolism, these fibre types are defined by their unique biochemical and functional characteristics. These can be as diverse as acetylcholinesterase (AChE) activity (Sketelj 1997), sodium (Na) channel density (Ruff 1992), myoglobin expression levels (Ordway 2004), and GLUT4 expression/translocation (Schiaffino 2011). In general, slow-oxidative type I fibres are designed to sustain continuous, low-intensity contractions for extended periods of time, whereas fast-glycolytic type IIb-x fibres are built for short, powerful bursts of contractile activity. This translates to several adaptations at the subcellular level that are specific to each fibre type. (**Figure 1.4**)

At the NMJ, fast fibres demonstrate a significantly higher quantity of acetylcholine (ACh) neurotransmitter release, a greater density of ACh receptors and a prevalence of voltage-dependent sodium channels in the surrounding postsynaptic folds (Schiaffino 2011). This excess of neurotransmitter release, receptors, and ion channels guarantees successful neuromuscular transmission, but it cannot be maintained for long periods of time, which results in a rapid depression (Schiaffino 2011). Predictably, slow, oxidative type I muscles are capable of responding to continuous stimulation due to their characteristically low synaptic depression. In terms of ion homeostasis, type I and type II muscle fibres exhibit some key differences. Fast, type II fibres have significantly more sodium channels to accommodate the high discharge rate of the motor neurons (Ruff 1993). However, this may

contribute to their susceptibility to fatigue, as the large sodium influx can overwhelm the Sodium-Potassium (Na/K)-ATPase pumps' ability to maintain ionic homeostasis. Slow, oxidative fibres need mechanisms in place to counteract the accumulation of ions that results from long-lasting stimulations (Schiaffino 2011). One such adaptation is the increased efficiency of the Na/K pump in response to prolonged activity (Everts 1992).

Another important area of deviation between type I and type II skeletal muscle fibres is their handling of calcium shuttling and sequestration within the cell. Calcium is a critical messenger in skeletal muscle, carrying several functions, which include triggering contractions via binding to troponin (Schiaffino 2011). As compared to slow, oxidative muscle fibres, their fast, glycolytic counterparts have a lower cytosolic concentration of free calcium. This is due, in part, to the superior buffering capabilities of the troponin C and parvalbumin isoforms that are characteristic of this fibre type (Füchtbauer 1991). In addition, fast, glycolytic fibres have a greater abundance of calcium release channels, calcium pumps, and a more developed sarcoplasmic reticulum (SR), which affords them the ability to release and utilize larger amounts of calcium in less amount of time (Schiaffino 2011). In conjunction with contractile machinery that can take advantage of these rapid calcium transients, type II fibres are capable of eliciting powerful bursts of activity.

Finally, in terms of energy metabolism, ATP regeneration based on oxidative respiration is much more effective in slow than in fast fibres due to the greater mitochondrial density and greater TCA cycle fuelling in type I fibres (Schiaffino 2011). Interestingly, once mitochondrial respiration is activated in slow fibres, ATP consumption can be completely balanced by ATP regeneration (Schiaffino 2011). This scenario is never realized in fast, type IIb-x fibres, where anaerobic glycolysis is the main avenue of energy production.

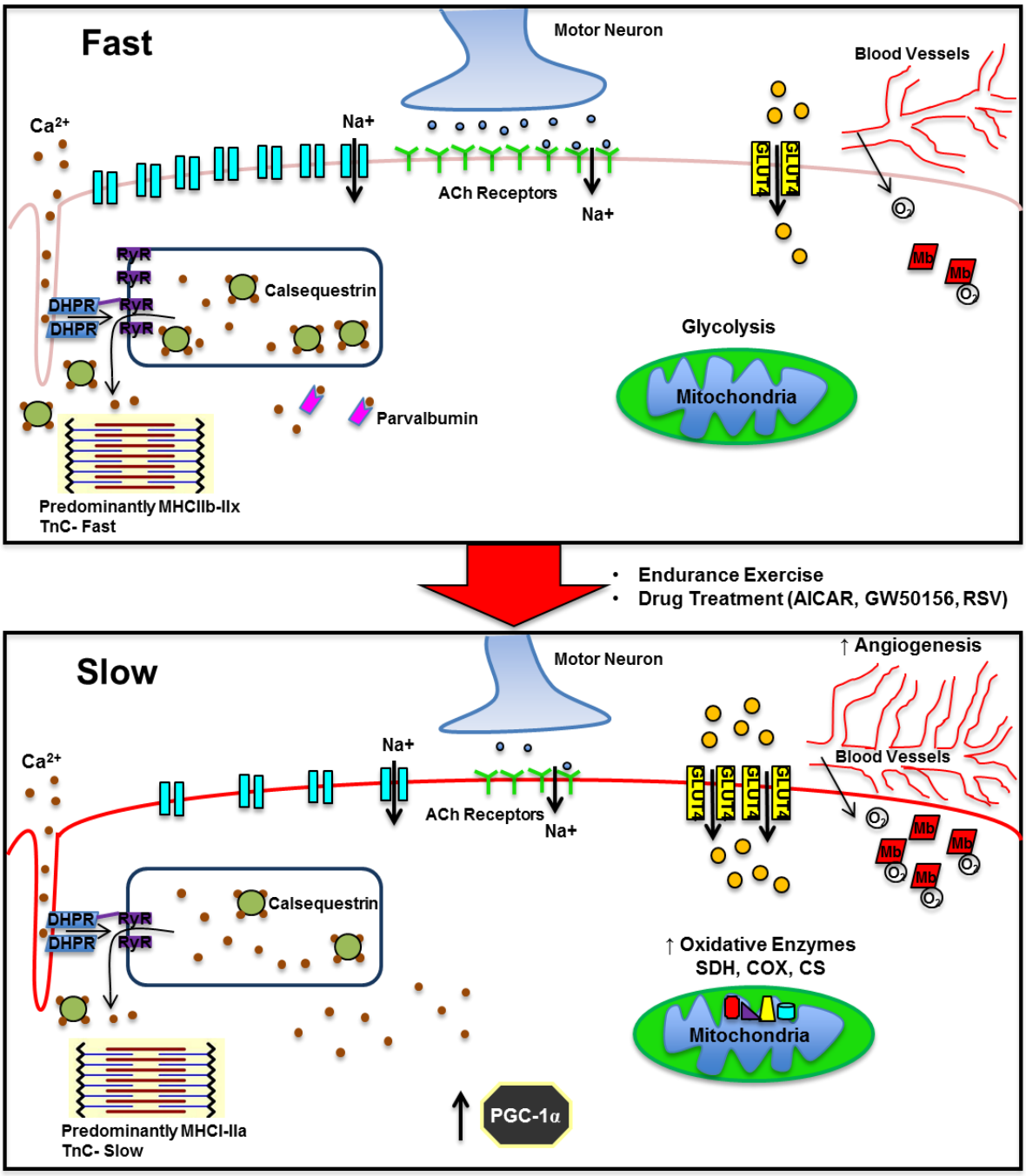

Figure 1.4 – Schematic representation of distinguishing characteristics of fast, glycolytic type II skeletal muscle (top panel) and slow, oxidative type I skeletal muscle (bottom panel)

Fast muscle has a number of characteristics that make them optimally-suited for rapid, phasic activity. These include a larger motor end plate, a higher density of acetylcholine receptors, and enhanced calcium buffer systems. Slow muscle is different in that it is designed for slow, continuous activity. Oxidative metabolism, increased myoglobin concentration and enhanced glucose transport systems allow these muscles to function under such conditions. SDH- succinate dehydrogenase, COX- cytochrome c oxidase, CS- citrate synthase, Mb- myoglobin, DHPR- dihydropyridine receptor, RyR- ryanodine receptor, GLUT4, glucose transporter type 4. Note: yellow circles represent glucose.

Although these differences are evident among individual muscle fibres, skeletal muscles are often laced with heterogeneity, which allows them to perform a variety of tasks, ranging from continuous low-intensity activity (e.g., posture) to fast maximal contractions (e.g., jumping) (Schiaffino 2011). In other words, skeletal muscles contain a continuous spectrum of fast and slow fibres, rather than distinct fibre types, which have the ability to change in response to hormonal and neural influences (Schiaffino 2011). Understanding different mechanisms responsible for this muscle plasticity is important, as certain phenotypes carry inherent benefits under the right context. For example, during fasting or conditions of muscle wasting, including cancer cachexia, type II glycolytic muscle fibres demonstrate a higher degree of atrophy, compared to type I oxidative muscle fibres (Matsakas 2009). In the context of DMD, the slower, more oxidative muscle fibres in diseased patients are more resistant to the dystrophic pathology, as compared to the faster, more glycolytic fibres (Webster 1988). This phenomenon also holds true in the *mdx* mouse (Moens 1993).

Interestingly slow muscle contains higher amounts of structural proteins, including dystrophin, and utrophin A (Gramolini 2001b; Miura 2006). Immunofluorescence indicates that utrophin A can be found at low levels extrasynaptically along the sarcolemma in slow, oxidative soleus muscles, whereas utrophin A expression is restricted to the NMJ in fast, glycolytic extensor digitorum longus (EDL) muscles (Gramolini 2001a). Furthermore, the expression of transcripts encoding synaptic proteins, including AChE, ColQ and utrophin A is elevated and extended to extrasynaptic regions of slow muscle fibres (Gramolini 2001a). This pattern of increased expression of utrophin A in slow-twitch muscle fibres translates to reduced damage in both the *mdx* mouse and DMD patients (Webster 1988; Miura 2009).

1.5 Promotion of the slow oxidative myogenic program (SOMP) as a therapeutic strategy to increase utrophin A expression and protect dystrophic muscle

1.5.1 Calcineurin/NFAT Pathway

The mechanisms responsible for the increase in sarcolemmal utrophin A expression, observed in slow, oxidative skeletal muscle, have been under investigation in recent years. Intracellular calcium levels are an element of distinction between slow type I and fast type II muscle fibres that may help explain this phenomenon. Due to sustained activation patterns, slow muscles demonstrate consistent elevations of intracellular calcium concentrations (Schiaffino 2011). Calcium is an important signaling molecule that interacts with a number of different pathways and proteins, including calcineurin. Interestingly, calcineurin is a protein phosphatase that is implicated in the control of the SOMP by acting on nuclear factor of activated T cells (NFAT) transcription factors (Chin 1998; Schiaffino 2007; Mallinson 2009). These observations led researchers to explore the ability of calcineurin to promote the SOMP and stimulate utrophin A expression in pre-clinical trials. Constitutive activation of calcineurin through transgenic means resulted in increased utrophin A expression in skeletal muscles of mice (Chakkalakal 2003). Conversely, inhibition of this calcineurin pathway through cyclosporine A (CsA) injection had the opposite effect, as mice showed an 80% decrease in utrophin A mRNA levels (Chakkalakal 2003). NFAT binding sites, located in the utrophin A promoter region suggest a possible mechanism for this calcineurin-induced increase in utrophin A mRNA levels (Chakkalakal 2003). Indeed, constitutively active forms of NFATc1 and calcineurin trigger utrophin A promoter activity (Chakkalakal 2003). Establishing this relationship allowed researchers to move to the diseased context.

The Jasmin lab crossed mice carrying enhanced muscle calcineurin activity with *mdx* mice to understand whether increased calcineurin activity had any therapeutic value in ameliorating the dystrophic pathology (Chakkalakal 2004). Muscles from these mice showed evidence of a fibre type shift towards the slower phenotype, as well as significant increases in utrophin A expression. These changes were accompanied by reductions in centrally-nucleated myofibres and fibre size variability (Chakkalakl 2004). Improvements in sarcolemmal integrity were also evident, judging by IgM and Evans blue dye staining (Chakkalakal 2004).

Stupka and colleagues took a different approach, electing to disrupt the calcineurin pathway via CsA treatment in *mdx* mice. They found that inhibiting the calcineurin pathway had a significant deleterious effect (Stupka 2004). CsA-treated *mdx* mice demonstrated extensive collagen and connective tissue infiltration, as well as a significant decrease in force production, when compared to vehicle-treated *mdx* mice (Stupka 2004). To solidify the role of this calcineurin/NFAT pathway in *mdx* mice, Chakkalakal and colleagues also explored the consequences of inhibiting its activity in skeletal muscle (Chakkalakal 2006). They focused their attention on calcium and calmodulin (CaM), which are both upstream regulators of calcineurin (Chakkalakal 2006). Ca^{2+}/CaM play critical roles in the initiation of calcineurin's phosphatase activity, which then leads to the dephosphorylation, nuclear translocation and binding of NFAT to target promoters, including utrophin A (Chakkalakal 2006). They generated an *mdx* mouse strain, expressing a transgene that encodes for a small peptide inhibitor of CaM, called CaM-binding protein (CaMBP). By doing so, Chakkalakal and colleagues were able to successfully disrupt the CN/NFAT pathway, reducing utrophin A expression and exacerbating the dystrophic phenotype (Chakkalakal 2006). In addition to

its influence on utrophin A promoter activity, calcineurin is also implicated in regulating utrophin A mRNA stability through interactions with an AU-rich element (ARE) located in the 3'UTR (Gramolini 2001a; Chakkalakal 2008). Therefore, there is clear evidence that calcineurin is an important factor in maintaining utrophin A expression and protecting slow muscle from the dystrophic pathology, operating at the transcriptional and post-transcriptional levels.

1.5.2 PGC-1α

The transcriptional co-activator peroxisome proliferator-activated receptor (PPAR) ϒ coactivator α (PGC-1α) is another key factor than can influence the formation of slow, oxidative muscle fibres (Puigserver 1998; Lin 2002). PGC-1α has been described as the master regulator of skeletal muscle phenotypic plasticity, and when it is expressed at physiological levels in transgenic mice, a fibre type conversion is observed: muscles originally rich in type II fibres become redder and activate genes of mitochondrial oxidative metabolism (Lin 2002). The link between PGC-1α and utrophin A in skeletal muscle was first established by the Jasmin lab (Angus 2005). They demonstrated that overexpression of PGC-1α through transfection was sufficient to transcriptionally activate the utrophin A promoter (Angus 2005). This induction was potentiated by co-expression of PGC-1α with GABP, a transcription factor involved in the expression of NMJ and slow/oxidative genes. This led researchers to explore the role of PGC-1α in the *mdx* context. *Mdx* mice were crossed with muscle-specific PGC-1α overexpressing mice, resulting in significant improvements in serum creatine kinase levels, myofibre damage/necrosis, and acute exercise tolerance. (Handschin 2007). These changes were concomitant with an increase in utrophin A mRNA content (Handschin 2007). More recently, Selsby and colleagues solidified this

relationship between PGC-1α overexpression and utrophin A upregulation. They injected *mdx* mice with recombinant AAV, driving expression of PGC-1α (Selsby 2012). This genetic intervention resulted in increased expression of utrophin A, type I myosin heavy chain, and mitochondrial proteins (Selsby 2012). Functional improvements, including resistance to contraction-induced damage and resistance to muscle fatigue, were also observed (Selsby 2012). The importance of PGC-1α in promoting the SOMP is undeniable. Manipulation of this pathway through transgenic and physiological means has proved beneficial in ameliorating the dystrophic pathology. It is interesting to note that PGC-1α expression is inherently higher in *mdx* mice, compared to wild-type strains. Like utrophin A, this may serve as a compensatory mechanism to counteract the debilitating effects of the disease.

Taken together, PGC-1α and calcineurin/NFAT are powerful factors that have the ability to stimulate the SOMP. Activation of these molecules and their associative pathways can remodel skeletal muscle and induce the expression of a number of structural proteins, including utrophin A. In the *mdx* context, overexpression of PGC-1α and calcineurin is sufficient to yield significant improvements in the dystrophic pathology. These findings highlight the importance of identifying other molecules or pathways that target the SOMP.

1.6 Molecules that target SOMP

1.6.1 PPARβ/δ

PPARs are ligand-dependent nuclear receptors that belong to a broad family of nuclear transcription factors (Gervois 2007). PPARβ/δ is one such transcription factor that stimulates genes involved in lipid metabolism and oxidative respiration via PPAR-response elements located in their promoter regions (Ehrenborg 2009). PPARβ/δ is the most abundant

PPAR isoform in skeletal muscle (Muoio 2002; Ehrenborg 2009) and is more highly expressed in oxidative type I muscle fibres compared with glycolytic type II muscle fibres (Wang 2004). In addition, transgenic mice engineered with targeted skeletal muscle overexpression of PPARβ/δ exhibit changes in muscle morphology that are consistent with the slower, more oxidative phenotype (Luquet 2003; Wang 2004; Gaudel 2008; Gan 2011). These changes include increased myoglobin, troponin, and GLUT4 protein levels, mitochondrial biogenesis, angiogenesis, and improved exercise performance (Luquet 2003; Wang 2004; Guadel 2008; Gan 2011). These changes are comparable to those seen in mice overexpressing PGC-1α, insinuating that the pathways may overlap.

Recently, our lab administered GW501516, a PPARβ/δ agonist, to *mdx* mice, over a six week period. (Miura 2009). Treatment resulted in attenuation of the dystrophic pathology and increased utrophin A expression along the sarcolemma (Miura 2009). In addition, there was evidence of a phenotypic shift in skeletal muscle fibres towards the slower, more oxidative phenotype, including a significantly higher percentage of slow myosin heavy chain isoforms in both the EDL and SOL (Miura 2009). Interestingly, the utrophin A promoter contains PPAR response elements, which may be responsible for the observed changes in utrophin A expression, following GW501516 treatment.

1.6.2 AMPK

AMP-activated protein kinase (AMPK) has emerged as a critical regulator of skeletal muscle metabolism, transcription and phenotype. Activation of AMPK occurs in response to increased cellular AMP concentrations, which arise during cellular metabolic stress. AMPK's involvement in promoting the slow myogenic program is due, in large part, to the plethora of substrates which it acts upon, either directly or indirectly. These include the

PGC-1α, GLUT4, MEF2, Sirtuin1 (SIRT1), and PPARβ/δ (Kramer 2005; Canto 2009; Canto 2010). The co-ordinated increase in expression of these regulators in response to AMPK stimulation provides the cellular machinery required for skeletal muscle plasticity. Indeed, several AMPK activators, including adenosine analogue 5-amino-4-imidazolecarboxamide riboside (AICAR), have the ability to trigger phenotypic changes in skeletal muscle morphology (Holmes 1999; Winder 2000). These alterations can include myosin isoform shifts from type IIb to IIx, mitochondrial biogenesis, augmented PGC-1α, PPARδ and GLUT4 expression, and improved insulin sensitivity (Jorgensen 2007; Narkar 2008; Leick 2010).

Recently, we administered AICAR to *mdx* mice in the hope of activating the SOMP and, consequently, increasing utrophin A expression (Ljubicic 2011). Beneficial adaptations were observed at the level of the mitochondria and contractile apparatus, including increased utrophin A expression, which manifested as functional improvements, such as sarcolemmal structural integrity during damaging eccentric muscle contractions (Ljubicic 2011).

Activation of AMPK and PPARβ/δ through the use of small molecules was effective at increasing utrophin A expression and improving the dystrophic pathology in *mdx* mice. These effects were comparable to those observed in studies using transgenic mice overexpressing PGC-1α or calcineurin, which speaks to the potency of these drugs. It also supports the idea that promotion of the SOMP is an effective therapeutic strategy in the DMD context. Identifying other drugs that are capable of triggering the SOMP and inducing utrophin A expression is of utmost importance.

1.7 Does SIRT1 activation promote the SOMP?

SIRT1 is another important protein that plays a role in skeletal muscle plasticity and, as a result, may affect utrophin A expression. It is a class III histone deacetylase (HDAC), whose activity is dependent on the presence of NAD+. SIRT1 acts as an energy sensor and transcriptional regulator by manipulating the acetylation states of histones and non-histone proteins alike (Imai 2000). Some of these non-histone targets include, nuclear factor κB (NF-κB) (Salminen 2008), the forkhead box class O (FOXO) family members (Huang 2007), p53 (Van Leeuwen 2009), peroxisome proliferator-activated receptor gamma (PPARϒ), and PGC-1α (Gurd 2011). This plethora of targets affords SIRT1 the ability to modify the expression of many different genes in a wide range of tissues, including skeletal muscle. SIRT1 is almost ubiquitously expressed throughout the body, but the level of SIRT1 expression and/or activity can range between tissues, and even among different skeletal muscle fibre types. Suwa *et al.* observed that SIRT1 protein content in Wistar rats is significantly higher in the red, oxidative muscles, compared to their white, glycolytic counterparts (Suwa 2008). A similar finding was shown in mice, where both SIRT1 mRNA and protein levels were higher in the red gastrocnemius muscle, compared to the white gastrocnemius muscle (White 2011). SIRT1 is believed to influence the slow, oxidative myogenic program, predominantly, through its interaction with PGC-1α, which is considered a master regulator of mitochondrial biogenesis (Lin 2002). Essentially, SIRT1 deacetylates PGC-1α, thereby increasing its activity and function. Over-expression of SIRT1 in hepatocytes and C2C12 myotubes leads to increases in PGC-1α deacetylation and the expression of mitochondrial genes (Rodgers 2005; Gerhart-Hines 2007). Conversely, in

SIRT1 knockout or SIRT1-ablated myotubes, PGC-1α activity is reduced and there is a predictable decrease in PGC-1α target genes (Gerhart-Hines 2007; Amat 2009).

The relationship between SIRT1, PGC-1α and mitochondrial biogenesis in transgenic mammalian models is more contentious. Some transgenic mouse models, overexpressing SIRT1, have shown similar results to those found *in vitro*, including improved insulin sensitivity, fatty acid oxidation, motor function, and increased deacetylation of PGC-1α (Bordone 2007; Banks 2008; Gerhart-Hines 2011). However, there is also evidence that SIRT1 negatively correlates with PGC-1α protein and markers for mitochondrial content in skeletal muscle (Gurd 2009).

There is limited research on the role of SIRT1 in the DMD context and its influence on utrophin A expression. Ljubicic and colleagues have observed that SIRT1 protein levels, much like utrophin A and PGC-1α, are increased in *mdx* mice as compared to wild-type groups (Ljubicic 2011). But, direct manipulation of SIRT1 through pharmacological or other means has not been explored in great detail.

Discovering pharmacological agents that can interact with these proteins and activate the slow, oxidative myogenic program is of great interest to researchers of muscular dystrophy. The positive effects of skeletal muscle fibre type remodelling are evident in this context. This has led us to explore the potential therapeutic value of the SIRT1 activator, known as resveratrol, which interacts with several members known to be involved in promoting the SOMP, including AMPK and PGC-1α.

1.7.1 Resveratrol

Resveratrol is a polyphenolic compound that is found naturally in fruits and vegetables, such as the skin of grapes and the roots of peanuts (Wenzel 2005). It began to receive significant interest, following the discovery of its ability to potently activate SIRT1 and mimic the effects of caloric restriction in *C. elegans* (Howitz 2003). More recently, it has been heralded for its apparent cancer chemo-preventive properties (Wenzel 2005), its ability to act as an antioxidant (Jackson 2010), and its capacity to lower plasma glucose levels and improve insulin sensitivity (Milne 2007). However, the ability of resveratrol to increase mitochondrial biogenesis and oxidative capacity in skeletal muscle is most interesting (Lagouge 2006). It has also been suggested that resveratrol is involved in converting muscle fibres to the slower, more oxidative phenotype (Lagouge 2006). Lagouge and colleagues have shown that mice on a high-fat diet, supplemented with resveratrol, had increased mitochondrial DNA, citrate synthase activity, an overall improvement in mitochondrial function, and a gene expression pattern characteristic of the SOMP (Lagouge 2006). Skeletal muscle of resveratrol-treated mice had increased expression of PGC-1α, myoglobin, and slow-type troponin I; as well as a reduction in the proportion of acetylated PGC-1α (Lagouge 2006). Resveratrol also shows a retentive effect of the slow, oxidative skeletal muscle profile under conditions of muscle atrophy (Momken 2011). Rats subjected to prolonged muscle disuse, were able to maintain normal slow MHC I expression, maximal force contraction, mitochondrial oxidative capacity, and expression levels of SIRT1, PGC-1α and COXIV in the soleus muscle (Momken 2011). Therefore, it seems that resveratrol can orchestrate myofibre remodeling, similar to that seen in exercise training, but in the absence

of an increase in physical exertion. Obviously, this is of particular interest to patients with DMD, who have significant restrictions when it comes to exercise.

The effects of resveratrol on human muscle metabolism have not been studied in great depth. Some studies have shown resveratrol-induced improvements in measures of insulin sensitivity and oxidative stress (Brasnyo 2011; Crandall 2012), but few have looked at markers of skeletal muscle plasticity and the SOMP. Timmers and colleagues provided some insight on this topic, after treating 11 healthy, obese men with 150mg/day resveratrol for 30 days (Timmers 2011). Following treatment, human subjects demonstrated increased SIRT1 and PGC-1α protein content in skeletal muscle (Timmers 2011). This was accompanied by increased citrate synthase activity, improved insulin sensitivity and improvements in muscle fat oxidative capacity, suggesting that resveratrol enhances mitochondrial efficiency in human subjects (Timmers 2011). Although the effects were modest, they were consistent, and substantiate some of what has been found in animal models.

The mechanisms or pathways of resveratrol action are not fully elucidated, but an increase in the expression and/or activity of PGC-1α is almost ubiquitously observed (Lagouge 2006; Barger 2008; Um 2010). Resveratrol does not directly interact with PGC-1α; instead, resveratrol influences its activity through two metabolic sensors, AMPK and SIRT1 (Canto 2010). SIRT1 is necessary for resveratrol to exert its effects on skeletal muscle morphology. Evidence for this is found using SIRT1 knockout mouse embryonic fibroblasts (MEFS), as the resveratrol-induced increases in PGC-1α expression are not observed in the absence of SIRT1 (Lagouge 2006). Price and colleagues extended this to the *in vivo* context. They implemented a tamoxifen-inducible system to delete SIRT1 in adult mice (Price 2012).

This inducible strategy is significant because it circumvents many of the issues faced by researchers using SIRT1 knockout mice, including impaired growth and developmental abnormalities (Cheng 2003; Price 2012). Using this model, they discovered that the effects of moderate doses of resveratrol on mitochondrial biogenesis, mitochondrial function, AMPK activation and the NAD+/NADH ratio, were entirely dependent upon SIRT1 (Price 2012). In addition, overexpression of SIRT1 replicates the effects of resveratrol on mitochondrial function and AMPK activation, reinforcing the importance of SIRT1

Activation of AMPK results in many of the same effects in skeletal muscle that are seen following resveratrol treatment, including glucose uptake, fatty acid oxidation, and mitochondrial biogenesis (Jorgensen 2006). Add this to the fact that AMPK can directly influence PGC-1α activity through phosphorylation events (Jorgensen 2006), and it becomes difficult to ignore the possible relationship between resveratrol and AMPK. Um and colleagues examined this potential pathway in AMPK-deficient mice and AMPK knockout MEFS (Um 2010). They discovered that resveratrol-induced increases in glucose tolerance, endurance, PGC-1α expression, mitochondrial enzyme activity, and mtDNA content were abolished in the knockout strains, suggesting that AMPK is required for resveratrol's effects on muscle physiology (Um 2010). This dependency of resveratrol action on the presence of AMPK has been replicated in other studies as well (Canto 2010; Do 2012; Park 2012).

Thus, it appears that resveratrol can elicit changes in muscle morphology towards the slower, more oxidative phenotype by activating PGC-1α through a pathway involving SIRT1 and AMPK activation. However, at the commencement of this study it was unknown whether resveratrol could achieve this and induce utrophin A expression in animal models for Duchenne muscular dystrophy.

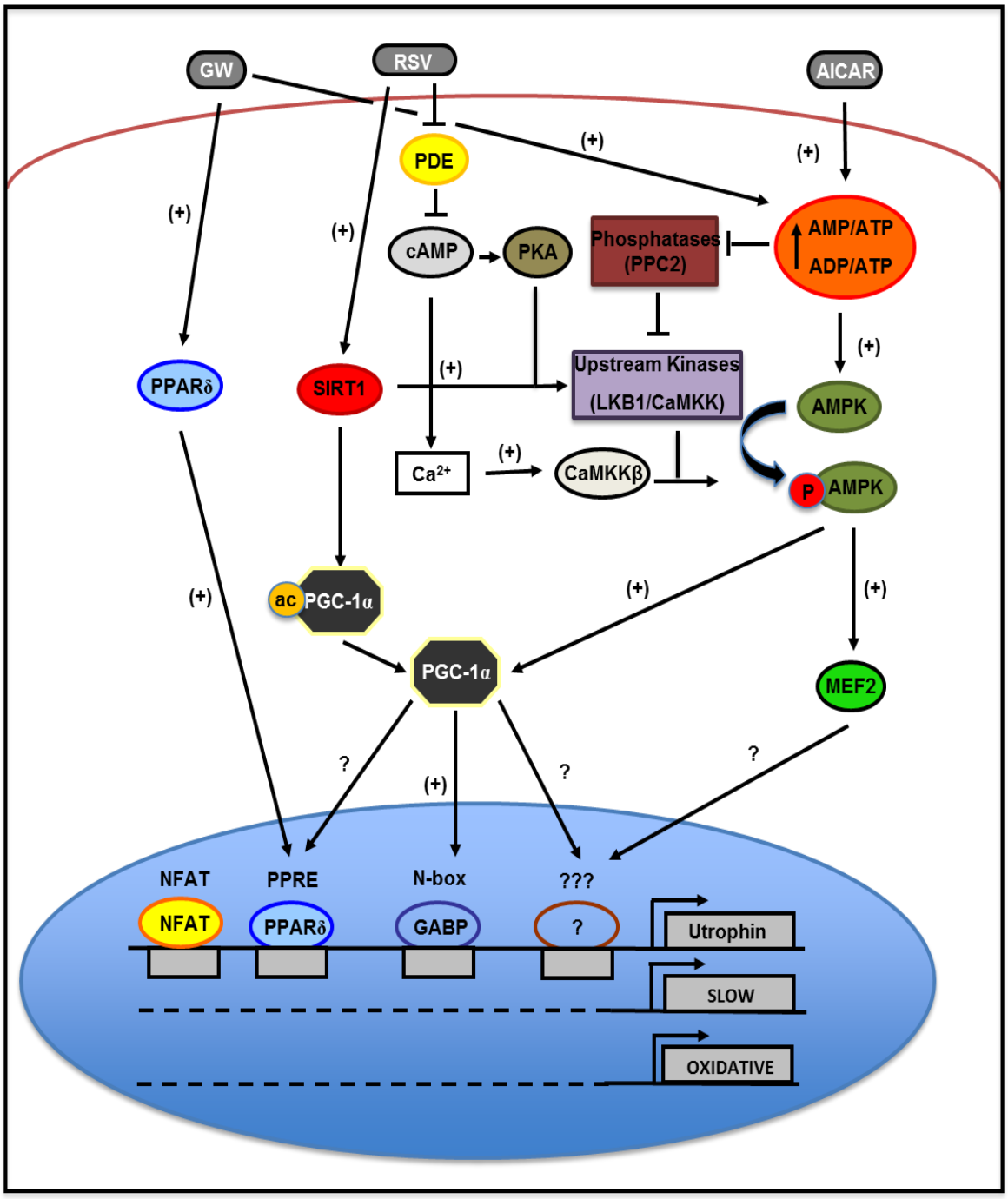

Figure 1.5 – Pharmacological-induced promotion of the SOMP and utrophin A expression in skeletal muscle cell

GW501516 (GW), resveratrol (RSV) and AICAR all carry the putative ability to activate genes involved in regulating the SOMP. PGC-1α, often labeled the master regulator of the SOMP, is a converging target of RSV and AICAR. GW acts as a PPARδ agonist but also influences the energy state of the cell. Each small molecule has a unique mechanism of action. However, there is considerable cross-talk between the pathways.

1.8 Statement of Problem

DMD is a lethal neuromuscular disease that is the result of a lack of functional dystrophin. Although there is no cure, pre-clinical trials have demonstrated that utrophin A has the ability to compensate for the absence of dystrophin in dystrophic muscle fibres (Tinsley 1998; Blake 2002; Jasmin 2002). Thus, making a determination of the factors that influence utrophin A expression patterns and localisation has been of utmost importance. In recent years, several papers have emerged demonstrating that slow-twitch, oxidative myofibres possess a greater utrophin A content, and enriched levels of utrophin A in extra-synaptic regions, as compared to their faster, more glycolytic counterparts (Gramolini 2001b; Chakkalakal 2003). Interestingly, these slower, more oxidative muscle fibres are also more resistant to the dystrophic pathology (Webster 1988). In light of these findings, our lab has made a focus of identifying clinically-approved small molecules capable of promoting the SOMP and triggering utrophin A expression (Miura 2009; Ljubicic 2011).

1.9 Hypothesis

Based on previous findings that resveratrol-induced activation of SIRT1 and downstream PGC-1α promotes the SOMP (Lagouge 2006; Um 2010; Timmers 2011; Price 2012), we hypothesize that chronic administration of resveratrol to *mdx* mice will prevent the progression of the dystrophic pathology and trigger utrophin A expression.

1.10 Objectives

To this end, our main objectives are as follows:

1) Determine whether resveratrol activates key phenotypic modifiers of the SOMP, as well as utrophin A expression in C2C12 cells.
2) Characterize the effects of chronic resveratrol treatment on the expression and activity of phenotypic modifiers of the SOMP and utrophin A expression and localization in *mdx* mice. Furthermore, evaluate whether there is evidence of a fibre-type conversion with treatment and whether these changes translate to improvements in central nucleation and fibre size variability.
3) Compare the effectiveness of an elevated dose of resveratrol to a moderate dose of resveratrol

2: Materials and Methods

2.1 Muscle cell culture treatment

Mouse C2C12 muscle cells (American Type Culture Collection, Manassas, VA) were cultured as described previously (Ljubicic 2011). Briefly, cells were maintained in 6-well culture dishes coated with Matrigel in DMEM, containing 10% fetal bovine serum and 1% antibiotic/antimycotic (Invitrogen, Burlington, Canada). Cells were grown in a humidified chamber at 37°C with 5% CO_2.

Cells were treated for different time periods as myoblasts or myotubes. Myoblasts were grown to 80-90% confluency before being treated with vehicle (DMSO) or resveratrol at a concentration of 50 µM (Sigma-Aldrich, Missouri, USA). They were treated for 24 h before being extracted for analyses. Myotubes were switched to DMEM, containing 5% heat-inactivated horse serum and 1% antibiotic/antimycotic, at 80-90% confluency. They were then treated for 24h, 48 h, and 72 h with DMSO or resveratrol at a concentration of 50 µM.

2.2 Animal treatment with resveratrol

All experimental protocols were approved by the University of Ottawa Institutional Animal Care Committee and were in accordance with Canadian Council of Animal Care guidelines. Six-to-seven-week-old male C57BL/10 and *mdx* mice (C57BL/10ScSn-Dmd^{mdx}/J, Jackson Laboratory, Bar Harbor, USA) were maintained in the Animal Care and Veterinary Service of the University of Ottawa, under a constant 12 h light/dark cycle. Mice were housed separately and given free access to food and water. We conducted two animal studies, which differed in the dose of resveratrol administered and the duration of the treatment period. In the first study, treated *mdx* mice were given a standard chow diet

(Harlan Research Models and Services, Wisconsin, USA), supplemented with 0.05% resveratrol (~100 mg/kg/day), for a duration of six weeks (Sigma-Aldrich, Missouri, USA).This is considered a moderate dose and short duration (**MDSD**). The control mice groups were fed a standard control diet without resveratrol, but their food had undergone the same process as the reconstituted chow, in order to maintain consistency. Following the six week treatment period, the tissues were harvested, and immediately frozen in liquid nitrogen, or in melting isopentane cooled with liquid nitrogen for histological and immunofluorescence analyses. For the second treatment protocol, treated *mdx* mice were given a standard control diet, supplemented with 0.375% resveratrol (~500 mg/kg/day), for a duration of 12 weeks. This is considered a high dose and a long duration (**HDLD**).

2.3 mRNA analysis

Total RNA was isolated from muscle and C2C12 cells using TRIzol reagent (Invitrogen, Carlsbad, USA) and treated with DNAse I (Fermentas, Burlington, Canada) to eliminate possible DNA contamination. Reverse transcription (RT) was performed using an RT mixture containing 5 mM MgCl2, 1x PCR buffer, 1 mM dNTP, 1 U/µl RNase inhibitor, 5 U/µl MuLV reverse transcriptase, and 2.5 µM random hexamers (Applied Biosystems, CA). Diethylpyrocarbonate (DEPC)-treated water was added to RT mix to act as a negative control. RT reactions lacking MuLV reverse transcriptase were also carried out to confirm that there was no DNA contamination. Endogenous mRNAs were measured by real-time quantitative reverse transcription-polymerase chain reaction (Agilent Tech, Mississauga, Canada), and the delta CT method was used to quantify the expression of utrophin A, SIRT1, PPARδ, COXVI and PGC-1a relative to glyceraldehyde (GAPDH) or 18S, as previously described (Ljubicic 2011).

2.4 Protein extraction and immunoblot analyses

Frozen muscle sections were ground to a powder with mortar and pestle on dry ice. Proteins were extracted from powdered muscles by homogenization at 4°C in RIPA buffer (Sigma-Aldrich, Missouri, USA), supplemented with cOmplete Mini Protease Inhibitor Cocktail and PhosSTOP (Roche, Laval, Canada). Homogenates were centrifuged at 12,000 *g* for 12 min at 4°C, and supernatants were collected and stored at -80°C. Protein concentration was determined using the Bio-Rad DC Protein Assay kit. For Western blotting, 50-100 μg of proteins were resolved by sodium dodecyl sulfate–polyacrylamide gel electrophoresis (6–8% polyacrylamide) and subsequently transferred to nitrocellulose membranes (Bio-Rad, Mississauga, Canada). Equal gel loading was checked by staining membranes with Ponceau S (Sigma-Aldrich). Membranes were subsequently washed with 1× TBST [Tris-buffered saline Tween 20: 25 mM Tris–HCl (pH 7.5), 1 mM NaCl and 0.1% Tween 20] and blocked (1 h) with a 5% skim milk in TBST solution. Blots were then incubated in blocking solution with an antibody directed against utrophin A (Novocastra), PGC-1a (Abcam ab72230), SIRT1 (Millipore 09-844, Temecula, USA), MHCI (Dr. Jean-Marc Renaud Laboratory, University of Ottawa, Canada), AMPKα (New England Biolabs 2532, Pickering, Canada), GAPDH (Advanced ImmunoChemical 2-RGM2 6C5, Long Beach, USA), β-actin (Santa Cruz Biotechnology) overnight at 4^{o}C with gentle agitation. After 3 × 5 min washes with TBST, blots were incubated at room temperature (1 h) with the appropriate secondary antibody coupled to horseradish peroxidase. Blots were then washed again 3 × 5 min with TBST, followed by visualization with enhanced chemiluminescence (Western Lightning ECL, PerkinElmer, Woodbridge, Canada). Films (CL-X Posure, Thermo Scientific, Rockford, USA) were then scanned and analyzed using ImageJ (NIH).

2.5 PGC-1α immunoprecipitation

Proteins extracted from the gastrocnemius muscle homogenates were incubated with an anti-PGC-1 antibody (H-300, Santa Cruz) overnight at 4°C. Complexes were immunoprecipitated using protein G Sepharose (Sigma Aldrich, St Louis, MO) for 4 hours at 4°C and then washed with RIPA buffer, supplemented with protease and phosphatase inhibitors. Western blotting was then carried out using an acetyl-lysine antibody (Cell Signaling, Massachusetts, USA) (Lagouge 2006).

2.6 SIRT1 activity

SIRT1 activity was measured using a SIRT1 fluorometric assay kit (BIOMOL, Plymouth Meeting, Pennsylvania, USA) as described by the manufacturer. Briefly, 25 μg of skeletal muscle protein homogenate was incubated with 15 μl of Fluor de Lys-SIRT1 substrate (100 μM) and NAD+ (100 μM) and assay buffer for 30 min at 37◦C. The reaction was then stopped by the addition of a mixture of 50 ml of developer reagent and nicotinamide (2mM). The fluorescence was subsequently measured at 360 nm (excitation) and 460 nm (emission).

2.7 Assessment of muscle fibre central nucleation and size

Cross-sections (10 μm) of EDL and soleus muscles were stained with hematoxylin and eosin, dehydrated through a series of alcohol solutions, cleared with xylene and mounted using Permount (Fisher Scientific, Ottawa, Canada). The extent of central nucleation was determined by counting the number of muscle fibres and those with centralized myonuclei from four 10× cross-sectional views of myofibres from the mid-belly of the muscle, facilitated by Northern Eclipse Software (NES; Empix Imaging, Mississauga, Canada). CSAs for each individual fibre were also measured using NES.

2.8 MHC immunofluorescence

Immunofluorescent fibre-type analysis was performed using undiluted antibodies to detect MHC I, MHC IIa and MHC IIb (Dr. Jean-Marc Renaud Laboratory, University of Ottawa, Canada). Cross-sections (10 μm) were double-stained with a polyclonal anti-laminin antibody at 1:1000 dilution (Sigma-Aldrich, St Louis, USA) to permit identification of individual fibre boundaries and detection of extracellular matrix surrounding the sarcolemma. Secondary detection was performed using appropriate FITC-conjugated anti-mouse antibodies and/or a TRITC-conjugated anti-rabbit antibody. High-resolution 10× views of the cryosections were used for counting, and NES and ImageJ were used to quantify the percentage of fibres that were MHC-positive.

2.9 Utrophin A immunofluorescence

For immunofluorescence analysis of utrophin A, images were acquired at 20× magnification on a Zeiss Axioshop-2 microscope. Muscle cryosections were stained with monoclonal utrophin A (Novocastra NCL-DRP2, Newcastle upon Tyne, UK). Immunostaining was performed on the EDL, TA, and soleus muscles at the same time for all experimental groups in order to minimize variability in background fluorescence intensity. For each animal, three fields of view were analyzed per cross-section obtained from the midbelly of the EDL and soleus muscles. Quantification of the fluorescence intensity was performed using NES and ImageJ (NIH).

2.10 Ex vivo EC protocol

The EC protocol was performed on the EDL muscles from WT mice on a control diet, *mdx* mice fed a control diet and *mdx* mice fed a diet supplement with resveratrol, as described previously (Ljubicic 2011; Miura 2009). Essentially, one tendon was attached to a

Cambridge ergometer (model 300, Aurora Scientific, Aurora, Canada), whereas the other was affixed to a metal pin, and muscles were continuously superfused by physiological saline solution containing 0.1% procion orange dye (Sigma-Aldrich) at 15 ml/min and maintained at 25°C. Prior to the ECs, muscle length was adjusted to give maximum force output, and subsequently muscles were allowed to equilibrate for 30 min. Following equilibration, the EDL muscle was subjected to a set of five maximal twitch contractions (10 V, 0.3 ms square pulse) every 100 s for the determination of contractile kinetics. Next, an EC protocol was employed consisting of 12 ECs applied at 1 min intervals. For each EC, force was elicited with a 700 ms train duration of supramaximal 10 V, 0.3 ms square pulses at 200 Hz (model S88, Grass Technologies, West Warwick, USA) with a 10% lengthening at a velocity of 0.5 Le/s applied during the last 200 ms. Force was recorded using a Keithley data acquisition board (model KPCI-3104, Cleveland, USA) at a sample rate of 5 KHz throughout the experiment. Following the contraction protocol, cross-sections from the mid-belly of EDL muscles were examined at 10× magnification for intracellular green fluorescence, indicative of procion orange dye infiltration into the core of the muscle. The fibres around the periphery of the EDL section were omitted from this analysis due to the potential for myofibre damage artifact caused by the muscle excision process.

2.11 Statistical analysis

The data were analyzed using paired and unpaired Student's t-tests as appropriate. Statistically significant distinctions between groups represented in the graphs depicted as fold differences are computed using the raw data sets prior to conversion to the fold difference values. Significance was accepted at $P < 0.05$.

3: Results

3.1Utrophin A mRNA levels increase with resveratrol (RSV) treatment in C2C12 cells

The first part of our study focused on characterizing the effects of resveratrol treatment in C2C12 skeletal muscle cells. More specifically, we wanted to confirm the beneficial changes on skeletal muscle plasticity that have been shown previously in different contexts (Lagouge 2006; Um 2010). We decided to implement the C2C12 mouse cell line due to the fact that it has been used with success in similar drug treatment studies and translates well to the *in vivo* setting (Miura 2009; Ljubicic 2011).

C2C12 myoblasts and myotubes were treated with 50uM resveratrol for different time periods so that we could monitor the changes in gene expression throughout muscle differentiation. The concentration of resveratrol was selected based on previous studies (Park 2007; Liu 2010; Kaminski 2012). Myoblasts at 60-70% confluency were treated for 24 hours, whereas myotubes were for 24, 48, and 72 hours. Upon completion of the time course, cells were extracted for protein and RNA analyses. Initial experiments, using qRT-PCR, showed a 1.2-1.5 fold increase in utrophin A mRNA levels in the resveratrol-treated group, as compared to the DMSO-treated cells ($n=3\text{-}4$, $P < 0.05$) (**Figure 3.1**). Similarly, both SIRT1 and PPARδ mRNA levels were also significantly increased in the resveratrol-treated group ($n=3\text{-}4$, $P < 0.05$) (**Figure 3.1**). Changes in PGC-1α mRNA levels were less consistent, but showed a slight, non-significant increase in expression ($n=3\text{-}4$, $P > 0.05$ (**Figure 3.1**). All of these genes are implicated in the slow, oxidative myogenic program and their increased expression indicates that resveratrol may be driving changes that affect skeletal muscle plasticity.

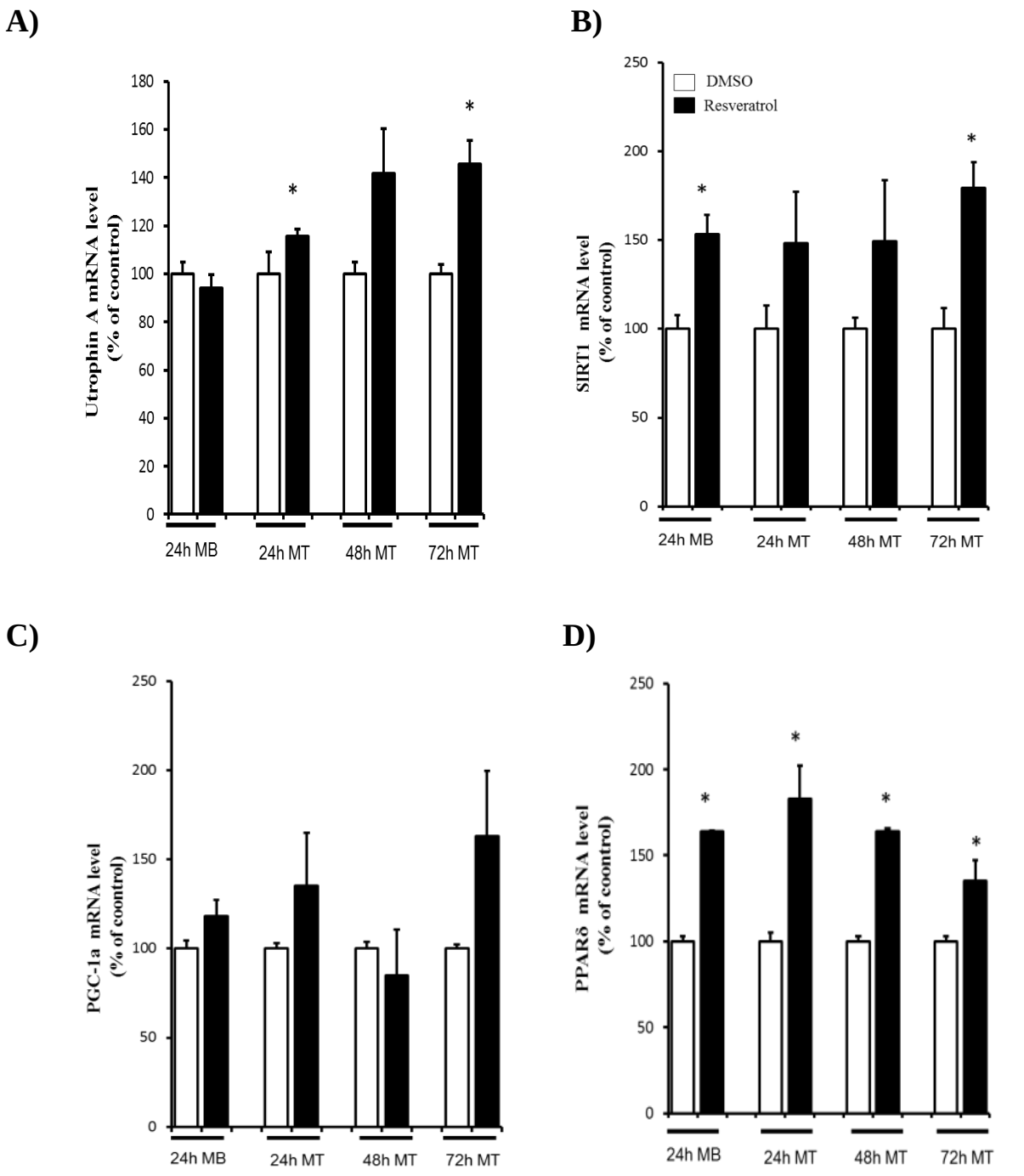

Figure 3.1 – Expression of phenotypic modifiers following resveratrol treatment in C2C12 cells

Treatment of C2C12 cells with resveratrol induces a significant increase in utrophin A, SIRT1, and PPARδ mRNA levels as measured by quantitative RT-PCR. C2C12 myoblasts (MB) were treated for 24 h with 50 μM resveratrol or a DMSO control. C2C12 myotubes (MT) were also treated with the same concentration of resveratrol for 24, 48, and 72 hours. Values were standardized to 18s mRNA levels (n=3–4, * < 0.05) Mean ± s.e.m. are shown.

The protein levels of utrophin A and PGC-1α, a putative target of resveratrol, were also evaluated by western blot. In all cases, resveratrol-treated cells had a ~40% elevation in protein content when compared to the vehicle-treated cells, but this relationship was not significant (n=3-4, $P > 0.05$) (**Figure 3.2**).

Together, the experiments *in vitro* demonstrate that resveratrol appears to be capable of activating several phenotypic modifiers that are involved in converting skeletal muscle from fast, glycolytic fibres, towards the slower, more oxidative phenotype. These pathways have been shown to trigger utrophin A expression, which can provide significant benefits in the DMD context. Based on these modest but consistent changes in mRNA and protein levels, as well as emerging literature in this field (Hori 2011; Moorwood 2011), we decided to expand the study to the *in vivo* context, specifically in *mdx* mice.

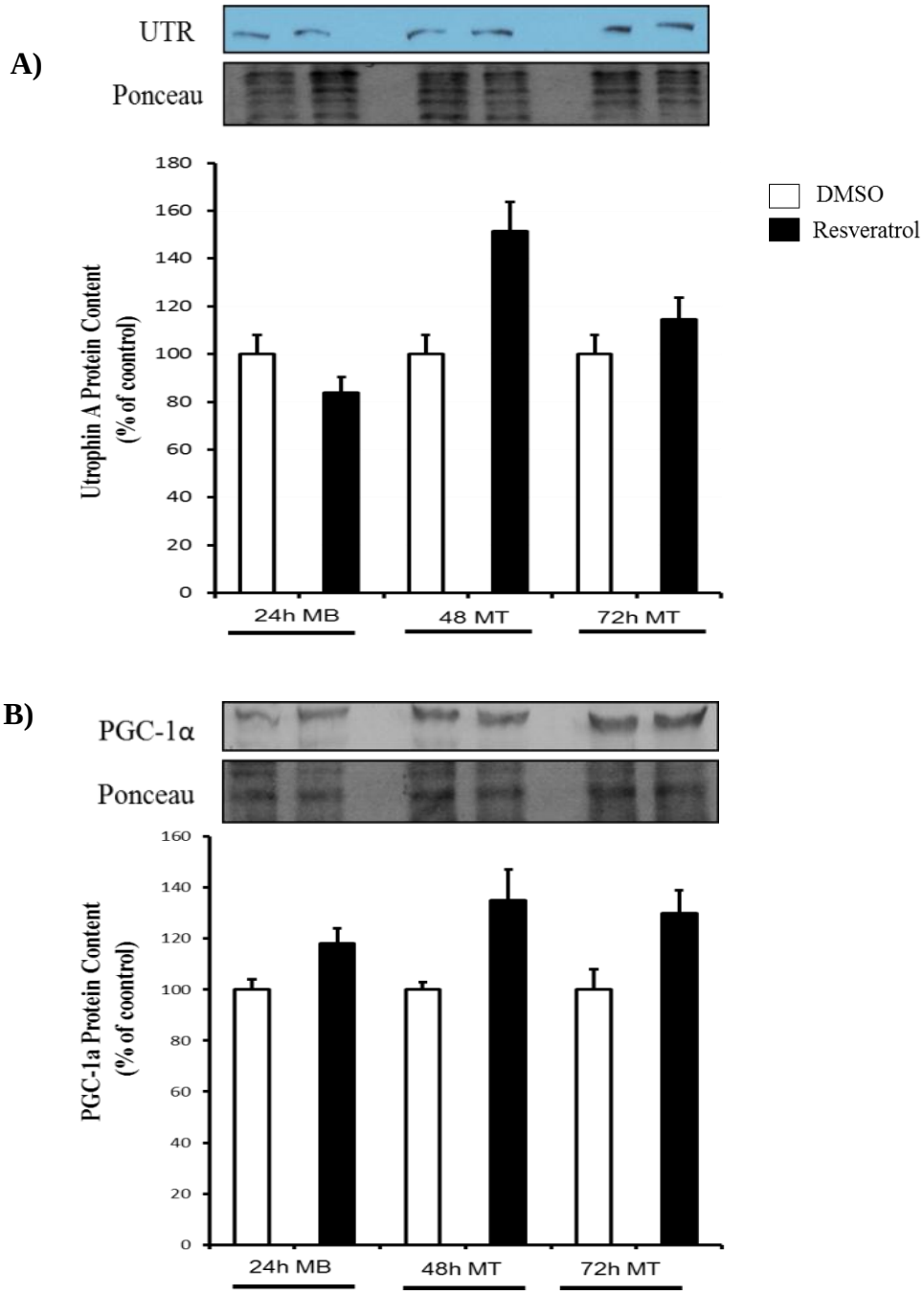

Figure 3.2 – Protein levels of UTRA and PGC-1α following resveratrol treatment

Treatment of C2C12 cells with resveratrol induces an increase in utrophin A and PGC-1α protein levels as measured by western blot analysis. C2C12 myoblasts (MB) were treated for 24 h with 50 uM resveratrol or a DMSO control. C2C12 myotubes (MT) were also treated with the same concentration of resveratrol for 48, and 72 hours. Values were standardized to ponceau-stained blots (n=3–4, * < 0.05) Mean ± s.e.m. are shown.

3.2 RSV-MDSD stimulates the SOMP in *mdx* mice

Male mice, 6-7 weeks of age, were divided into three groups based on genetic background and diet: **1)** C57BL/10 (wild-type) mice fed a standard control diet (WT-CTL), **2)** *mdx* mice fed a standard control diet (*mdx*-CTL), and **3)** *mdx* mice fed a diet supplemented with 0.05% resveratrol (~100 mg/kg/day) (*mdx*-RSV). This dosage was chosen based on previous studies (Baur 2006; Lagouge 2006; Ryan 2010). After a six-week treatment period, the mice were euthanized and their tissues removed for analysis. In order to evaluate changes in different muscle types, we focused our attention on the fast EDL muscle and the slow SOL muscle. The next few sections (**3.2.1 – 3.2.4**) concentrate exclusively on the fast, EDL muscle, unless stated otherwise.

3.2.1 RSV-MDSD activates SIRT1 and PGC-1α in fast skeletal muscle fibres of *mdx* mice

Initial experiments sought to ensure that the drug was being well received by the mice. We evaluated a number of positive controls for resveratrol, as well as phenotypic modifiers that relate to skeletal muscle plasticity. These included SIRT1 protein levels and activity, and PGC-1α protein levels and activity.

Resveratrol is considered an activator of SIRT1 (Smith 2009). The mechanism of interaction between the two has not been fully elucidated, but resveratrol has been shown to consistently upregulate SIRT1 expression and/or activity. Using western blot analysis, we show that SIRT1 protein levels exhibit a ~2-fold increase in the EDL of *mdx* mice treated with resveratrol, compared to *mdx* mice on the control diet ($n=9$, $P < 0.05$) (**Figure 3.3A**). In addition, we evaluated SIRT1 activity, using a SIRT1 fluorometric assay kit. The assay

works by measuring the fluorescence emitted when a known SIRT1 substrate is deacetylated. With this assay, we found a significant increase in SIRT1 activity in the EDL muscles of *mdx* mice treated with resveratrol (n=4-5, $P < 0.05$) (**Figure 3.3B**). This increase in SIRT1 protein levels and activity provided us with a strong positive control for the treatment group, indicating that the drug was having an effect on one of the desired phenotypic modifiers of skeletal muscle.

PGC-1α is another regulator of the slow, oxidative myogenic program, and is a downstream target of SIRT1 (Canto 2009). The activation of PGC-1α has been directly linked to phenotypic changes in skeletal muscle that are characteristic of the slower, more oxidative phenotype, including increased utrophin A expression (Lin 2002; Angus 2005; Handschin 2009). PGC-1α is regulated at the posttranslational level, as modifications including acetylation, can significantly impact its activity (Rodgers 2005). Furthermore, SIRT1 is a deacetylase enzyme, which has been shown to target PGC-1α (Lagouge 2006; Canto 2009). Therefore, we compared PGC-1α acetylation in the gastrocnemius muscle between the three groups of mice (**Figure 3.4A**). The ratio of acetylated PGC-1α protein to total PGC-1α protein was decreased 2-fold in the resveratrol-treated *mdx* mice, when compared to the *mdx* mice fed a control diet (n=4, $P < 0.05$). This lower proportion of acetylated PGC-1α in the treated group is suggestive of increased PGC-1α activity. We also evaluated PGC-1α mRNA and protein levels (**Figure 3.4B-C**). Resveratrol did not increase both mRNA and protein levels of PGC-1α, as compared to the *mdx* mice fed a control diet (n = 4-5, $P > 0.05$). This is consistent with what we observed in experiments with cultured cells.

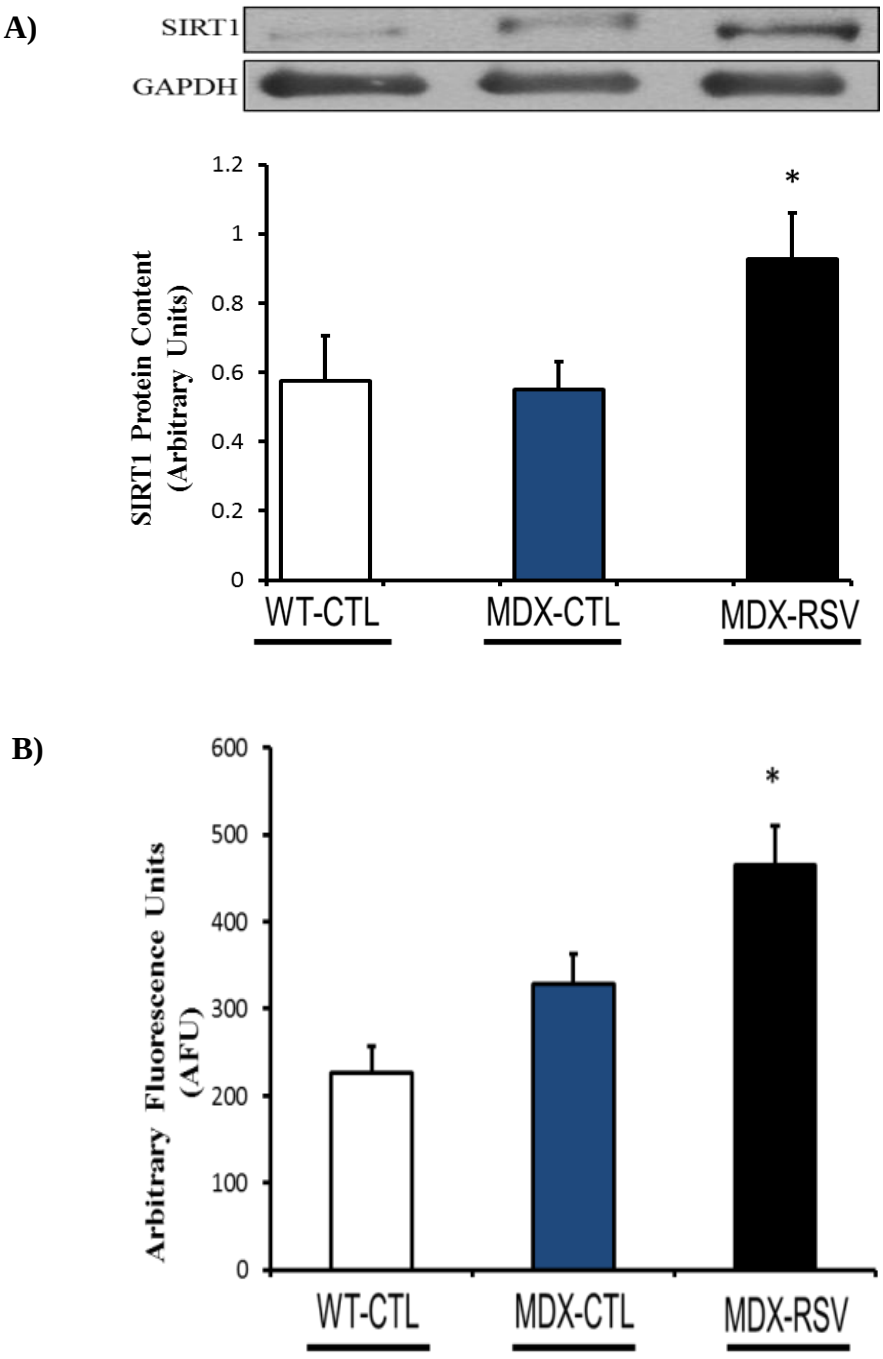

Figure 3.3 – Effects of resveratrol treatment on the protein expression and activity of SIRT1 in the EDL muscles of *mdx* mice

A) Representative SIRT1 and GAPDH western blots with quantification and **B)** SIRT1 activity, measured as arbitrary fluorescence units (AFU). Muscle extracts isolated from wild-type mice on a control diet (WT-CTL), *mdx* mice on a control diet (MDX-CTL) and *mdx* mice on a resveratrol supplemented diet (MDX-RSV) ($n = 9$, $* P < 0.05$ versus MDX-CTL). Mean $\pm$ s.e.m. are shown.

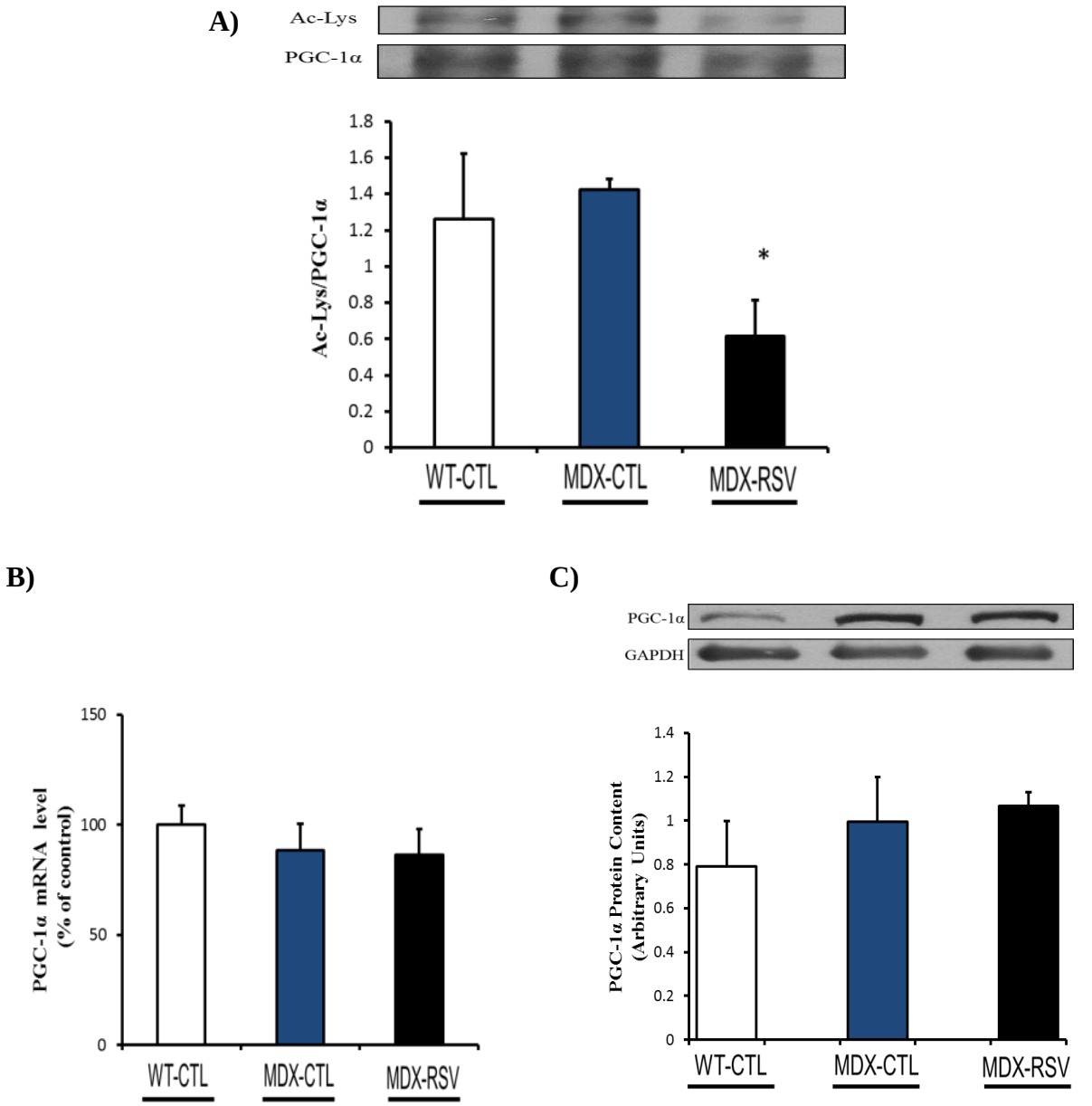

Figure 3.4 – Effects of resveratrol treatment on protein expression, mRNA expression and activity of PGC-1α in *mdx* mice

A) Representative blots and quantification showing the relative amount of acetylated versus total PGC-1α, for gastrocnemius muscle. PGC-1α was immunoprecipitated (IP) from muscle extracts and then immunoblotted with either an antiacetylated lysine antibody to determine the extent of PGC-1α acetylation (Ac-Lys) or a PGC-1α antibody to determine the total amount of PGC-1α (n = 4, $*$ P < 0.05 versus MDX-CTL) **B)** mRNA levels of PGC-1α from EDL muscles are shown, as measured by quantitative RT-PCR. Values were standardized to 18s mRNA levels. (n=3–4, P > 0.05 versus MDX-CTL). **C)** Representative PGC-1α and GAPDH western blots with quantification from EDL muscles (n = 9, P > 0.05 versus MDX-CTL). Muscle extracts isolated from wild-type mice on a control diet (WT-CTL), *mdx* mice on a control diet (MDX-CTL) and *mdx* mice on a resveratrol supplemented diet (MDX-RSV). Mean ± s.e.m. are shown.

3.2.2 RSV-MDSD treatment stimulates the SOMP in the EDL muscles of *mdx* mice

An increase in SIRT1 and PGC-1α activity generally correlates with muscle fibre-type conversion towards the slower, more oxidative phenotype, and an increase in markers for mitochondrial biogenesis. We wanted to evaluate if this was the case in our model as well. COXIV, a downstream target of PGC-1α, is involved in oxidative phosphorylation and is considered a marker for mitochondrial biogenesis (Lagouge 2006; Ljubicic 2011). The mRNA levels of COXIV were significantly increased in the fast, glycolytic, EDL muscle with resveratrol treatment (n=3-4, $P < 0.05$) (**Figure 3.5**). We also stained muscle sections with antibodies that detect myosin heavy chain (MHC) type IIa and IIb positive fibres. We discovered that these muscle sections had a much higher proportion of the slow MHC IIa isoform in the resveratrol-treated *mdx* mice, as compared to the *mdx* mice fed a control diet (n=3-4, $P < 0.05$) (**Figure 3.6**). There was also a tendency for a lowered percentage of the fast, type IIb MHC isoform in EDL muscle sections, although this difference was not considered significant (n=3-4, $P > 0.05$) (**Figure 3.6**).

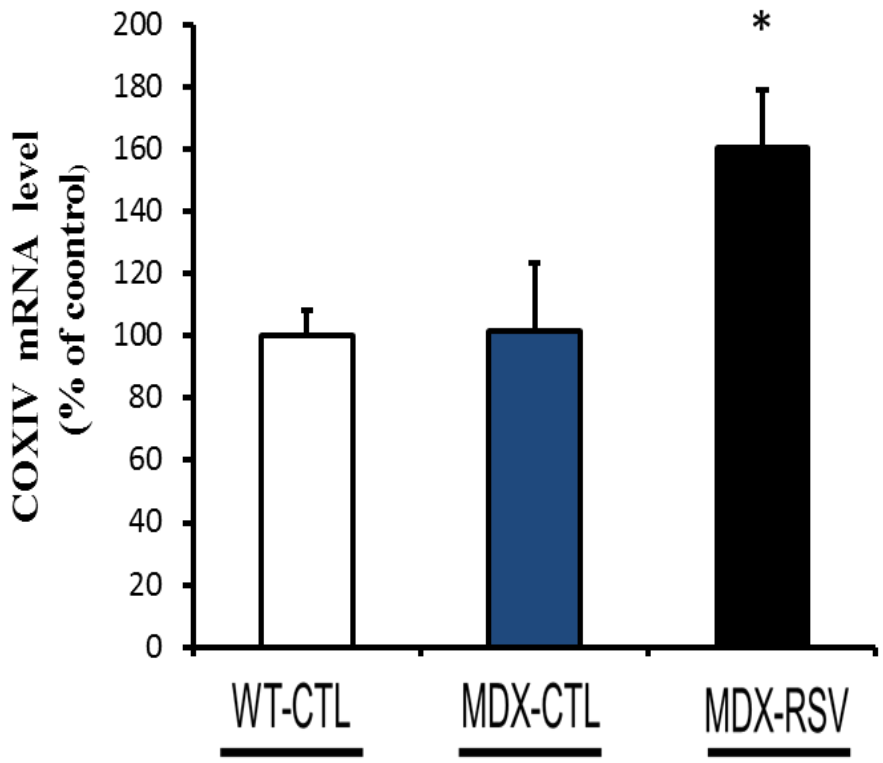

Figure 3.5 – Resveratrol treatment stimulates expression of COXIV, which is involved in promoting the slow, oxidative myogenic program, in EDL muscles of *mdx* mice

mRNA levels of COXIV are shown, as measured by quantitative RT-PCR. Values were standardized to 18s mRNA levels. Muscle extracts isolated from wild-type mice on a control diet (WT-CTL), *mdx* mice on a control diet (MDX-CTL) and *mdx* mice on a resveratrol supplemented diet (MDX-RSV) (n=3–4, * $P < 0.05$ versus MDX-CTL) Mean $\pm$ s.e.m. are shown.

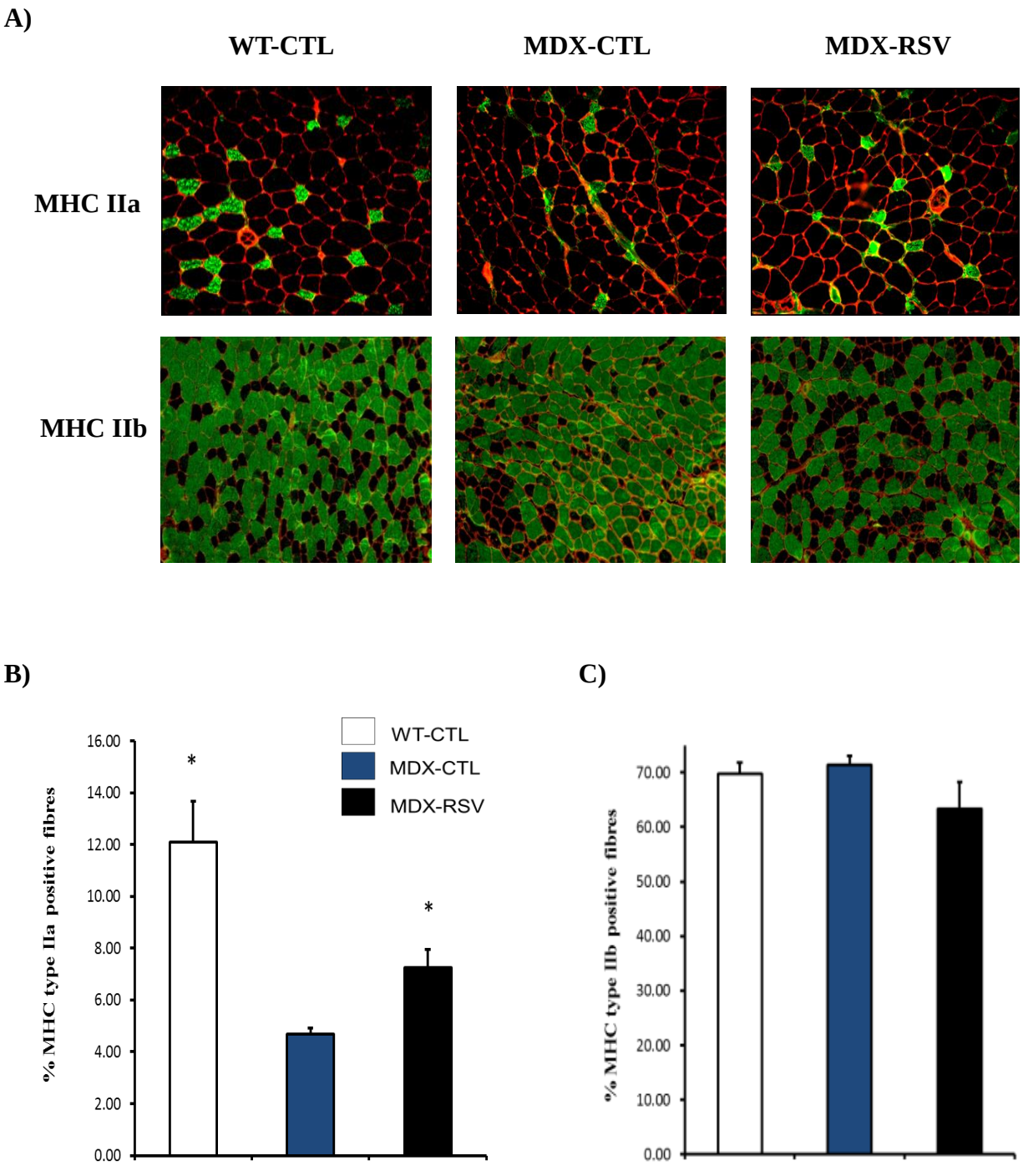

Figure 3.6 - Resveratrol treatment increases the appearance of the slow isoform of MHC in the EDL muscles of *mdx* mice

A) Representative micrographs of MHC IIa and MHC IIb immunofluorescence of EDL muscle cryosections. Graphical summaries of the percentages of (**B)** MHC IIa-positive fibres and (**C**) MHC IIb-positive fibres (n = 3-4, ∗ P < 0.05 versus MDX-CTL). Mean ± s.e.m. are shown. Red = laminin. Green = MHC-stained fibres.

3.2.3 Utrophin A mRNA levels increase in the EDL muscle of *mdx* mice treated with RSV-MDSD

Thus far, evidence suggests that resveratrol may be triggering a conversion in muscle fibre type towards the slower, more oxidative phenotype. As mentioned previously, these changes are often accompanied by increases in utrophin A expression, which is of great importance in the DMD context. Although utrophin A mRNA levels increased significantly with resveratrol treatment ($n=3\text{-}4$, $P < 0.05$), we observed a modest, non-significant increase in overall protein levels ($n=9$, $P > 0.05$) (**Figure 3.7A-B)**. This relationship is consistent with what was found in cell culture. To further understand this relationship we employed utrophin A immunofluorescence on serial cryosections of the EDL muscles. Utrophin A staining appeared slightly higher in the resveratrol treated mice, which supported our western blot analyses ($n=3\text{-}4$, $P > 0.05$) (**Figure 3.7C-D**). Therefore, there appears to be a tendency for moderate increased utrophin A expression with resveratrol treatment in *mdx* mice.

3.2.4 Histological analysis of EDL muscle sections from *mdx* mice treated with RSV-MDSD

We wanted to determine if the changes that we have observed in SIRT1 and PGC-1α activity, SOMP, and utrophin A would translate to improvements in skeletal muscle morphology in *mdx* mice. In terms of central nucleation, there was no observed difference between the resveratrol-treated and untreated *mdx* mice (**Figure 3.8A-B**). A decrease in central nucleation would indicate that the muscle fibres may be more protected from continuous cycles of degeneration and regeneration, as a result of muscle damage. We also measured the cross-sectional area (CSA) of individual fibres from the EDL muscles (**Figure**

3.8C). The untreated *mdx* mice have a greater proportion of smaller fibres than resveratrol-treated *mdx* mice. Furthermore, the resveratrol-treated *mdx* mice have a CSA profile that is much more similar to the wild-type mice. Essentially, the treated mice have a more uniform distribution of fibre size variability that closely resembles what one observes in healthy, wild-type skeletal muscle sections. This is corroborated by their similar average myofibre size and standard deviation.

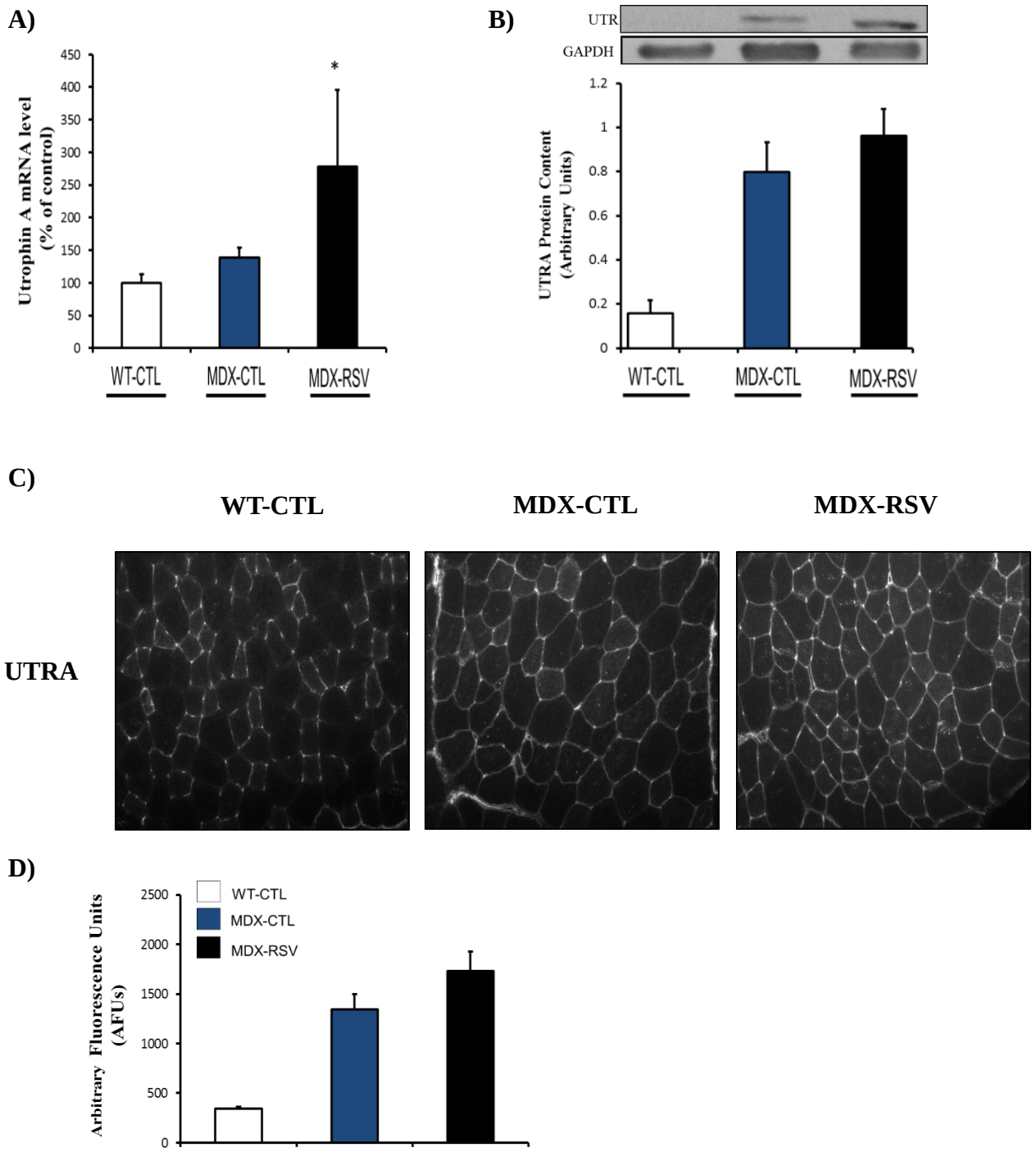

Figure 3.7 - Utrophin A expression increases with resveratrol treatment in EDL muscles of *mdx* mice

A) mRNA levels of utrophin A are shown, as measured by quantitative RT-PCR. Values were standardized to 18s mRNA levels (n=4-5, *P < 0.05 versus MDX-CTL). **B)** Representative western blots of utrophin A and GAPDH, and graphical summary of utrophin A protein content (n=9, P > 0.05). **C)** Typical micrographs of utrophin A immunostaining in EDL. **D)** Graphical summary of utrophin A fluorescence. (n= 4, P > 0.05). Mean ± s.e.m. are shown.

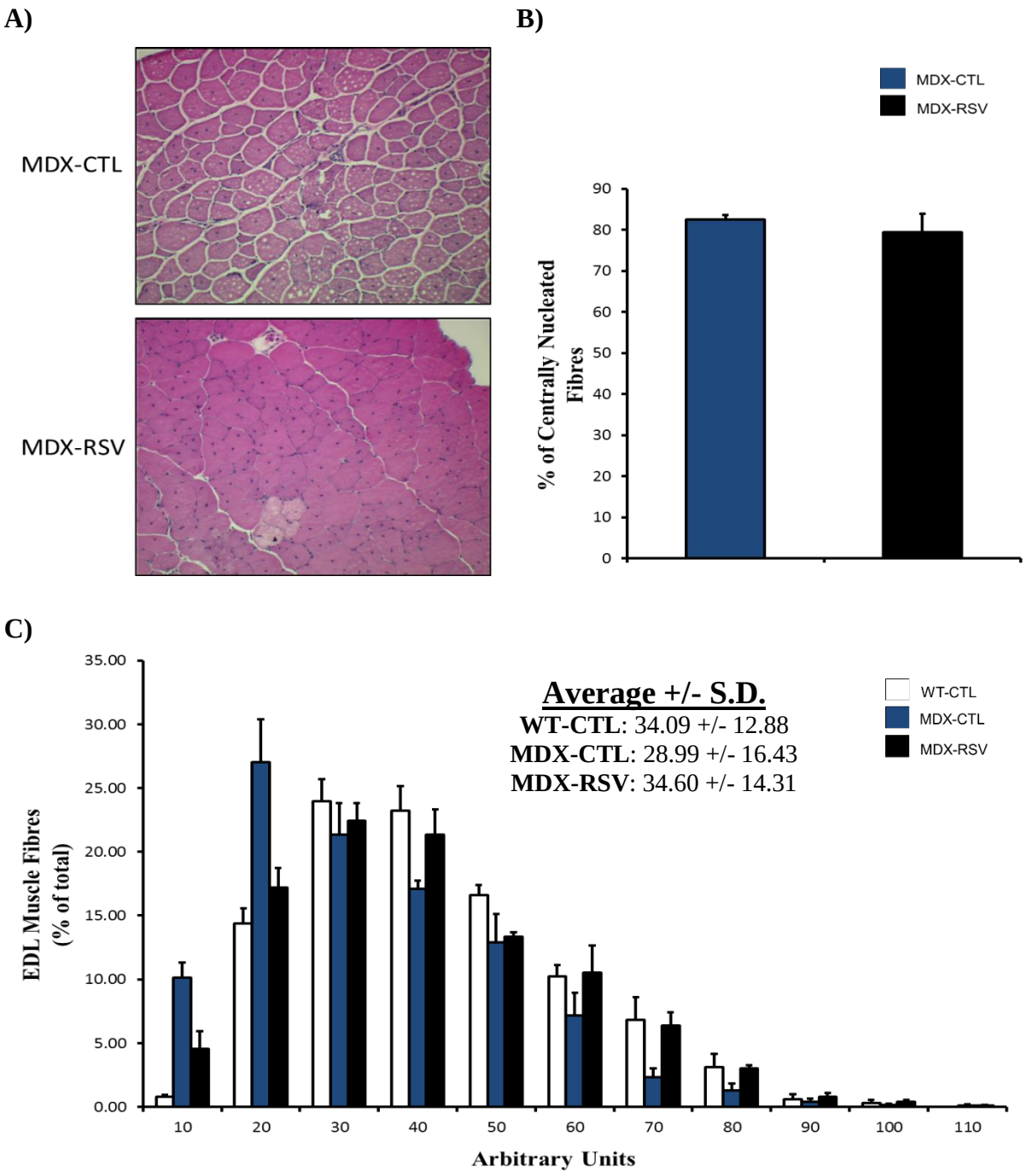

Figure 3.8 – Histological analysis of EDL muscle sections from *mdx* mice

A) H&E staining demonstrating the appearance of centrally nucleated myofibres and **B)** graphical representation of the percentage of fibres that exhibit central nucleation. **C)** Mean myofibre CSA, expressed as a percentage of the total number of fibres in EDL muscles from wild-type mice on a control diet (WT-CTL), *mdx* mice on a control diet (MDX-CTL) and *mdx* mice on a resveratrol supplemented diet (MDX-RSV) (n=4, $P > 0.05$). Mean $\pm$ s.e.m. are shown. Average CSAs (Arbitrary Units) with corresponding standard deviation of each muscle are displayed above the frequency histograms.

3.2.5 RSV-MDSD activates SIRT1 and PGC-1α in slow skeletal muscle fibres of *mdx* mice

We also analysed the slow, oxidative SOL muscles in the same manner to see if there were any changes in the activity of skeletal muscle phenotypic modifiers (**3.2.5 – 3.2.8**). Consistent with findings in the EDL muscles, both SIRT1 protein and activity were significantly increased with resveratrol treatment in the SOL muscles of *mdx* mice (n=9, * P < 0.05) (**Figure 3.9A-B**). This increase was approximately 2-fold when compared to the *mdx* mice fed a control diet **(Figure 3.9A-B**). Activation of SIRT1 often translates to deacetylation of its downstream targets, including PGC-1α. This deacetylation effect was shown previously in the gastrocnemius muscles of the resveratrol-treated *mdx* mice (n=4, * P < 0.05) (**Figure 3.4A**). PGC-1α mRNA levels in the SOL also showed a significant increase in the resveratrol-treated *mdx* mice, compared to the untreated *mdx* group (n=3-4, * P < 0.05) (**Figure 3.10A**). However, PGC-1α protein levels showed no significant difference among all three groups (n=9, * P > 0.05) (**Figure 3.10B**).

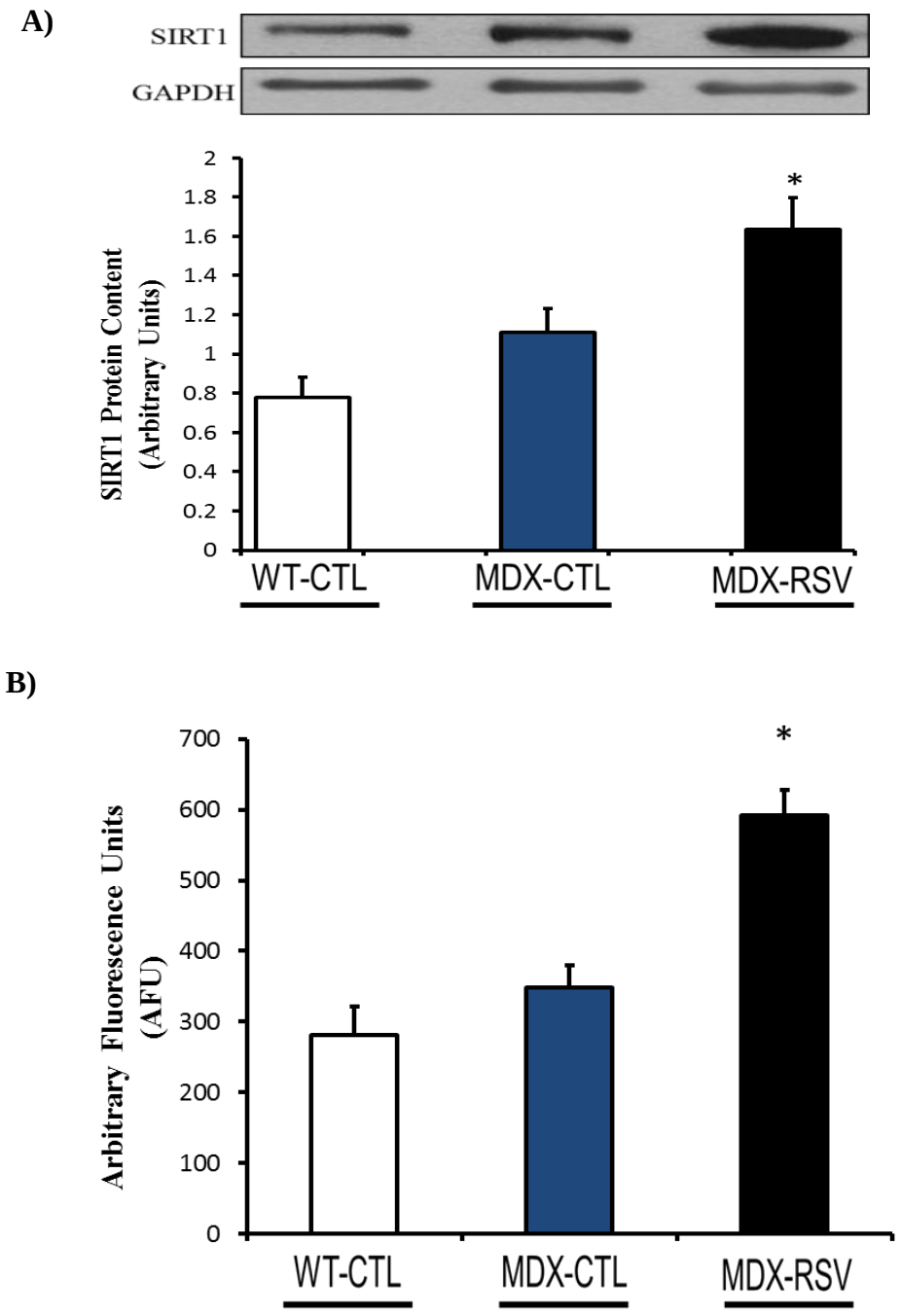

Figure 3.9 –Effects of resveratrol treatment on the protein expression and activity of SIRT1 in the SOL muscles of *mdx* mice

A) Representative SIRT1 and GAPDH western blots with quantification and **B)** SIRT1 activity, measured as arbitrary fluorescence units (AFU). Muscle extracts isolated from wild-type mice on a control diet (WT-CTL), *mdx* mice on a control diet (MDX-CTL) and *mdx* mice on a resveratrol supplemented diet (MDX-RSV) ($n = 9$, $* P < 0.05$ versus MDX-CTL). Mean $\pm$ s.e.m. are shown.

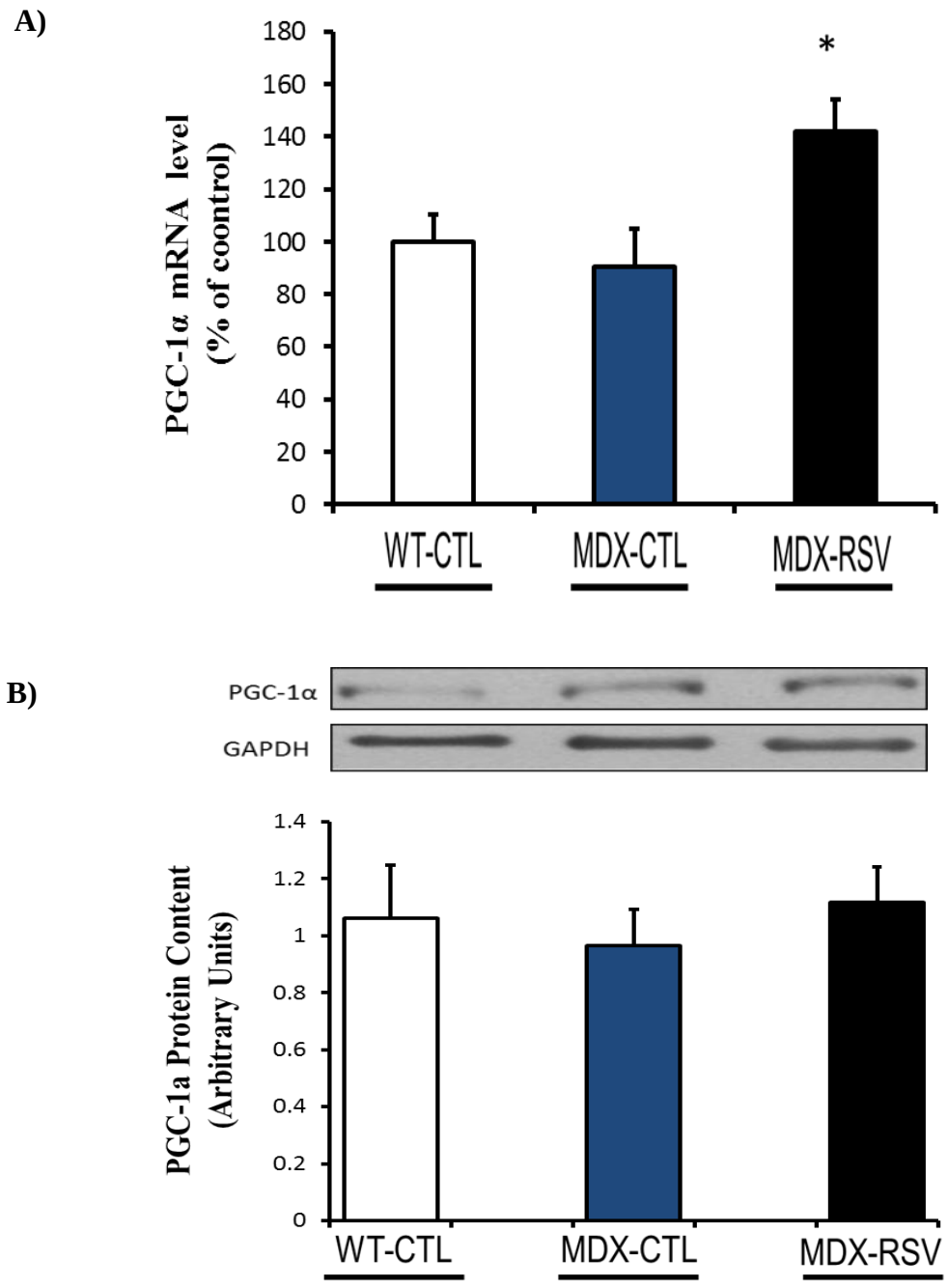

Figure 3.10 – Effects of resveratrol treatment on the protein and mRNA expression of PGC-1α in SOL muscles of *mdx* mice

A) mRNA levels of PGC-1α from SOL muscles are shown, as measured by quantitative RT-PCR. Values were standardized to 18s mRNA levels. (n=3–4, P > 0.05 versus MDX-CTL). **B)** Representative PGC-1α and GAPDH western blots with quantification from SOL muscles (n = 9, P > 0.05 versus MDX-CTL). Muscle extracts isolated from wild-type mice on a control diet (WT-CTL), *mdx* mice on a control diet (MDX-CTL) and *mdx* mice on a resveratrol supplemented diet (MDX-RSV). Mean ± s.e.m. are shown.

3.2.6 RSV-MDSD treatment stimulates the SOMP in the SOL muscle of *mdx* mice

After observing an increase in the activity of SIRT1 and PGC-1α mRNA in the SOL muscles of resveratrol-treated *mdx* mice, we analysed a number of markers that are characteristic of the slow, oxidative phenotype. COXIV, a mitochondrial enzyme, demonstrated a significant increase in mRNA levels in the SOL muscles of resveratrol-treated *mdx* mice, as measured by qRT-PCR (n=3-4, * $P < 0.05$) (**Figure 3.11**). To further evaluate whether resveratrol promoted the slow, oxidative myofibre program in *mdx* mice, we stained muscle sections with an antibody that detects myosin heavy chain (MHC) type I positive fibres. Analysis of SOL muscles revealed a ~1.5-fold increase in the percentage of slow, oxidative MHC type I fibres in the resveratrol-treated *mdx* mice compared with *mdx* mice fed a control diet (n=3-4, * $P < 0.05$) (**Figure 3.12A-B**). Western blot analysis revealed a similar trend in the MHC type I protein content. The resveratrol-treated *mdx* mice had significantly more MHC type I protein than the vehicle-treated *mdx* mice (n=4-5, * $P < 0.05$) (**Figure 3.12C**).

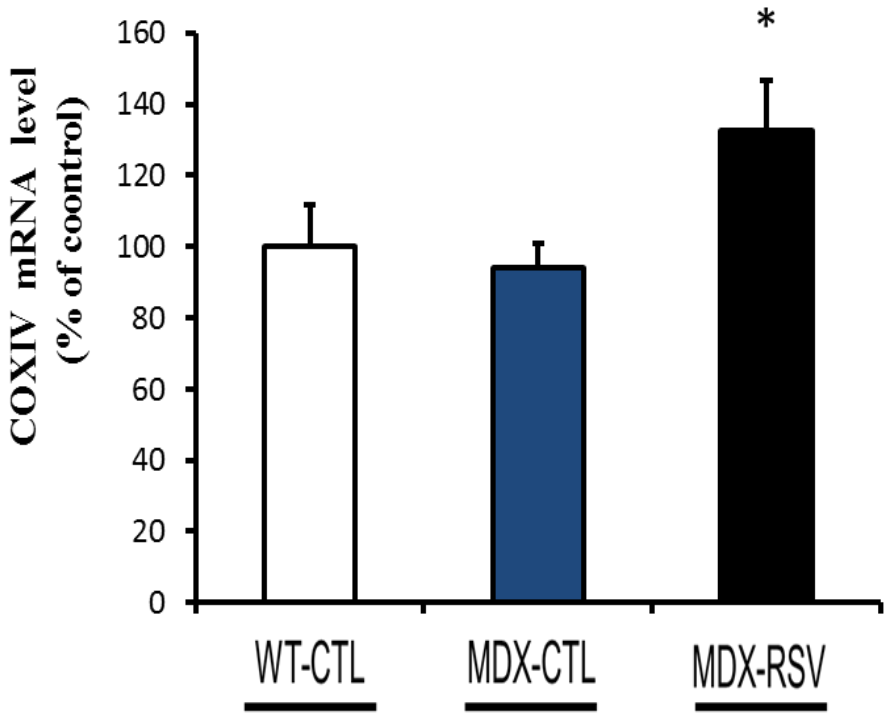

Figure 3.11 - Resveratrol treatment stimulates expression of COXIV, which is involved in promoting the slow, oxidative myogenic program, in SOL muscles of *mdx* mice

mRNA levels of COXIV are shown, as measured by quantitative RT-PCR. Values were standardized to 18s mRNA levels. Muscle extracts isolated from wild-type mice on a control diet (WT-CTL), *mdx* mice on a control diet (MDX-CTL) and *mdx* mice on a resveratrol supplemented diet (MDX-RSV) (n=3–4, * $P < 0.05$ versus MDX-CTL) Mean $\pm$ s.e.m. are shown.

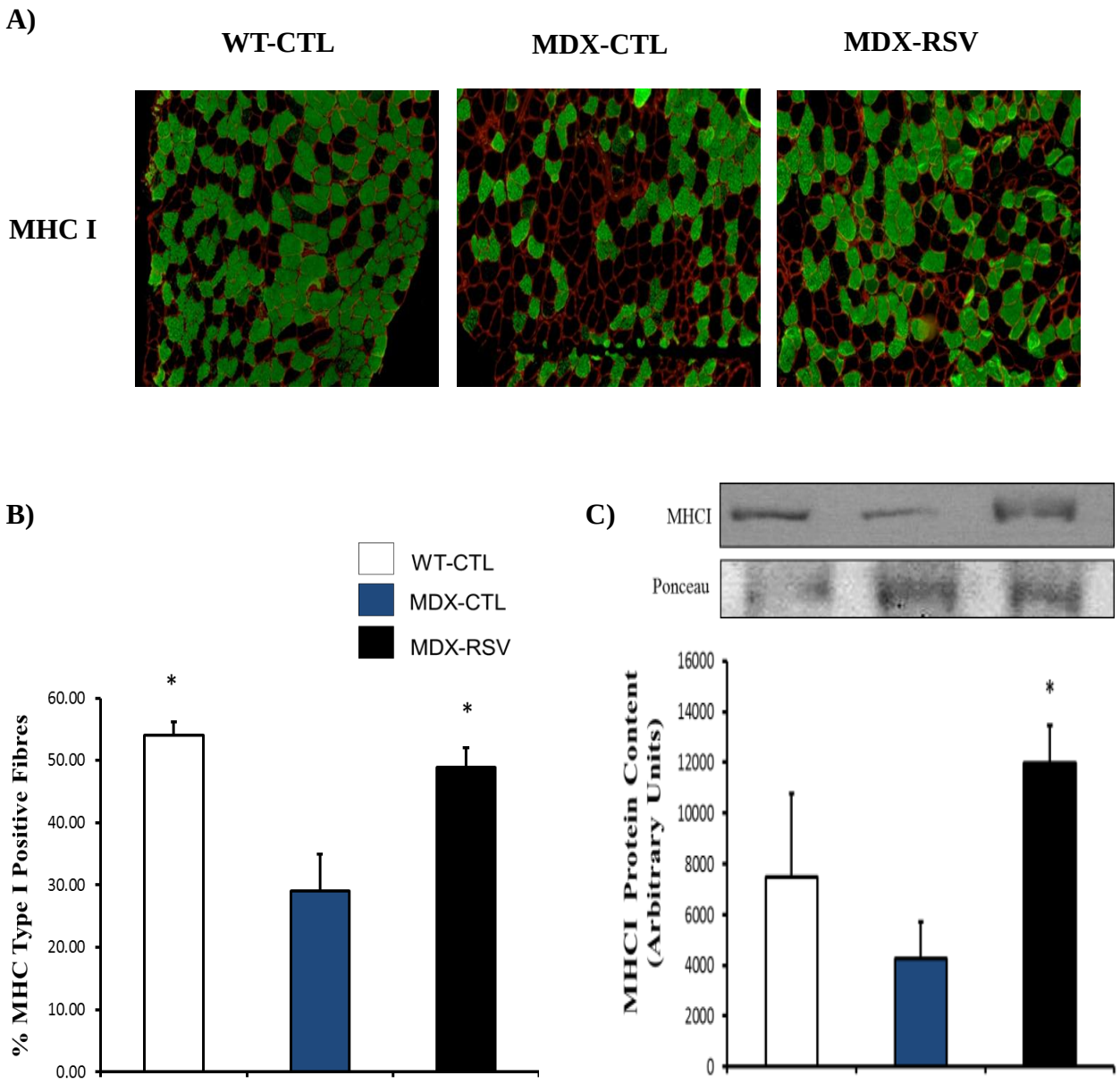

Figure 3.12 - Resveratrol treatment increases the appearance of the slow isoform of MHC in the SOL muscles of *mdx* mice

A) Representative micrographs of MHC I immunofluorescence of SOL muscle cryosections. **B)** Graphical summary of the percentage of MHC I-positive fibres (n = 3-4, ∗ P < 0.05 versus MDX-CTL). **C)** Representative blots with quantification of MHCI normalized to ponceau staining. (n=4-5, * P < 0.05 versus MDX-CTL)Mean ± s.e.m. are shown.

3.2.7 Utrophin A protein levels demonstrate a tendency to increase in the SOL muscles of *mdx* mice treated with RSV-MDSD

We measured mRNA levels, protein content and localization of utrophin A. mRNA levels exhibited no significant difference between all three mouse groups in the slow, oxidative, SOL muscle (n=3-4, $P > 0.05$) (**Figure 3.13A**). Using western blot analysis, we also observed that utrophin A protein levels were slightly higher in the SOL muscles of the resveratrol-treated *mdx* mice as compared to the vehicle-treated *mdx* mice, but this difference was not significant (n=9, $P > 0.05$) (**Figure 3.13B**). To further understand this relationship, we employed utrophin A immunofluorescence on serial cryosections of the SOL muscles. Utrophin A staining was slightly higher in the resveratrol treated mice, consistent with the changes observed in utrophin A protein levels (n=3-4, $P > 0.05$) (**Figure 3.13C-D**).

3.2.8 Histological analysis of SOL muscle sections from *mdx* mice treated with RSV-MDSD

Changes in phenotypic modifiers, specifically SIRT1, can result in morphological benefits for skeletal muscle. We examined central nucleation, as well as CSA of individual skeletal muscle fibres from the SOL muscles of *mdx* mice. This was used as a measure of the ability of the SOL to resist contraction-induced damage. Central nucleation was significantly reduced in the resveratrol-treated *mdx* mice as compared to the untreated group (n=4, $P < 0.05$) (**Figure 3.14A-B**). We also measured the CSA of individual fibres from the SOL muscles (**Figure 3.14C**). However, there were no observed differences between the *mdx* groups.

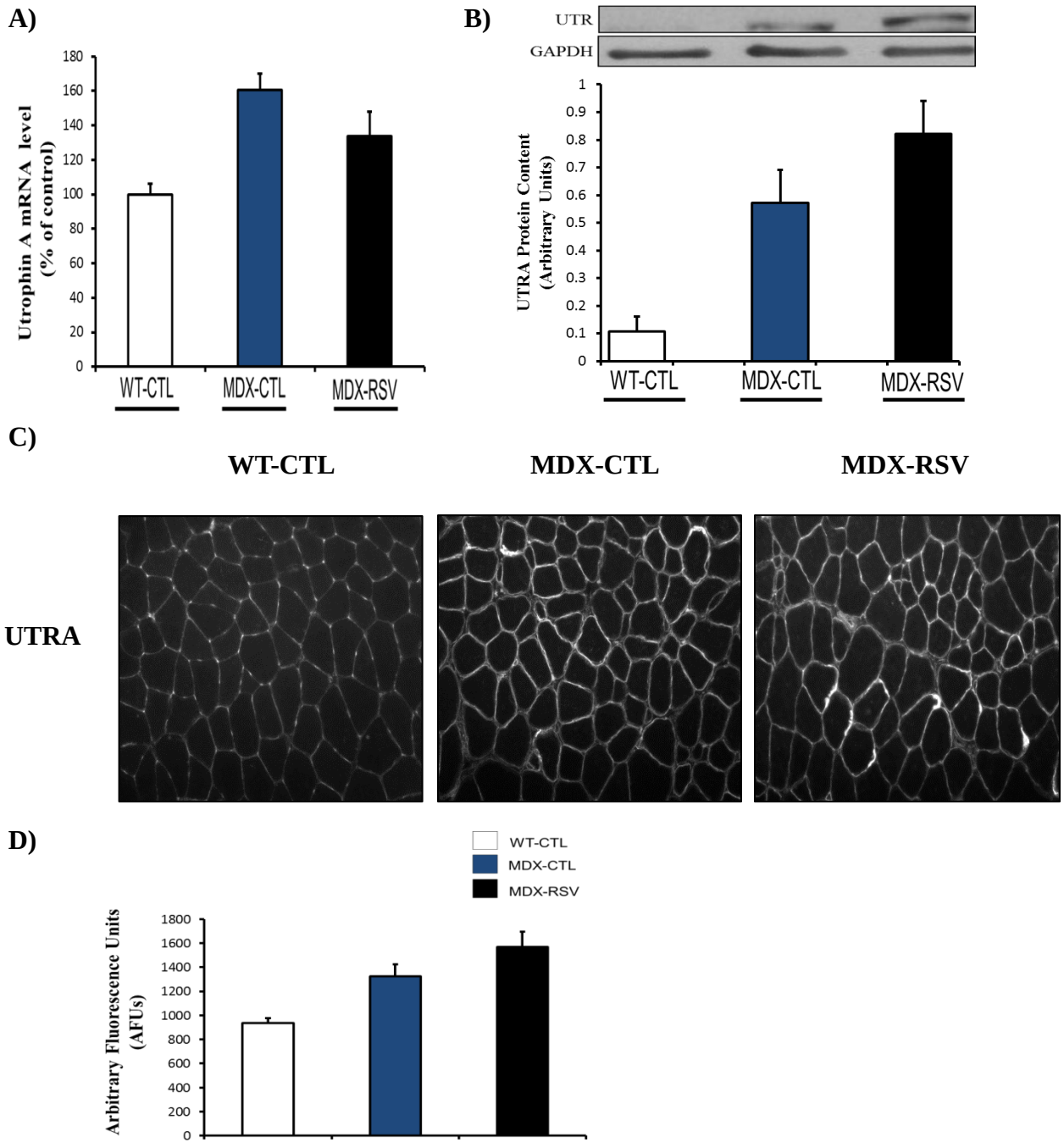

Figure 3.13 - Utrophin A expression increases modestly with resveratrol treatment in SOL muscles of *mdx* mice

A) mRNA levels of utrophin A are shown, as measured by quantitative RT-PCR. Values were standardized to 18s mRNA levels (n=4-5). **B)** Representative western blots of utrophin A and GAPDH, and graphical summary of utrophin A protein content (n=9). **C)** Typical micrographs of utrophin A immunostaining in SOL. **D)** Graphical summary of utrophin A fluorescence. (n= 4). Mean ± s.e.m. are shown.

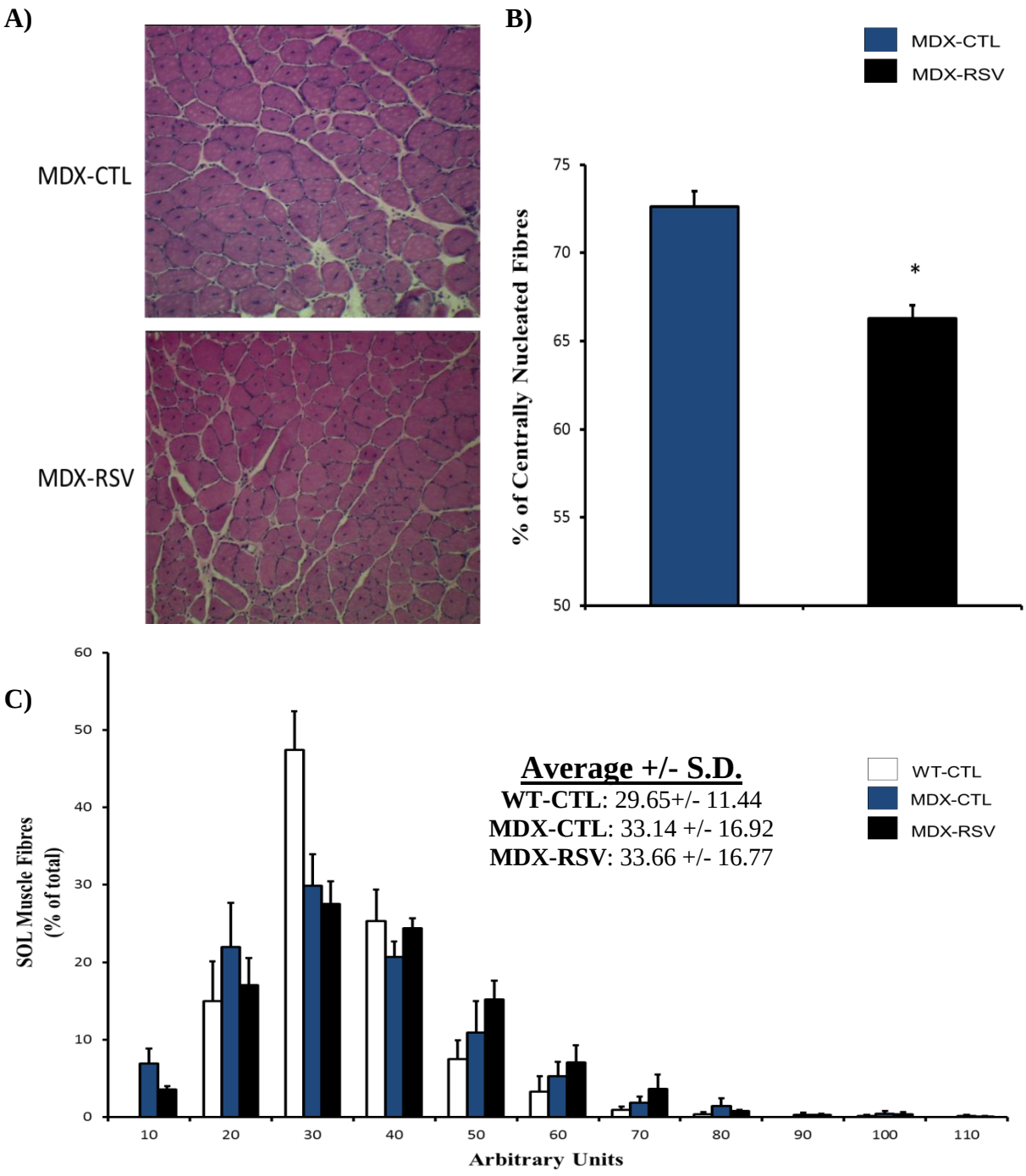

Figure 3.14 - Histological analysis of SOL muscle sections from *mdx* mice

A) H&E staining demonstrating the appearance of centrally nucleated myofibres and **B)** graphical representation of the percentage of fibres that exhibit central nucleation. **C)** Mean myofibre CSA, expressed as a percentage of the total number of fibres in SOL muscles from wild-type mice on a control diet (WT-CTL), *mdx* mice on a control diet (MDX-CTL) and *mdx* mice on a resveratrol supplemented diet (MDX-RSV) (n=4). Mean ± s.e.m. are shown. Average CSAs (Arbitrary Units) with corresponding standard deviation of each muscle are displayed above the frequency histograms.

Overall, it appears that the resveratrol treatment at a moderate dosage for a short duration (MDSD) is triggering a conversion in skeletal muscle towards the slower, more oxidative phenotype. These changes seem to be mediated through PGC-1α, which may be activated by the deacetylating action of the SIRT1 enzyme. Not only are SIRT1 protein levels elevated in the SOL and EDL of resveratrol-treated *mdx* mice, but SIRT1 activity is also significantly increased. PGC-1α protein levels demonstrate no significant change across all three groups, but the ratio of acetylated PGC-1α to total PGC-1α is significantly decreased in resveratrol-treated *mdx* mice, compared to vehicle-treated *mdx* mice. Activation of these phenotypic modifiers translates to an upregulation of several markers that are characteristic of the slow, oxidative skeletal muscle phenotype. The percentage of MHC type I- and MHC type IIa-positive fibres in the SOL and EDL, respectively, is significantly increased in the treated groups. As well, there is an increase in markers for mitochondrial biogenesis, such as COXIV expression. Utrophin A levels show a modest, but consistent increase in both the EDL and SOL of resveratrol-treated *mdx* mice. These changes result in significantly lower levels of central nucleation in the SOL and a pattern of CSA in the EDL that resembles wild-type mice. Histological changes of this nature are of benefit in the DMD context.

These results provide evidence for a resveratrol-induced conversion in skeletal muscle morphology towards the slower, more oxidative phenotype. Due to these promising results, we decided to perform an additional series of experiments and increase the dose of the drug and the duration of the treatment in an effort to yield a stronger conversion in muscle phenotype with greater benefit for muscle functionality.

3.3 RSV-HDLD does not stimulate the slower, more oxidative phenotype in *mdx* mice

In a separate series of experiments, we increased the dosage of resveratrol and the duration of the treatment. The dose was increased to ~500mg/kg/day, based on recently published papers (Hori 2011; Moorwood 2011) and the duration was extended to twelve weeks. Thus, male mice, 6-7 weeks of age, were divided into three groups based on genetic background and diet: **1)** C57BL/10 (wild-type) mice fed a standard control diet (WT-CTL), **2)** *mdx* mice fed a standard control diet (*mdx*-CTL), and **3)** *mdx* mice fed a diet supplemented with 0.375% resveratrol (*mdx*-RSV). After a twelve week treatment period the mice were euthanized and their tissues removed for analysis. In order to evaluate changes in different muscle types, we focused our attention on the fast EDL and TA muscles, and the slow SOL muscle. The next few sections (**3.3.1 – 3.3.4**) concentrate exclusively on the fast, EDL and TA muscles, unless stated otherwise. The TA muscles were used for molecular analysis due to the fact that the EDL muscles were relegated for electrophysiological experiments.

3.3.1 RSV-HDLD does not activate SIRT1 or PGC-1α in fast skeletal muscle fibres of *mdx* mice

We evaluated SIRT1 protein levels and activity in the TA muscles of all three groups of mice. We expected the higher dose of resveratrol to increase SIRT1 activity, based on past studies (Lagouge 2006; Hori 2011) and our own data from the previous sections. However, we observed no difference in both SIRT1 protein levels and SIRT1 activity between the resveratrol-treated *mdx* group and the untreated *mdx* group (n=5-6, $P > 0.05$) (**Figure 3.15A-B**). Based on these observations, one would surmise that PGC-1α activity may be unaffected

by resveratrol treatment as well because PGC-1α is a target of SIRT1's deacetylase mechanism. To evaluate the activity of PGC-1α, we compared PGC-1α acetylation in the gastrocnemius muscle between the three groups of mice (**Figure 3.16A**). The proportion of deacetylated-PGC-1α over total-PGC-1α was almost identical in both the resveratrol-treated and untreated groups, indicating that PGC-1α activity was not increased in the presence of a high dose of resveratrol (n=4, $P > 0.05$) (**Figure 3.16A**). Despite no change in activity, PGC-1α protein levels were surprisingly increased in the *mdx* mice treated with resveratrol, as compared to the *mdx* group fed a control diet (n=5-6, * $P < 0.05$) (**Figure 3.16B**).

A)

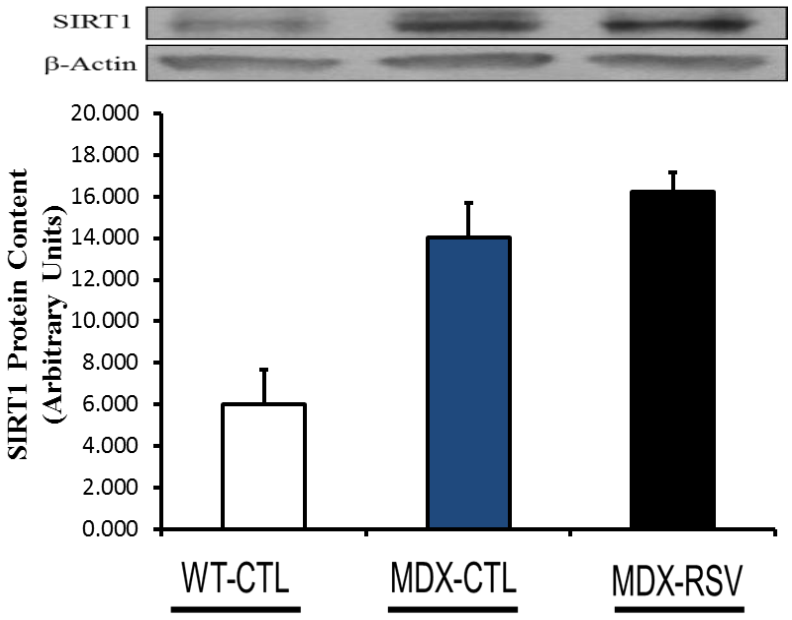

B)

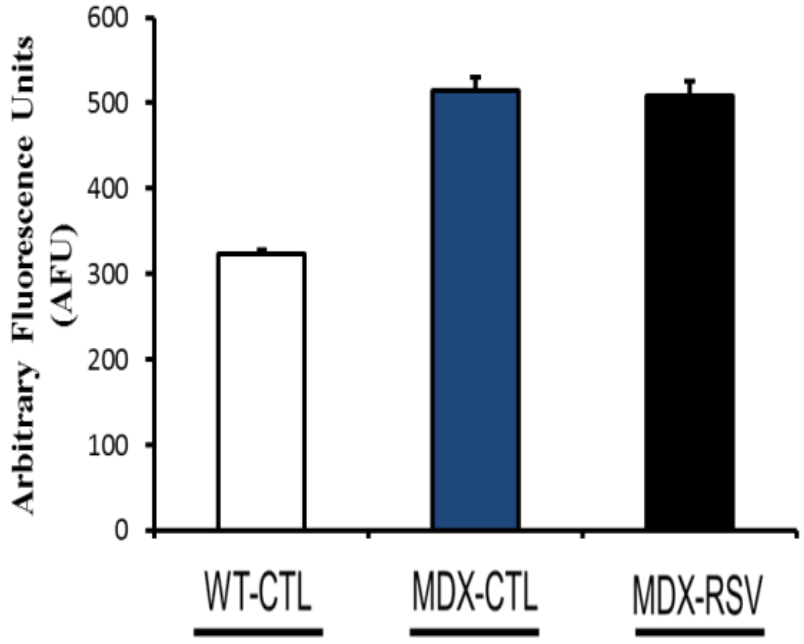

Figure 3.15 – Effects of resveratrol treatment on the protein expression and activity of SIRT1 in the TA muscles of *mdx* mice

A) Representative SIRT1 and β-actin western blots with quantification and **B)** SIRT1 activity, measured as arbitrary fluorescence units (AFU). Muscle extracts isolated from wild-type mice on a control diet (WT-CTL), *mdx* mice on a control diet (MDX-CTL) and *mdx* mice on a resveratrol supplemented diet (MDX-RSV) (n =5-6, P > 0.05 versus MDX-CTL). Mean ± s.e.m. are shown.

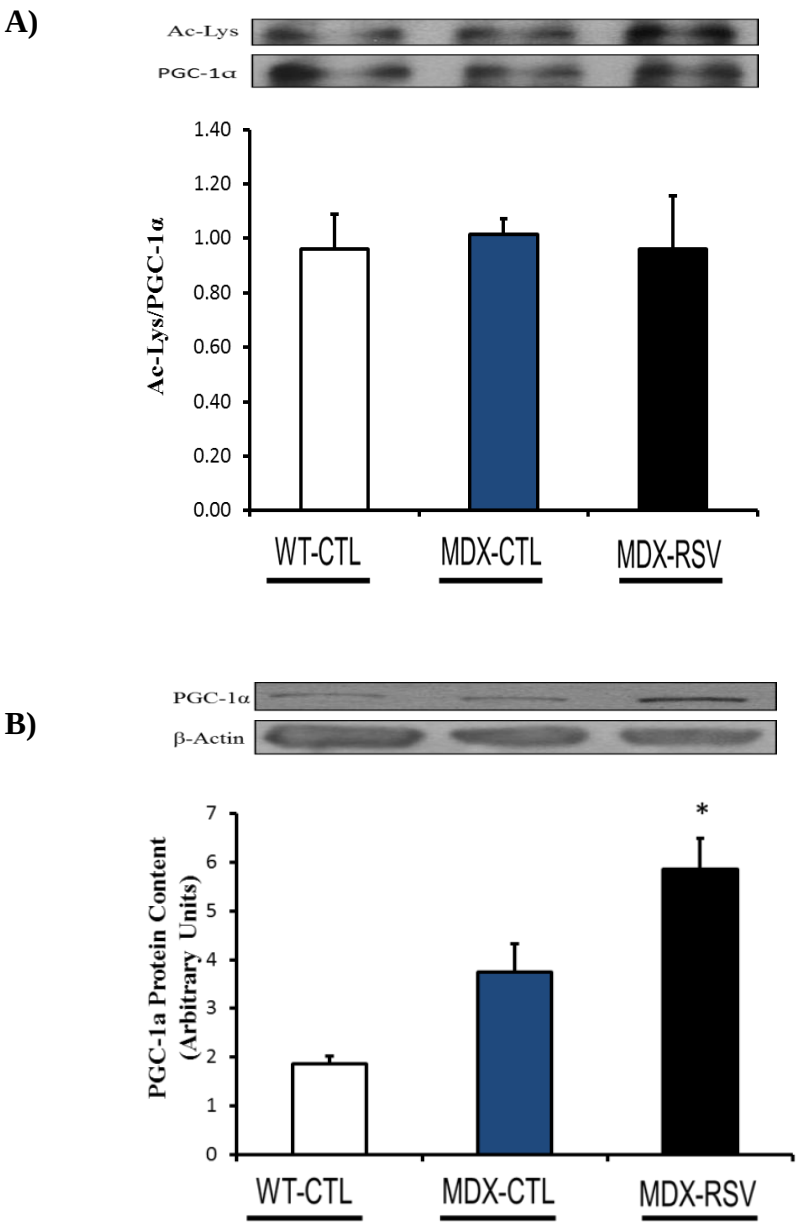

Figure 3.16 – Effects of resveratrol treatment on protein expression and activity of PGC-1α in *mdx* mice

A) Representative blots and quantification showing the relative amount of acetylated versus total PGC-1α, for gastrocnemius muscle. PGC-1α was immunoprecipitated (IP) from muscle extracts and then immunoblotted with either an antiacetylated lysine antibody to determine the extent of PGC-1α acetylation (Ac-Lys) or a PGC-1α antibody to determine the total amount of PGC-1α (n = 4, P > 0.05) **B)** Representative PGC-1α and GAPDH western blots with quantification from TA muscles (n = 5-6, * P < 0.05 versus MDX-CTL). Muscle extracts isolated from wild-type mice on a control diet (WT-CTL), *mdx* mice on a control diet (MDX-CTL) and *mdx* mice on a resveratrol supplemented diet (MDX-RSV). Mean ± s.e.m. are shown.

3.3.2RSV-HDLD has modest effects on promoting the SOMP in the fast TA muscles of *mdx* mice

We next examined some common markers that are characteristic of the slow, oxidative skeletal muscle phenotype. COXIV mRNA levels in the TA muscles were unchanged in the resveratrol-treated *mdx* group, when compared to the untreated *mdx* group (n=3-4, $p > 0.05$) (**Figure 3.17**). We also stained TA muscle sections, using antibodies designed for the detection of the slow MHC IIa isoform and the fast MHC IIb isoform (**Figure 3.18A**). We observed that the resveratrol-treated *mdx* mice had, on average, TA muscle sections with a higher proportion MHC IIa-positively stained fibres , as compared to the *mdx* mice fed a control diet (n=3-4, * $P < 0.05$) (**Figure 3.18A-B**).The treated *mdx* mice had a lower proportion of MHC IIb-positive fibres in the TA muscles, as compared to the untreated *mdx* group, but this difference was not significant (n=3-4, $P > 0.05$) (**Figure 3.18C**).

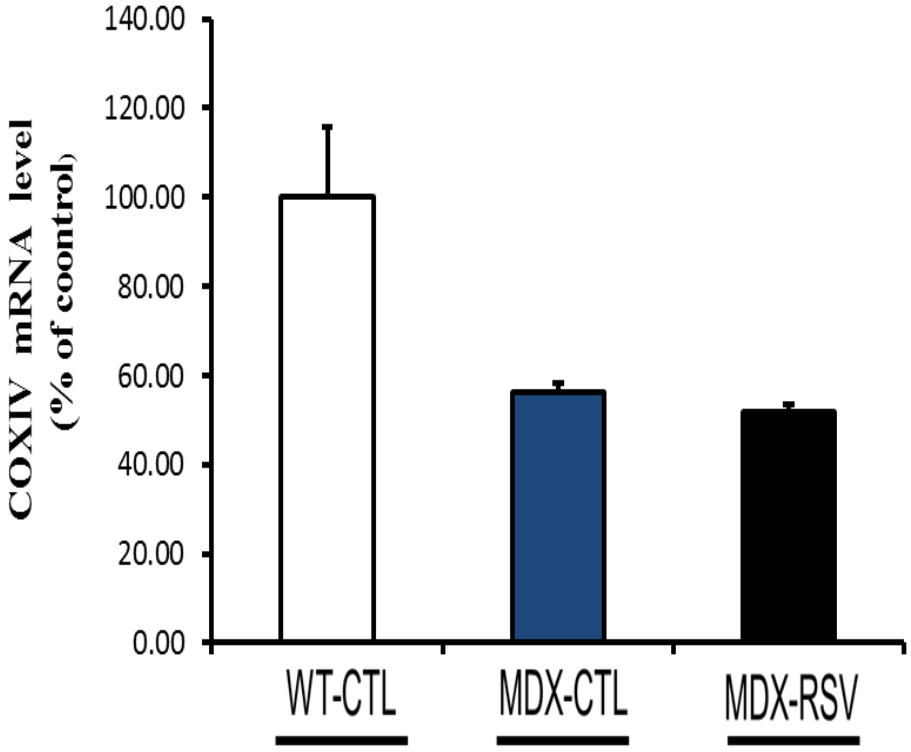

Figure 3.17 – A high dose of resveratrol does not stimulate expression of COXIV in TA muscles of *mdx* mice

mRNA levels of COXIV are shown, as measured by quantitative RT-PCR. Values were standardized to 18s mRNA levels. Muscle extracts isolated from wild-type mice on a control diet (WT-CTL), *mdx* mice on a control diet (MDX-CTL) and *mdx* mice on a resveratrol supplemented diet (MDX-RSV) (n=3–4, $P > 0.05$) Mean ± s.e.m. are shown.

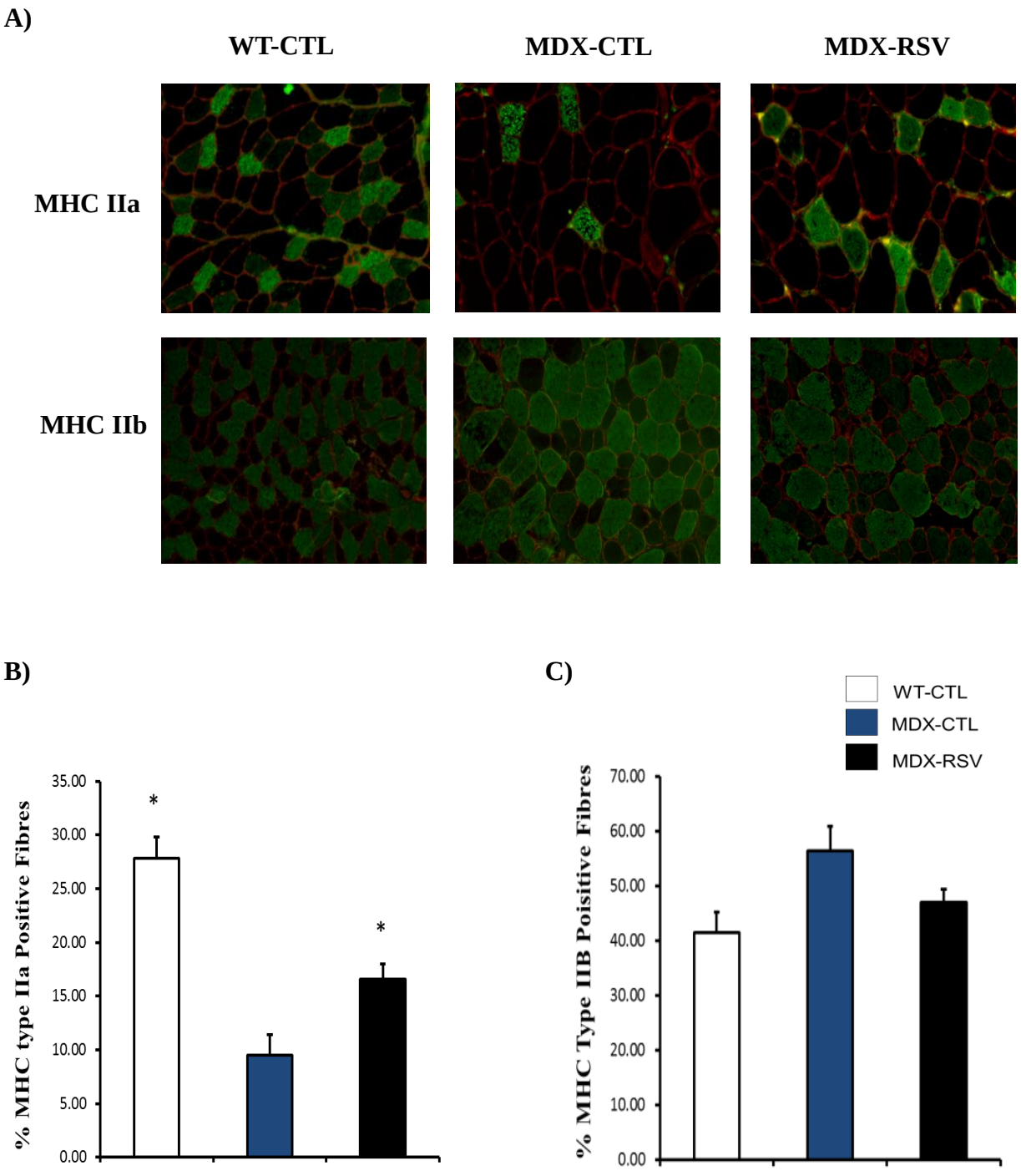

Figure 3.18 - Resveratrol treatment increases the appearance of the slow isoform of MHC in the TA muscles of *mdx* mice

A) Representative micrographs of MHC IIa and MHC IIb immunofluorescence of TA muscle cryosections. Graphical summaries of the percentage of (**B)** MHC IIa-positive fibres and (**C**) MHC IIb-positive fibres (n = 3-4, ∗ P < 0.05 versus MDX-CTL). Mean ± s.e.m. are shown.

3.3.3 Utrophin A mRNA and protein levels do not to increase in the TA muscles of *mdx* mice treated with RSV-HDLD

We analysed mRNA levels, protein content, and localization of utrophin A. Utrophin A mRNA levels showed a slight, but non-significant increase in the resveratrol-treated group as compared to the *mdx* mice on a control diet (n=4-5, $P > 0.05$) (**Figure 3.19A**). Using western blot analysis, we also observed that utrophin A protein levels increased ~25% in the TA muscles of the resveratrol-treated *mdx* mice as compared to the vehicle-treated *mdx* mice, but this difference was also non-significant (n=5-6, $P > 0.05$) (**Figure 3.19B**). Utrophin A staining increased by approximately 20% in the resveratrol treated *mdx* mice, reinforcing the lack of change in utrophin A protein levels (n=3-4, $P > 0.05$) (**Figure 3.19C-D**).

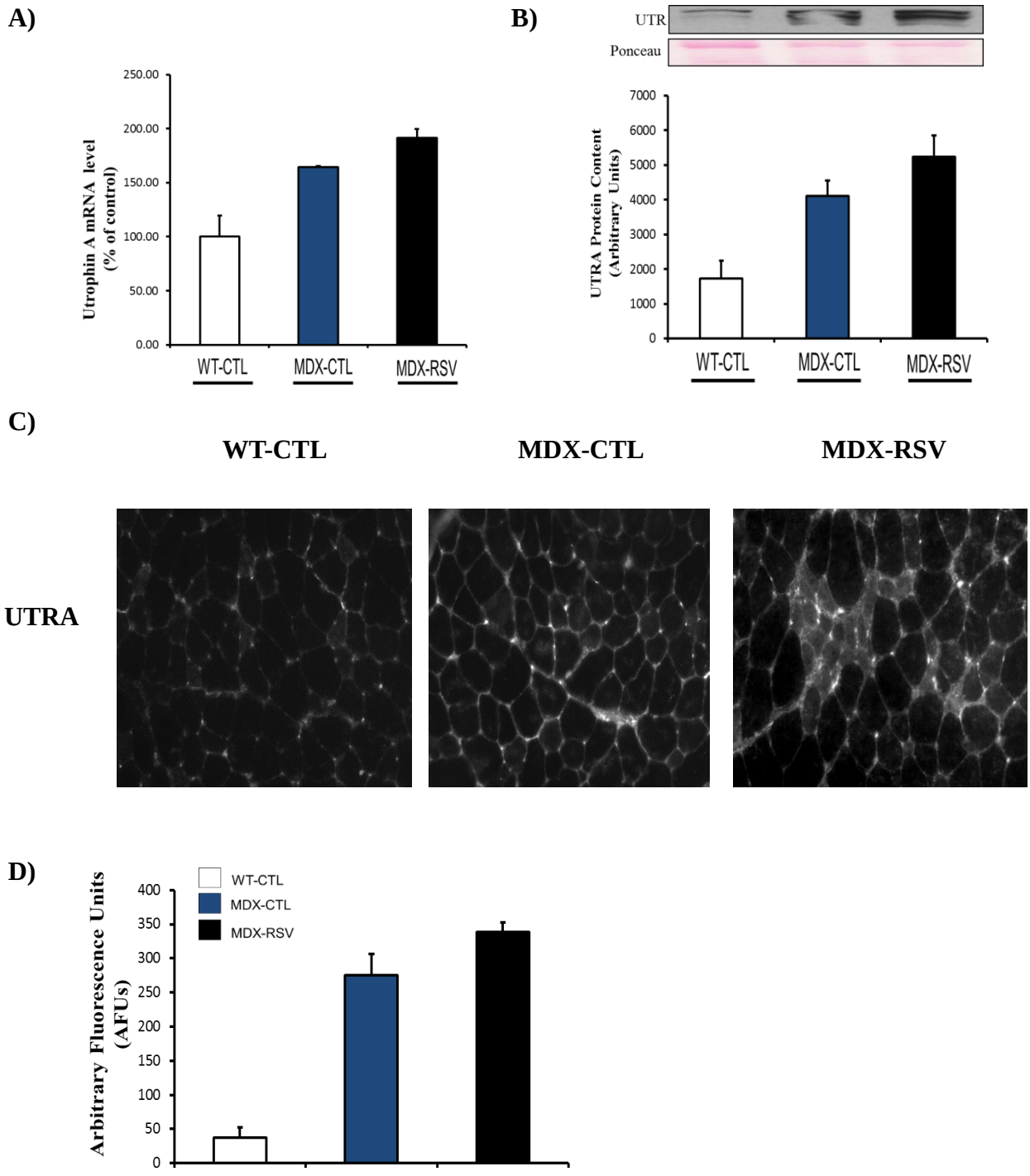

Figure 3.19 - Utrophin A expression increases modestly with resveratrol treatment in TA muscles of *mdx* mice

A) mRNA levels of utrophin A are shown, as measured by quantitative RT-PCR. Values were standardized to 18s mRNA levels (n=4-5, P > 0.05). **B)** Representative western blots of utrophin A and ponceau, and graphical summary of utrophin A protein content (n=5-6). **C)** Typical micrographs of utrophin A immunostaining in TA. **D)** Graphical summary of utrophin A fluorescence. (n= 4). Mean ± s.e.m. are shown.

3.3.4 Fast, EDL muscles of *mdx* mice treated with RSV-HDLD demonstrate modest improvements in function

Since we expected phenotypic improvement in *mdx* animals due to RSV-HDLD, we tested EDL myofibre structural integrity during repetitive electrically stimulated eccentric contractions (ECs) ex vivo. Force generation decreased to 53.51+6.0, 21.52+4.26, and 25.42+8.73% of initial tension in wild-type mice on a control diet, *mdx* mice fed a control diet, and resveratrol-treated *mdx* animals, respectively, after 12 contractions (**Figure 3.20A**). Therefore, resveratrol treatment did not have any effect on force maintenance in *mdx* mice. We also measured the maximum force generated by each muscle, prior to the EC protocol, as a measure of muscle strength. The resveratrol-treated *mdx* group showed a higher peak force than the untreated *mdx* group, but this difference was not significant (n=4, $P > 0.05$) (**Figure 3.20B**). During the EC protocol, EDL muscles were bathed in 0.1% procion orange solution. This dye infiltrates the cytosol of myocytes whose sarcolemma has been disrupted, allowing for determination of the extent of cell membrane damage caused by the ECs. We found that procion orange fluorescence intensity in EDL myofibres from resveratrol-treated animals was approximately 40% lower than that measured in untreated *mdx* mice (n=3-4, * $P < 0.05$) (**Figure 3.21A-B**).

A)

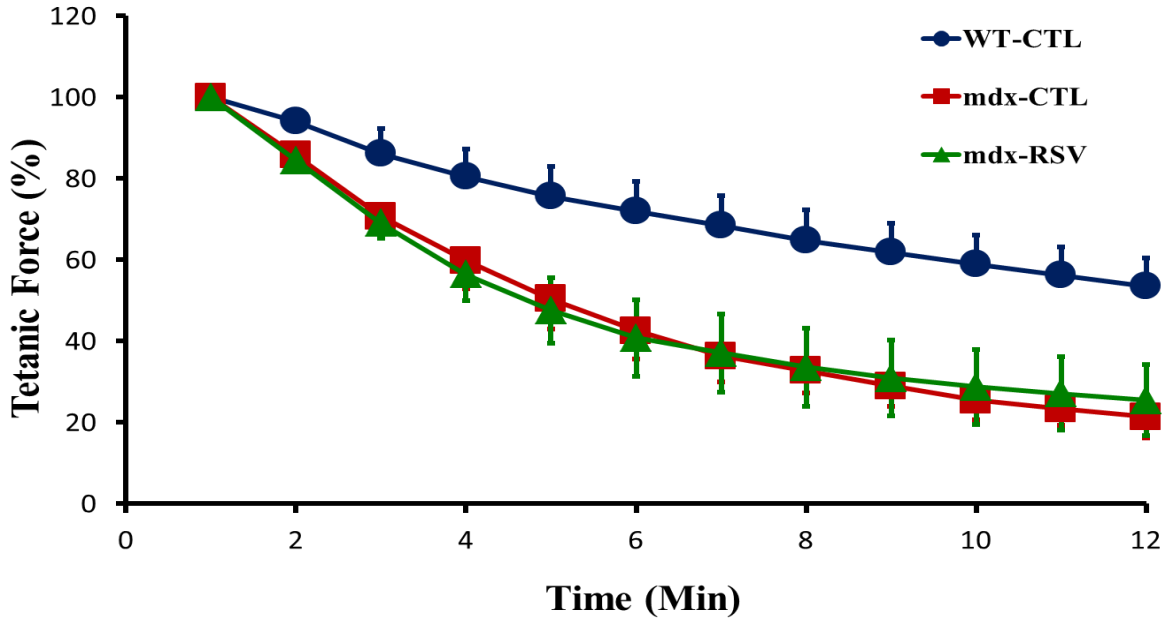

B)

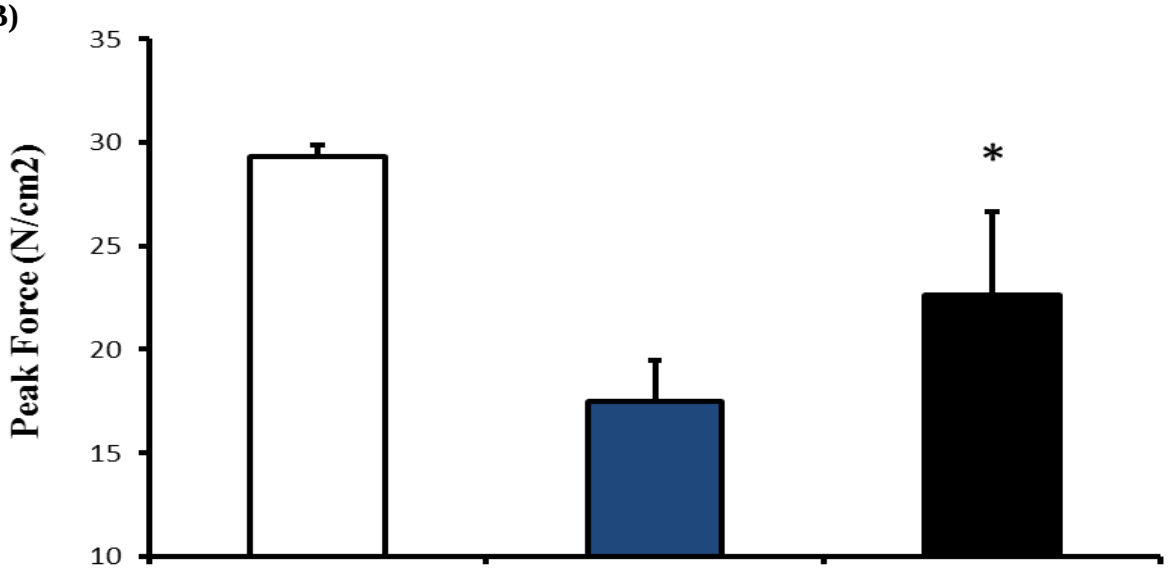

Figure 3.20 – Effects of resveratrol administration on *ex vivo mdx* skeletal muscle contractile performance

A) Maximal force development of EDL muscles, expressed as a percentage of the initial contraction, during twelve electrically stimulated eccentric contractions **B)** Graphical representation of mean peak force of EDL muscles from wild-type mice on a control diet (WT-CTL), *mdx* mice on a control diet (MDX-CTL) and *mdx* mice on a resveratrol supplemented diet (MDX-RSV) (n=3–4, ∗ $P < 0.05$ versus MDX-CTL) Mean ± s.e.m. are shown.

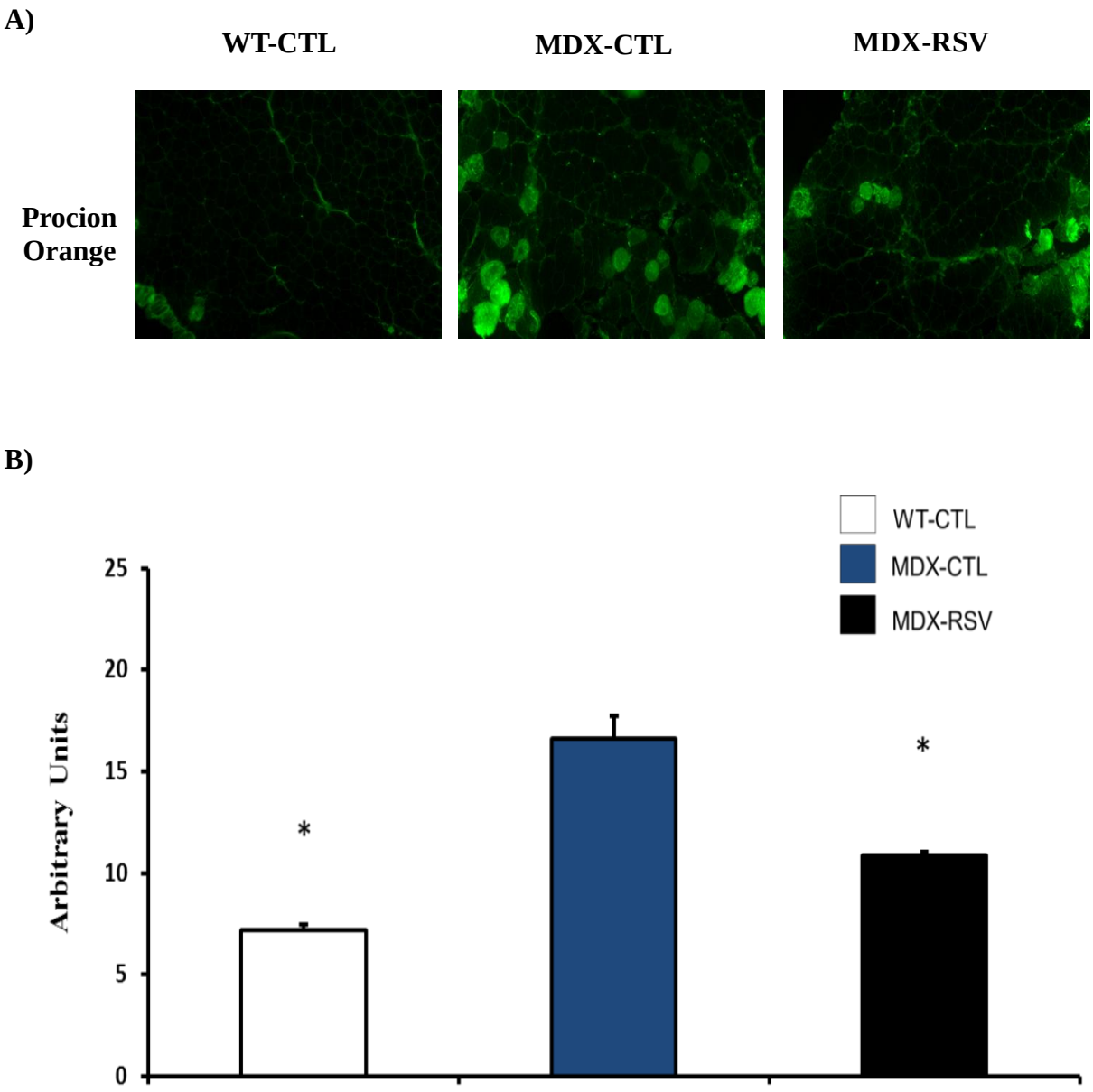

Figure 3.21 - Effects of resveratrol administration on sarcolemmal structural integrity

A) Typical procion orange staining of the EDL cryosections after undergoing eccentric contractions. **B)** Graphical summary of the total intramuscular procion orange fluorescence from wild-type mice on a control diet (WT-CTL), *mdx* mice on a control diet (MDX-CTL) and *mdx* mice on a resveratrol supplemented diet (MDX-RSV) (n=3–4, $*$ $P < 0.05$ versus MDX-CTL) Mean $\pm$ s.e.m. are shown.

3.3.5 RSV-HDLD does not significantly increase the activity of key phenotypic modifiers in slow skeletal muscle fibres of *mdx* mice

We also analysed the slow, oxidative SOL muscles in a similar manner to see if there were any changes in the activity of skeletal muscle phenotypic modifiers (**3.3.5 – 3.3.7**). SIRT1 protein levels increased approximately 30% in the resveratrol treated group, compared to the untreated *mdx* group (**Figure 3.22A**). However, this change was not significant (n=5-6, $P > 0.05$). SIRT1 activity in the SOL muscles was unchanged between the resveratrol-treated *mdx* group and the *mdx* mice fed a control diet (n=5-6, $P > 0.05$) (**Figure 3.22B**). These findings were similar to what was observed in fast TA muscles after HDLD. Furthermore, resveratrol treated *mdx* mice showed no change in PGC-1α protein levels in the SOL muscles when compared to untreated *mdx* animals (n=5-6, $P > 0.05$) (**Figure 3.23**).

3.3.6 RSV-HDLD does not stimulate the SOMP in the SOL muscle of *mdx* mice

We examined several common markers that are characteristic of the slow, oxidative skeletal muscle phenotype in the SOL muscles. COXIV mRNA levels of resveratrol-treated *mdx* mice show modest increases as compared to the *mdx* group fed a control diet, but this relationship was not significant (n=3-4, $P > 0.05$) (**Figure 3.24**). In addition, we evaluated the percentage of MHC I-stained fibres in SOL muscle cryosections from all three animal groups. Again, we observed a slight increase of approximately 20% in MHCI-positive fibres in the treated *mdx* mice group, but, this difference was not significant (n=3-4, $P > 0.05$) (**Figure 3.25A-B**). Western blot analysis confirmed that resveratrol was not stimulating

MHCI expression (**Figure 3.25C**). In fact, quantification of the blots demonstrated a modest decrease in protein levels of MHCI in the resveratrol-treated group, compared to the untreated *mdx* animals (**Figure 3.25C**)

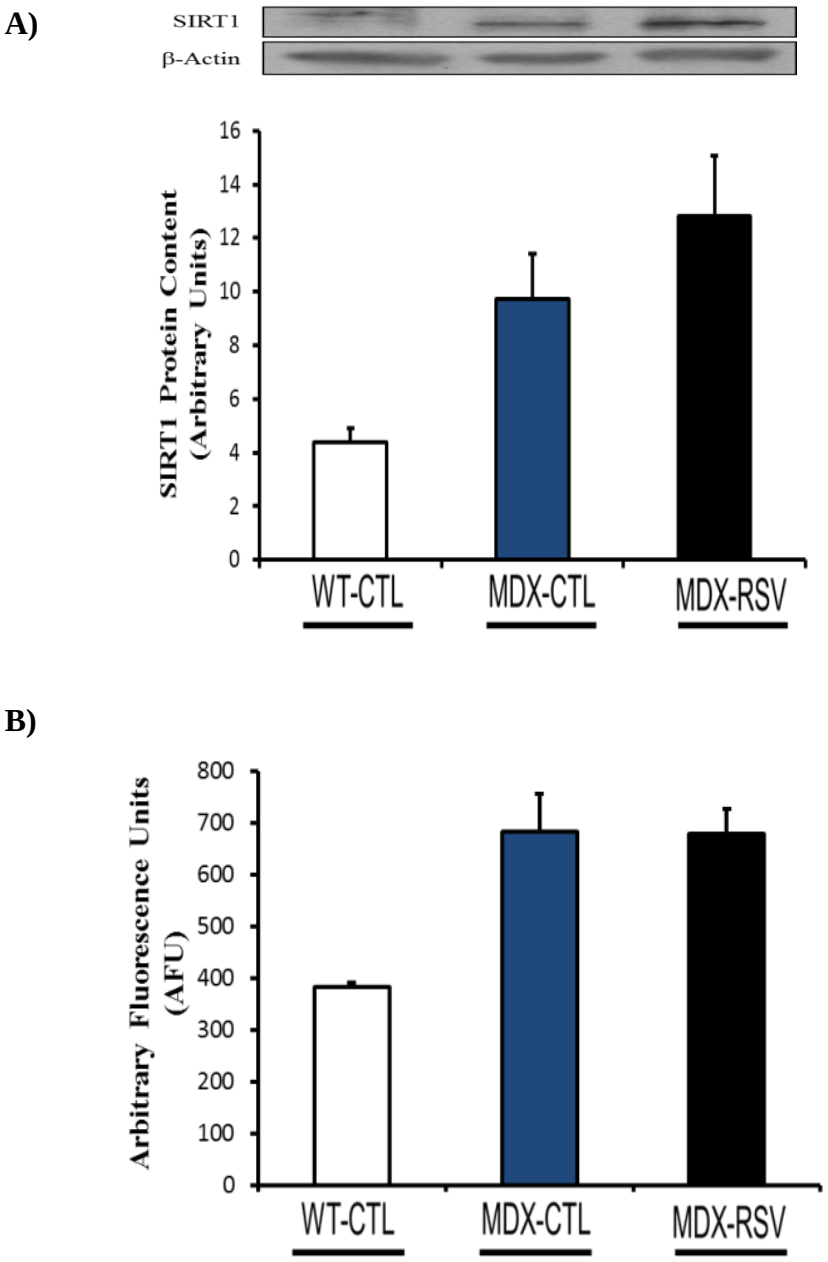

Figure 3.22 - Effects of resveratrol treatment on the protein expression and activity of SIRT1 in the SOL muscles of *mdx* mice

A) Representative SIRT1 and β-actin western blots with quantification and **B)** SIRT1 activity, measured as arbitrary fluorescence units (AFU). Muscle extracts isolated from wild-type mice on a control diet (WT-CTL), *mdx* mice on a control diet (MDX-CTL) and *mdx* mice on a resveratrol supplemented diet (MDX-RSV) (n =5-6, P > 0.05 versus MDX-CTL). Mean ± s.e.m. are shown. wild-type mice on a control diet (WT-CTL), *mdx* mice on a control diet (MDX-CTL) and *mdx* mice on a resveratrol supplemented diet (MDX-RSV) (n =5-6,). Mean ± s.e.m. are shown.

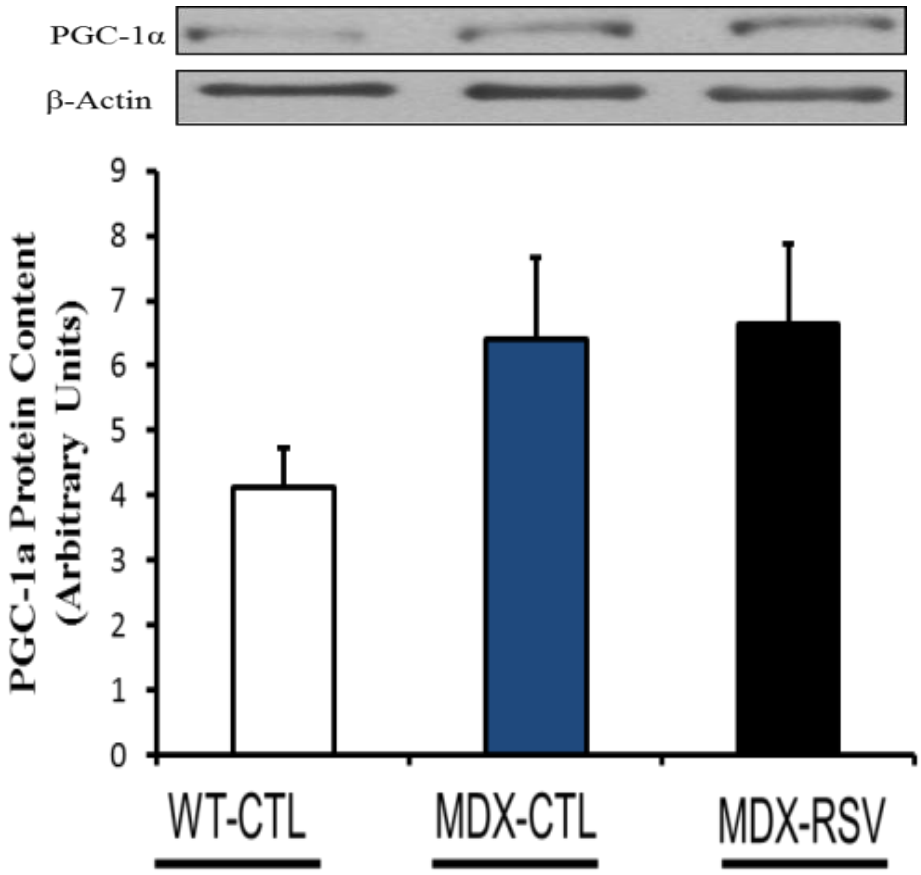

Figure 3.23 – Effects of resveratrol treatment on the protein expression of PGC-1α in the SOL muscles of *mdx* mice

Representative PGC-1α and GAPDH western blots with quantification from SOL muscles (n = 5-6, P > 0.05 versus MDX-CTL). Muscle extracts isolated from wild-type mice on a control diet (WT-CTL), *mdx* mice on a control diet (MDX-CTL) and *mdx* mice on a resveratrol supplemented diet (MDX-RSV). Mean ± s.e.m. are shown.

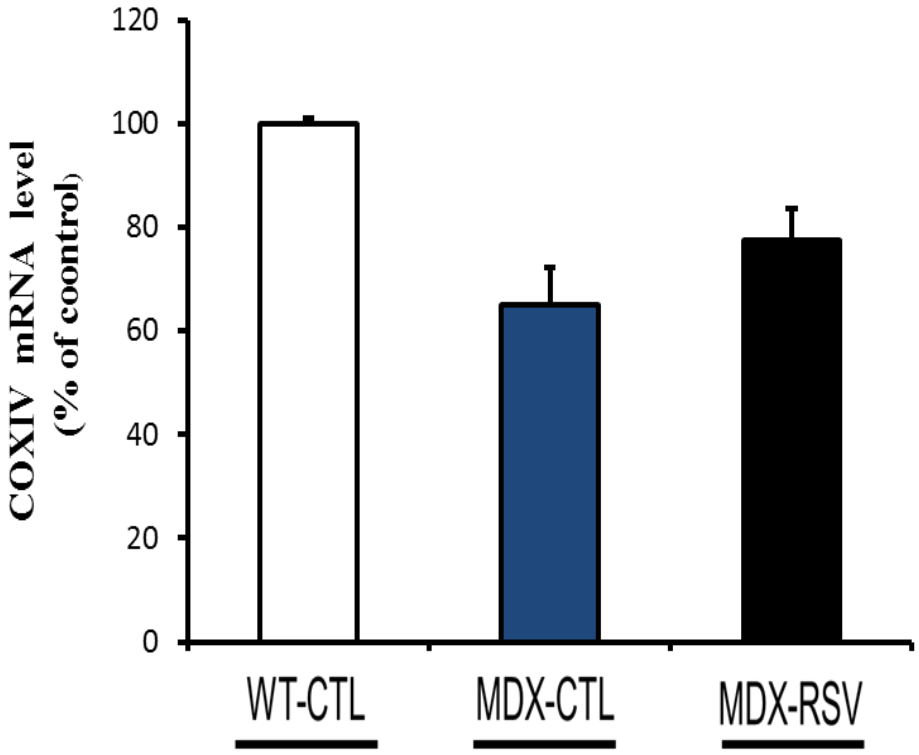

Figure 3.24 - A high dose of resveratrol does not stimulate expression of COXIV in the SOL muscles of *mdx* mice

mRNA levels of COXIV are shown, as measured by quantitative RT-PCR. Values were standardized to 18s mRNA levels. Muscle extracts isolated from wild-type mice on a control diet (WT-CTL), *mdx* mice on a control diet (MDX-CTL) and *mdx* mice on a resveratrol supplemented diet (MDX-RSV) (n=3–4, $P > 0.05$ versus MDX-CTL) Mean $\pm$ s.e.m. are shown.

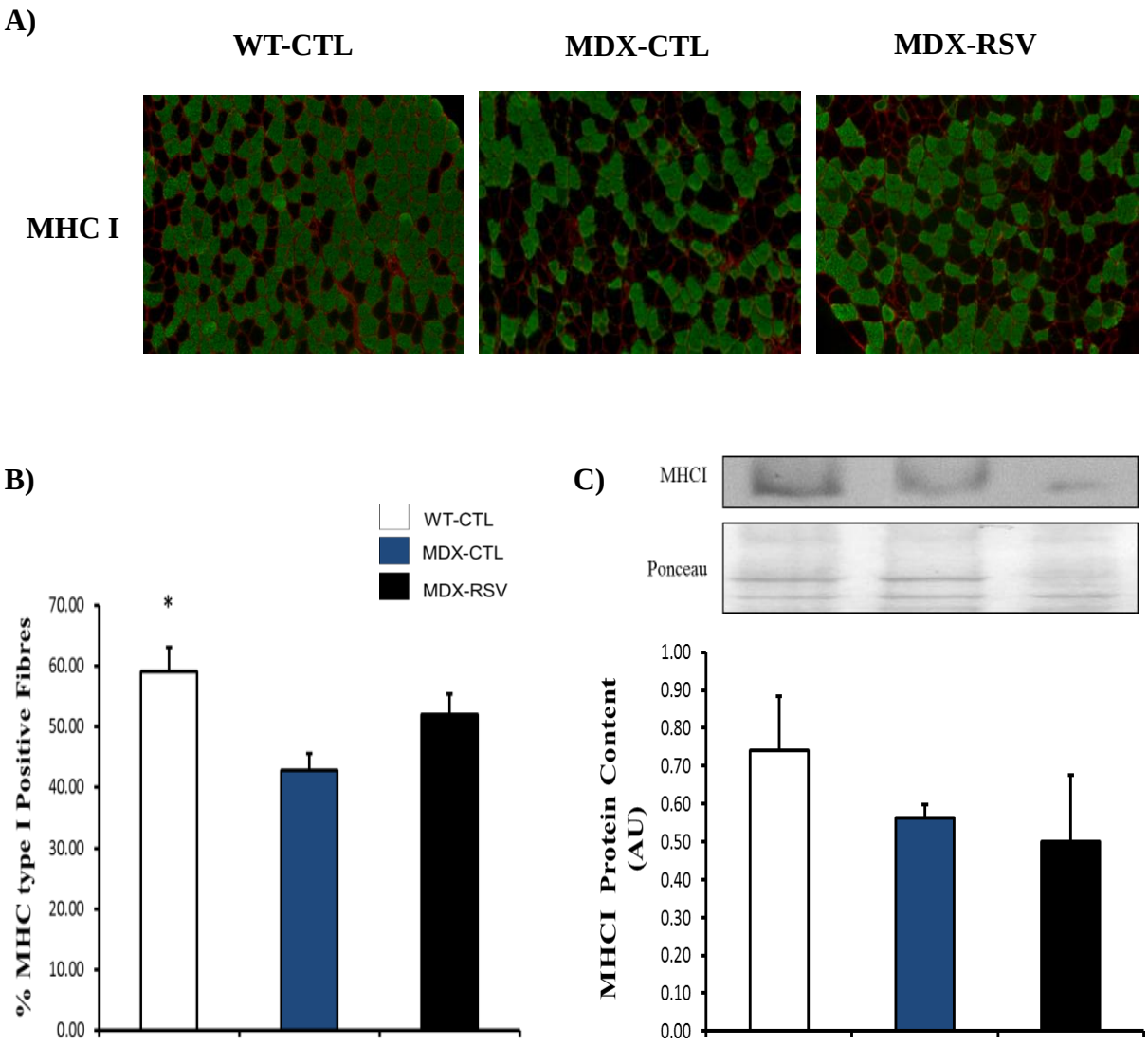

Figure 3.25 - Resveratrol treatment does not increase the appearance of the slow isoform of MHC in the SOL muscles of *mdx* mice

A) Representative micrographs of MHC I immunofluorescence of SOL muscle cryosections. **B)** Graphical summary of the percentage of MHC I-positive fibres (n = 3-4, P > 0.05). **C)** Representative blots with quantification of MHCI normalized to ponceau staining. (n=4-5, P > 0.05) Mean ± s.e.m. are shown.

3.3.7 Utrophin A mRNA and protein levels in the SOL muscle of *mdx* mice are unaffected by treatment with RSV-HDLD

We analysed mRNA levels, protein content and localization of utrophin A. mRNA levels exhibited no significant different between all three animal groups in the slow, oxidative, SOL muscle (n=3-4, $P > 0.05$) (**Figure 3.26A**). Using western blot analysis, we also observed that utrophin A protein levels in the SOL muscles of *mdx* mice did not change in response to resveratrol treatment (**Figure 3.26B**). In fact, utrophin A levels decreased slightly in the treated group, compared to the *mdx* mice fed a control diet (n=5-6, $P > 0.05$) (**Figure 3.26B**). To evaluate utrophin A localization and expression, we stained SOL muscle cryosections, using a utrophin A antibody (**Figure 3.26C**). Utrophin A fluorescence intensity was slightly lower in the resveratrol treated mice, when compared to the *mdx* mice fed a control diet (n=3-4, $P > 0.05$) (**Figure 3.26C-D**).

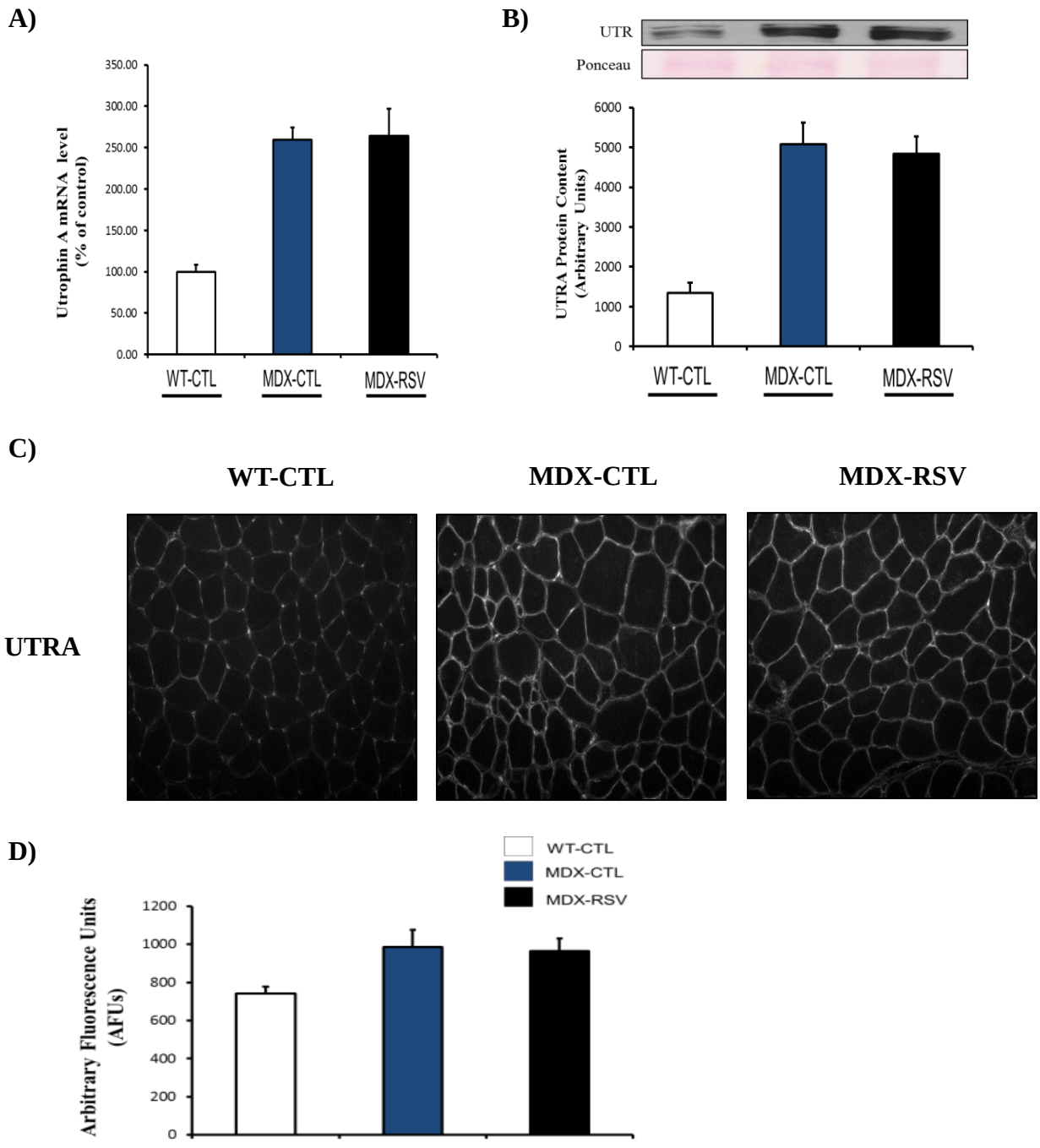

Figure 3.26 - Utrophin A expression does not increase with resveratrol treatment in SOL muscles of *mdx* mice

A) mRNA levels of utrophin A are shown, as measured by quantitative RT-PCR. Values were standardized to 18s mRNA levels (n=3-4, $P > 0.05$). **B)** Representative western blots of utrophin A and ponceau, and graphical summary of utrophin A protein content (n=5-6, $P > 0.05$). **C)** Typical micrographs of utrophin A immunostaining in SOL. **D)** Graphical summary of utrophin A fluorescence. (n= 4, $P > 0.05$). Mean $\pm$ s.e.m. are shown.

Taken together, the results indicate that the higher dose of resveratrol was not effective in promoting the SOMP in the slow, oxidative SOL muscles of *mdx* mice. None of the proteins that are typically activated by resveratrol were increased significantly, including SIRT1 and PGC-1α. There were no changes in the proportion of MHCI-positive stained myofibres between the treated and untreated animals. In addition, there were no significant changes in utrophin A expression with resveratrol treatment at this dosage in the SOL muscle.

The fast, glycolytic EDL and TA muscles were also largely unaffected by RSV-HDLD. There were no changes in SIRT1 protein levels and activity. Surprisingly, we did observe an elevation in the percentage of MHCIIa-stained fibres and a slight reduction in MHCIIb-stained fibres. Utrophin A did not exhibit significant increases with RSV-HDLD when compared to the untreated *mdx* group. Functional analysis revealed no improvements in terms of percentage of force drop, following ECs.

4: Discussion

In recent work, we have shown that promoting the slow, oxidative myogenic program (SOMP), through the use of small molecules, can have an ameliorative effect on the DMD pathology (Miura 2009; Ljubicic 2011). In the present study, we evaluated the therapeutic potential of resveratrol, a putative activator of SIRT1 and AMPK (Lagouge 2006; Canto 2009; Um 2010; Park 2012). We discovered that resveratrol treatment can activate several key signaling molecules, involved in skeletal muscle plasticity, both *in vitro* and *in vivo*. More specifically, these resveratrol-induced changes led to a shift in skeletal muscle fibre type in *mdx* mice towards the slower, more oxidative phenotype. We also learned that resveratrol's ability to remodel skeletal muscle in the *mdx* context is largely dose-dependent. Overall, a moderate dose of resveratrol seems to be much more effective than a relatively high dose of the drug. At the commencement of this study, there was no knowledge of the interaction between resveratrol and dystrophic skeletal muscle. Although some papers have emerged since (Hori 2011; Selsby 2012; Gordon 2013), they do not characterize the conversion in muscle fibre type and/or limit their analyses to short treatment periods. Our work is very timely, as it outlines a promising role for resveratrol in promoting the SOMP in the diseased context and highlights the importance of optimizing the drug dose.

4.1 Resveratrol activates SOMP signaling molecules in C2C12 model

Our preliminary work focused on gaining an understanding of resveratrol's ability to activate SOMP signaling molecules in an *in vitro* skeletal muscle cell model. C2C12 cells were used due to their predictable patterns of differentiation and their response to drug

treatment has been shown to translate well to the *mdx* context (Xiong 2007; Miura 2009; Seow 2010; Ljubicic 2011). We observed resveratrol-induced increases in the expression levels of many key markers involved in skeletal muscle remodeling, including SIRT1, PGC-1α, and PPARδ. In addition utrophin A mRNA increased in the resveratrol-treated group. However, these significant changes in mRNA levels resulted in only modest increases at the protein level. This observation is not unusual, as several factors can cause discordance between mRNA and protein levels, including translational regulation, and protein degradation (Gramolini 1999; Gygi 1999; Tian 2004; Miura 2009). Indeed, resveratrol has been shown to act directly on SIRT1, which targets downstream proteins at the post-translational level, affecting their stability and activity (Baur 2006; Lagouge 2006; Amat 2009). Nonetheless, these initial results were encouraging in terms of increasing the expression of several important signaling molecules, thus we were interested in exploring the effects of resveratrol in the *mdx* mouse model. Note that the interaction between resveratrol and dystrophic muscle was completely unknown at this point of our study.

4.2 Resveratrol promotes elements of the SOMP in *mdx* mice

In experiments using pharmacological agents, it is often advised to implement the lowest effective dose to reduce the possibility of off target effects. Toxicological studies demonstrate that rodents can safely tolerate resveratrol at doses as high as 700mg/kg/day (Williams 2009), but mice have been treated effectively at much lower doses (Barger 2008). Targeting specific tissues adds complexity to the issue because the metabolic profile of resveratrol varies across different tissues. For example, in rats fed low to moderate doses of the drug, the greatest number of resveratrol metabolites was found in the liver and adipose tissue, whereas the presence of these metabolites was significantly lower in muscle (Andres-

Laceuva 2012). Thus, the context for which the drug is purposed can influence the optimal dose. The majority of recent studies that evaluate the effect of resveratrol on skeletal muscle use a dose in the range of ~50-400 mg/kg/day (Lagouge 2006; Um 2010; Park 2012; Price 2012; Menzies 2013). We initially implemented a dose of ~100mg/kg/day of resveratrol, based on previous studies (Baur 2006; Lagouge 2006; Ryan 2010), and started treating mice at six to seven weeks of age. At this point, the characteristic cycles of degeneration/regeneration and necrosis are well under way (De Luca 2012). Thus, our aim was to maintain the integrity of existing healthy fibres and/or prevent the progression of the disease phenotype (De Luca 2012).

Following treatment, the *mdx* mice showed evidence of skeletal muscle remodelling towards the SOMP, including a higher proportion of the slower MHC isoforms and an increased expression of oxidative genes, including COXIV. This is important because augmented mitochondrial biogenesis and promotion of the SOMP is associated with increased fatigue resistance (Hood 2001), decreased metabolic abnormalities (Millay 2008), improved insulin sensitivity (Leng 2004), and retention of muscle mass/function (Da Cruz 2012). In the context of DMD, the slower, more oxidative muscle fibres in diseased patients are more resistant to the dystrophic pathology, as compared to the faster, more glycolytic fibres (Webster 1988). This may be due, in part, to the fact that slow muscle contains higher amounts of structural proteins, including dystrophin and utrophin A (Gramolini 2001b; Miura 2006). Utrophin A localisation is also expanded to the extrasynaptic regions in slow, oxidative muscle, whereas it is restricted to the NMJ's in fast, glycolytic muscle (Gramolini 2001b, Chakkalakal 2003). Indeed, induction of the SOMP through functional muscle overload or transgenic activation of calcineurin is accompanied by significant increases in utrophin A expression (Chakkalakal 2003).

4.3 Importance of triggering SOMP in skeletal muscle diseases

Promoting the SOMP is not only beneficial in the DMD context. There is evidence that it helps patients with amylotrophic lateral sclerosis (ALS) (Da Cruz 2012), Huntington's disease (Johri 2012), cancer cachexia (Wang 2013), and diabetes (Stuart 2013), which speaks to the therapeutic value of stimulating the SOMP under a variety of conditions that stress muscle functionality. ALS and Huntington's disease are neurodegenerative disorders that result in muscle wasting, mitochondrial dysfunction, and motor neuron death (Da Cruz 2012; Johri 2012). In mouse models of these diseases, activation of PGC-1α and promotion of the SOMP results in significant improvements in mitochondrial function and biogenesis, as well as muscle performance, including resistance to fatigue (Da Cruz 2012; Johri 2012). Furthermore, the conversion in muscle fibre type towards the more oxidative phenotype protects the animals from skeletal muscle atrophy and increases fatty acid oxidation (Da Cruz 2012; Johri 2012). Under conditions of cancer cachexia, patients suffer from severe skeletal muscle atrophy which is more pronounced in type II, glycolytic myofibres, as compared to type I, oxidative fibres (Wang 2013). This may be due, in part, to the lower abundance of PGC-1α, which is characteristic of type IIB muscle fibres (Schiaffino 2011). PGC-1α overexpression can delay the progression of skeletal muscle atrophy by inhibiting the FoxO-dependent upregulation of ubiquitin liagases atrogin-1 and MuRF1 (Schiaffino 2011; Wang 2013). In the context of diabetes, the ability of skeletal muscles to act as a sink for plasma glucose is critically important (Schiaffino 2011). A defect in the glucose uptake process can lead to insulin resistance and hyperglycemia, which are characteristic features of type II diabetes (Schiaffino 2011). One of the main glucose transport proteins, GLUT4, is differentially expressed in type I and type II skeletal myofibres (Schiaffino 2011). Studies in

rabbits reveal that GLUT4 expression is significantly higher in oxidative fibres (Kong 1994). Furthermore, a direct relationship between insulin-triggered glucose uptake and the proportion of type I myofibres has been shown in humans (Zierath 1996). More recently, Stuart and colleagues have demonstrated that a lower proportion of type I muscle fibres correlates with higher severity of insulin resistance (Stuart 2013). Thus, there appears to be a clear benefit to promoting the SOMP in this disease context as it relates to glucose transport and insulin sensitivity. It is with this in mind that several pharmacological agents, possessing the ability to promote the SOMP, are currently being used in the treatment of diabetes. These include AICAR (Koistinen 2003), metformin (Zhou 2001) and resveratrol (Chen 2011). Taken together, these examples provide evidence for the benefits of inducing the SOMP under conditions of muscle wasting or dysfunction.

4.4 SIRT1 and PGC-1α regulate a shift in skeletal muscle towards the slower, more oxidative phenotype

The changes in skeletal muscle phenotype that we observed may have been mediated through activation of SIRT1 and subsequent deacetylation of PGC-1α. Deacetylated PGC-1α is considered the "active form", facilitating its incorporation into protein complexes at promoter regions and increasing the rates of transcription of several genes associated with the SOMP (Rodgers 2005; Gerhart-Hines 2007). PGC-1α is a master regulator of phenotypic plasticity, and its overexpression is sufficient to cause drastic changes in skeletal muscle fibre type towards the slower, more oxidative phenotype (Lin 2002; Handschin 2007; Rasbach 2010). These changes in skeletal muscle morphology are often accompanied by reorganization of the neuromuscular junction, including increased utrophin A expression (Chakkalakal 2004; Angus 2005; Stupka 2006; Handschin 2007). Histological analyses

revealed improvements in central nucleation and cross sectional area of myofibres. In addition, utrophin A levels demonstrated modest increases of ~1.4-fold in the treated animals. It is important to note that transgenic upregulation of utrophin A by only 2-fold is sufficient to completely prevent the dystrophic pathology (Tinsley 1998). These findings were promising, but the shift in skeletal muscle fibre type towards the slower, more oxidative phenotype was not complete. This raised the question of whether modifying the treatment regimen may result in a stronger effect on skeletal muscle plasticity and greater therapeutic benefits.

Surprisingly, we discovered that the elevated dose of 500mg/kg/day was ineffective in its promotion of the SOMP in both the fast, glycolytic muscle fibres, and the slow, oxidative muscle fibres. SIRT1 was not activated and there was no change in utrophin A levels with resveratrol treatment. Furthermore, the fast EDL muscles showed no significant improvement in peak force generation or resistance to force drop following eccentric contractions. It became evident that the dose of resveratrol plays a huge role in determining the effectiveness of the drug in dystrophic skeletal muscle.

4.5 Does therapeutic benefit of resveratrol depend on dose?

The first group to treat *mdx* mice with resveratrol did so at a dose of 500mg/kg/day for 32 weeks (Hori 2011). They observed a significant reduction in oxidative damage and fibrosis, and improved retention of overall muscle mass in the biceps femoris of treated *mdx* mice, when compared to the untreated group (Hori 2011). Although they focused on the secondary pathological features of DMD, this study demonstrates that the drug is well-tolerated at this elevated dose. More recently, two separate groups treated *mdx* mice with resveratrol at a moderate dose of 100mg/kg/day and high dose of 400mg/kg/day (Selsby

2012; Gordon 2013). Selsby and colleagues unexpectedly observed a high mortality rate in the *mdx* mice given the elevated dose of the drug and, consequently, focused their efforts on the mice treated with 100mg/kg/day (Selsby 2012). These mice demonstrated a trend towards increased utrophin A expression and showed an increased fatigue resistance in the soleus muscles (Selsby 2012). Gordon and colleagues did not see any effect on mortality rate, but did observe that only animals treated with the 100mg/kg/day exhibited increased expression of SIRT1 and a reduction in macrophage infiltration in skeletal muscle (Gordon 2013). Mice treated at the higher dose showed little to no improvements in the dystrophic pathology. A similar trend in dose-response was observed during a drug-screen for natural compounds that activate the utrophin A promoter (Moorwood 2011). Using a luciferase reporter promoter assay in the C2C12 context, it was discovered that resveratrol can activate the utrophin A promoter (Moorwood 2011). The maximum fold change in luciferase activity was seen at a relatively low dose of 6.25μM. Taken together, these studies provide mounting evidence that a low or moderate dose of resveratrol is much more effective at promoting the SOMP and, potentially, stimulating utrophin A promoter activity. This dose-response effect mirrors much of what we observed in our study.

Price and colleagues provide insight into the potential mechanism responsible for this dose-dependent reaction (Price 2012). They treated adult-inducible SIRT1 knockout mice with two doses of resveratrol, 30mg/kg/day and 230mg/kg/day, and evaluated their effects on skeletal muscle plasticity and mitochondrial function/biogenesis (Price 2012). The lower dose stimulated AMPK activity and promoted a conversion in skeletal muscle fibre type towards the slower, more oxidative phenotype, evidenced by improved mitochondrial respiration and increased expression of PGC-1α (Price 2012). These changes were entirely dependent on the presence of SIRT1, highlighting the importance of this enzyme in

resveratrol's mechanism of action. This agrees with data from our own study, which demonstrates clear increases in SIRT1 activity/protein and deacetylation of downstream PGC-1α, following treatment with a moderate dose of resveratrol. At the higher dose, Price and colleagues found that resveratrol had little effect on skeletal muscle morphology. However, they did show AMPK activation, even in the absence of SIRT1. This finding was replicated in their *in vitro* model, where they identified a potential toxic effect from the elevated dose. In cultured cells, those treated with a high dose of resveratrol suffered from impaired mitochondrial respiration and subsequent reductions in cellular ATP levels. By altering the energy state of the cell and, more specifically, the ADP/ATP ratio, AMPK may be activated, irrespective of SIRT1 (Hawley 2010; Price 2012). Bypassing SIRT1 and inhibiting the oxidative machinery may explain why this dose is ineffective for improving the skeletal muscle profile. Indeed, in our study we did not see any significant changes in SIRT1 activity or protein in *mdx* mice treated with the higher dose. This translated to minimal improvements in the dystrophic pathology and truly underscores the importance of dose in drug treatment studies.

4.6 How does resveratrol compare to the contextually novel small molecules, GW501516 and AICAR?

We were the first to demonstrate that promotion of the SOMP and, subsequent, amelioration of the dystrophic pathology, can be achieved in *mdx* animals via the chronic administration of a PPARδ agonist (GW501516) (Miura 2009), or using an activator of AMPK (AICAR) (Ljubicic 2011). In both cases, treatment of *mdx* animals with these compounds resulted in a significant increase in utrophin A expression as well as in a clear attenuation of the dystrophic phenotype (Miura 2009; Ljubicic 2011). Furthermore, both

GW501516 and AICAR resulted in a phenotypic conversion in skeletal muscle fibre type from fast type I to slow type II fibres, and improvements in sarcolemmal integrity (Miura 2009; Ljubicic 2011). More recently, it has been shown that AICAR is effective at triggering the autophagy-mitophagy pathway and eliminating defective mitochondria in skeletal muscles of *mdx* mice (Pauly 2012). Furthermore, combining both AICAR and GW501516 improves muscle strength and oxidative capacity of *mdx* skeletal muscle cells (Bueno Junior 2012; Jahnke 2012). These results were significant because they demonstrated that the DMD pathology could be partially rescued through the use of therapeutically relevant molecules.

In our current study, using a moderate dose of resveratrol, we observed similarities in terms of promotion of the SOMP. However, there were also agonist-specific variations in all three studies. Unlike GW501516 and AICAR, resveratrol was unable to induce a significant increase in utrophin A expression in *mdx* mice, despite a consistent trend in the positive direction. In addition, AICAR promoted phenotypic plasticity only in the fast, glycolytic muscles, whereas GW501516 and a moderate dose of resveratrol elicited adaptations in both fast EDL and slow SOL muscles (Miura 2009; Ljubicic 2011). Also, GW501516 improved resistance to force drop during consecutive EC's, whereas AICAR and resveratrol failed to do so.

Despite areas of overlap, the pathways associated with each drug are unique, which most likely contributes to the variation in the effects we have observed (**Figure 4.1**). GW501516 demonstrates some interaction with AMPK and its upstream effectors, but its relevance in the DMD context is largely based on its interaction with PPRE elements, located within the utrophin A promoter (Tanaka 2003; Wang 2004; Terada 2006; Miura 2009). AICAR is a synthetic compound that is phosphorylated to ZMP, following integration into myocytes (Witczak 2008). ZMP is an AMP analogue that mimics its influence on AMPK

activity, altering the energy state within the cell and encouraging transformations that are characteristic of the slow, oxidative phenotype skeletal muscle phenotype (Holmes 1999; Winder 2000; Narkar 2008; Witczak 2008; Friedrichsen 2013). Resveratrol is similar to AICAR in that they both have the capability to activate three main phenotypic modifiers: AMPK, SIRT1, PGC-1α (Holmes 1999; Winder 2000; Lin 2002; Ljubicic 2011; Suwa 2011; Park 2012; Price 2012). However, resveratrol is unique in that its effects on skeletal muscle plasticity and mitochondrial function are largely dependent on the presence of SIRT1 (Lagouge 2006; Chung 2010; Tennen 2012; Price 2012). By better defining the signaling mechanisms as well as their impact, we can optimize treatment strategies for individual patients and potentially combine different drugs to maximize their beneficial capabilities.

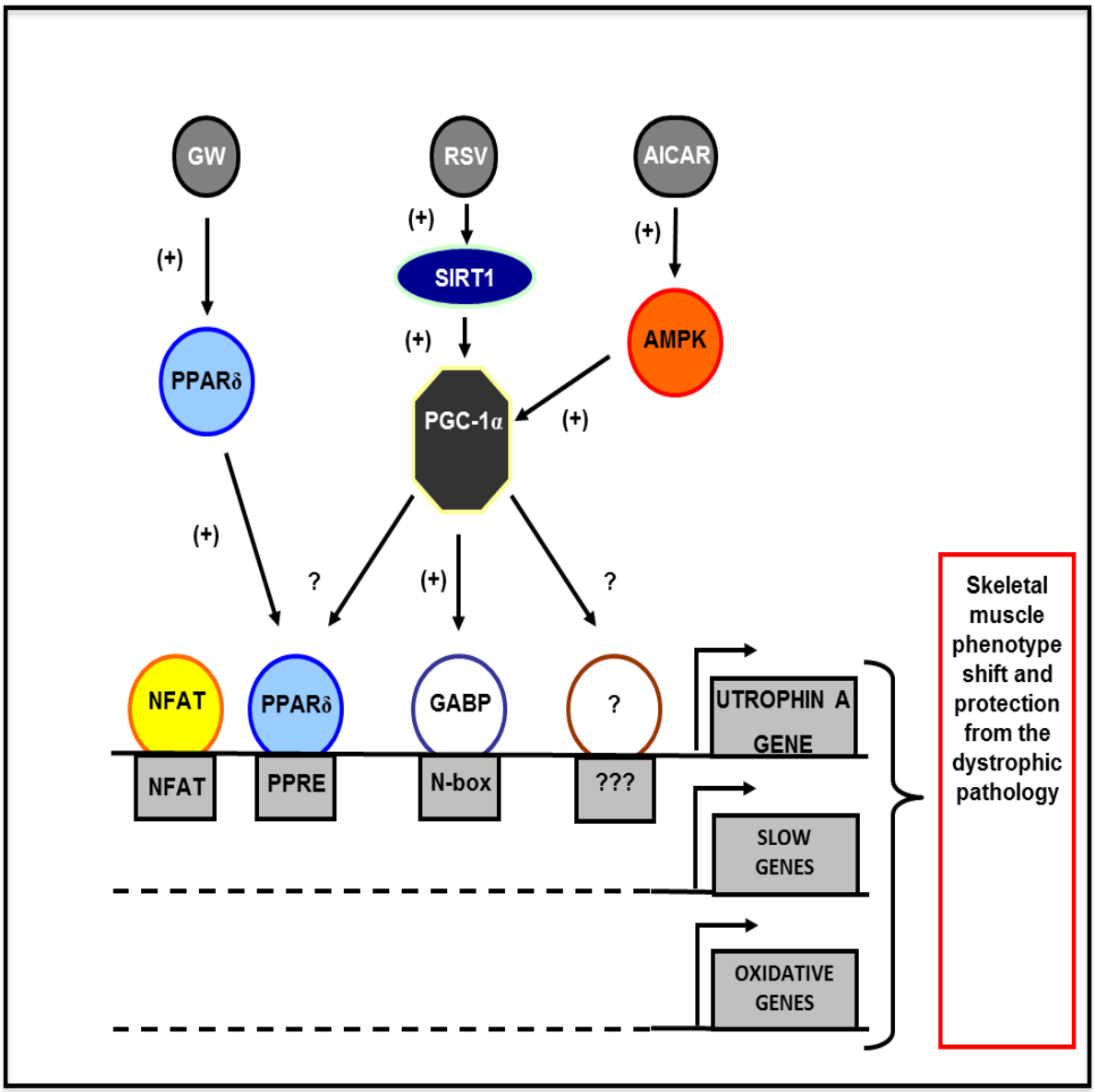

Figure 4.1 - Signaling cascades triggered by select compounds that converge on the utrophin A promoter, as well as other promoters for genes encoding the slow, oxidative myofibre program

The GW501516 (GW) compound targets the transcription factor (TF) PPARδ, which binds PPREs in upstream regions. Stimulated AMPK via AICAR treatment activates the transcriptional co-activator, PGC-1α. Resveratrol (RSV) also induces PGC-1α activity through a deacetylation event, involving SIRT1. PGC-1α interacts with TFs like GABP and PPARδ to transactivate gene expression. The activation of PPARδ, AMPK, SIRT1 and PGC-1α via agonist treatment has been shown to evoke the slow, oxidative phenotype resulting in numerous beneficial functional adaptations. This Figure has been adopted from Ljubicic (Jasmin Lab).

4.7 Combinatorial treatment strategies using transcriptional and post-transcriptional activators of utrophin A

Combinatorial treatment in the context of DMD or other disorders involving skeletal muscle is still in the very early stages of development. Recently, Bueno Junior and colleagues published a study, evaluating the effectiveness of a combined GW501516 and AICAR treatment in exercised *mdx* mice (Bueno Junior 2012). They observed instances of a synergistic effect with respect to muscle functionality and oxidative metabolism when the combinatorial treatment was coupled with exercise training (Bueno Junior 2012). Around the same time, another group evaluated these two metabolic remodeling agents, separately and in combination, in the *mdx* context (Jahnke 2012). There was no evidence of a synergistic effect with the combination of GW501516 and AICAR, but all three treatment groups managed to make significant improvements in the disease phenotype, including increased muscle strength and mitochondrial biogenesis (Jahnke 2012).

Resveratrol has also been used in combination with metformin, an AMPK activator commonly used for the treatment of diabetes, and hydroxymethylbutyrate, a leucine metabolite, in C2C12 cells and a diabetic mouse model (Bruckbauer 2013). The combination of these drugs is more effective at stimulating SIRT1 activity, improving insulin sensitivity, and inducing fatty acid oxidation than each of them on their own (Bruckbauer 2013). These are examples of combining drugs that are putative transcriptional activators of utrophin A.

It is interesting to speculate whether it would be more effective to couple transcriptional activation with drugs that act at the post-transcriptional level. Evidence suggests that utrophin A is subject to important post-transcriptional events that impact its

mRNA stability in skeletal muscle cells (Gramolini 2001a; Chakkalakal 2008). AU-rich elements (AREs), located within the 3'-untranslated region (UTR) of utrophin A, play a critical role in this process through their interactions with AU-rich element-binding poteins (AUBPs) (Gramolini 2001a; Chakkalakal 2008). Indeed, our lab has shown that stimulation of calcineurin signaling can improve utrophin A mRNA stability through an ARE-dependent mechanism (Chakkalakal 2008). Mutating the ARE sites abrogates the effect on mRNA stability, highlighting the importance of these sites in regulating mRNA steady-state levels (Chakkalakal 2008). More recently, our lab has explored the possibility of implementing small molecules to influence utrophin A mRNA stability at the post-transcriptional level. Heparin, a P38 activator, has the ability to decrease the functional availability of KSRP, an RNA-binding protein that can trigger the destabilization of ARE-containing transcripts, including utrophin A (Amirouche 2013). Treatment of *mdx* mice with this drug for 10 days was sufficient to significantly increase utrophin A expression in the diaphragm (Amirouche 2013). This was accompanied by an increase in p38 phosphorylation and a decrease in KSRP protein levels. Furthermore, heparin-treated C2C12 cells showed a drastic increase in the half-life of utrophin A mRNA, showing a stabilizing effect (Amirouche 2013). This paper reveals the powerful therapeutic potential of pharmacological agents that can enhance utrophin A expression at the post-transcriptional level through p38 activation. Other p38 activators that are already in clinical use may carry similar benefits in the DMD context, including celebrex (Hsiao 2007; Park 2010) and calcitriol (Buitrago 2012). The next logical step is to combine the transcriptional activators with post-transcriptional activators in an effort to maximize utrophin A expression in the DMD context (**Figure 4.2**).

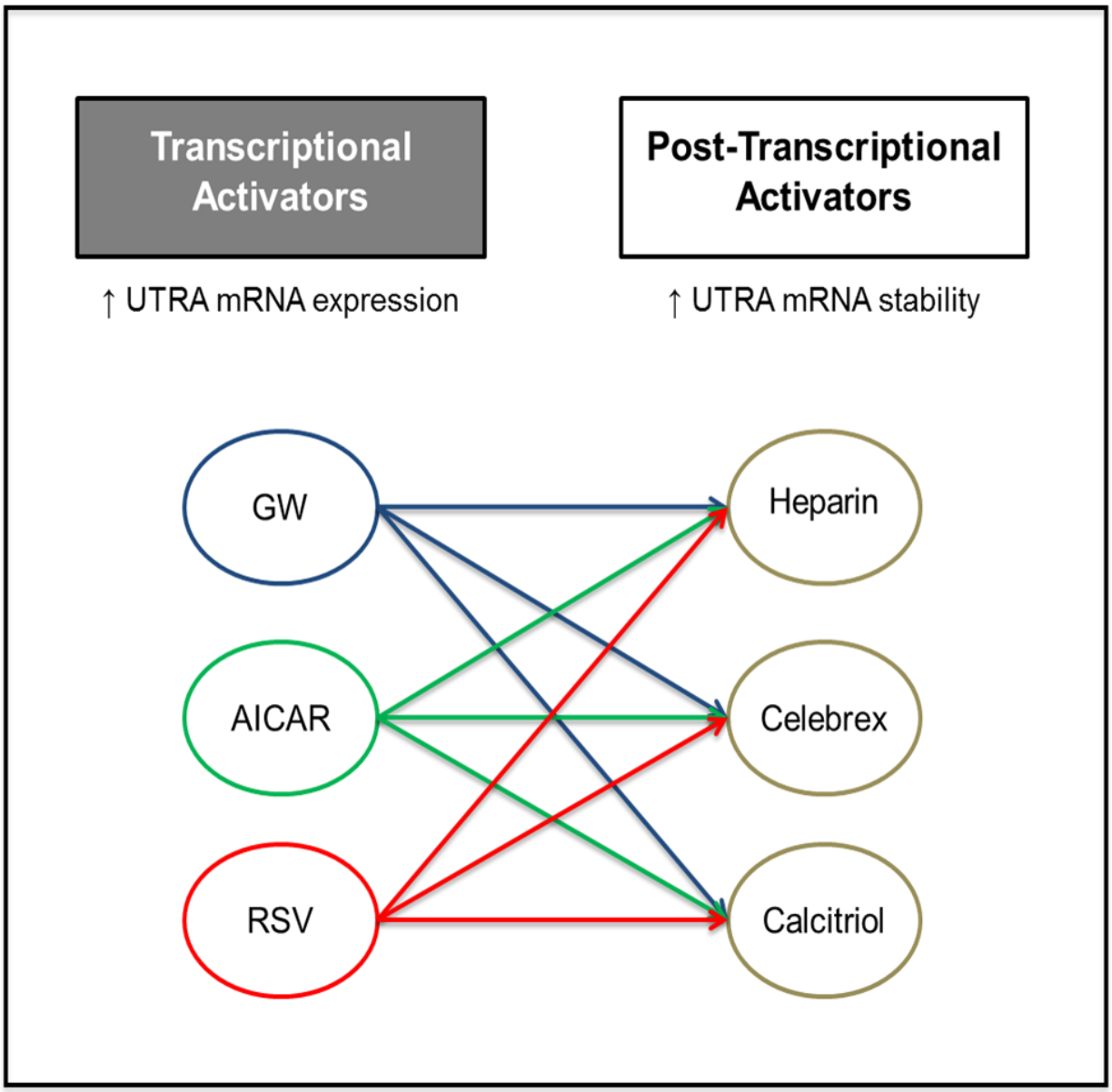

Figure 4.2 – Combinatorial treatment with transcriptional and post-transcriptional activators

GW501516 (GW), AICAR, and resveratrol (RSV) are considered transcriptional activators of utrophin A (UTRA) and other genes involved in the slow, oxidative myogenic program (SOMP). Combining these transcriptional activators with putative post-transcriptional activators, including heparin, celebrex and calcitriol, may yield synergistic effects on UTRA steady state mRNA levels. The idea is that the transcriptional activators increase UTRA mRNA expression and the post-transcriptional activators stabilize these transcripts. Many of these drugs have already been studied in pre-clinical trials using *mdx* mice, but a combinatorial treatment regime should be considered a high priority for future studies.

4.8 Conclusion

In summary, this study shows that SIRT1 activation, via chronic resveratrol administration, can promote the SOMP in both the fast EDL and slow SOL muscles of *mdx* mice. Utrophin A protein levels demonstrated modest, but consistent increases with resveratrol treatment and this may have contributed to improvements in myofibre central nucleation and cross sectional area variability. Interestingly, we found a clear dose-dependent response to resveratrol treatment. The moderate dose of resveratrol activated key phenotypic modifiers, including SIRT1 and PGC-1α, as well as key components of the SOMP, whereas the high dose resulted in minimal fibre type remodelling. Although the resveratrol-induced changes are not as robust as those seen using other drug therapies (Miura 2009; Ljubicic 2011), it is important to understand the potential therapeutic value of SIRT1 stimulation in the DMD context. Furthermore, SIRT1 is intimately linked to key signaling molecules involved in utrophin A regulation, such as AMPK and PGC-1α (Lan 2008; Canto 2009/2010; Suwa 2011). It is also worth noting that there are several other activators of SIRT1 in addition to resveratrol that are under investigation, such as SRT1720 and SRT2104 (Chauhan 2011; Minor 2011). These synthetic compounds boast more potent activation of SIRT1 and some are under investigation in clinical trials (Libri 2012; Hoffmann 2013). It would be interesting to evaluate their effectiveness in the *mdx* context relative to an optimal dose of resveratrol. In conclusion, resveratrol shows promise as a therapeutic agent for treatment of DMD.

5: Reference List

1. Acharyya S, Villalta SA, Bakkar N, et al. Interplay of IKK/NF-kappaB signaling in macrophages and myofibres promotes muscle degeneration in duchenne muscular dystrophy. *J Clin Invest*. 2007;117(4):889-901.

2. Ahn AH, Kunkel LM. The structural and functional diversity of dystrophin. *Nat Genet*. 1993;3(4):283-291.

3. Alderton JM, Steinhardt RA. How calcium influx through calcium leak channels is responsible for the elevated levels of calcium-dependent proteolysis in dystrophic myotubes. *Trends Cardiovasc Med*. 2000;10(6):268-272.

4. Amat R, Planavila A, Chen SL, Iglesias R, Giralt M, Villarroya F. SIRT1 controls the transcription of the peroxisome proliferator-activated receptor-gamma co-activator-1alpha (PGC-1alpha) gene in skeletal muscle through the PGC-1alpha autoregulatory loop and interaction with MyoD. *J Biol Chem*. 2009;284(33):21872-21880.

5. Amenta AR, Yilmaz A, Bogdanovich S, et al. Biglycan recruits utrophin to the sarcolemma and counters dystrophic pathology in mdx mice. *Proc Natl Acad Sci U S A*. 2011;108(2):762-767.

6. Amirouche A, Tadesse H, Lunde JA, Belanger G, Cote J, Jasmin BJ. Activation of p38 signaling increases utrophin A expression in skeletal muscle via the RNA-binding protein KSRP and inhibition of AU-rich element-mediated mRNA decay: Implications for novel DMD therapeutics. *Hum Mol Genet*. 2013.

7. Anderson MS, Kunkel LM. The molecular and biochemical basis of duchenne muscular dystrophy. *Trends Biochem Sci*. 1992;17(8):289-292.

8. Andres-Lacueva C, Macarulla MT, Rotches-Ribalta M, et al. Distribution of resveratrol metabolites in liver, adipose tissue, and skeletal muscle in rats fed different doses of this polyphenol. *J Agric Food Chem*. 2012;60(19):4833-4840.

9. Angelini C, Pegoraro E, Turella E, Intino MT, Pini A, Costa C. Deflazacort in duchenne dystrophy: Study of long-term effect. *Muscle Nerve*. 1994;17(4):386-391.

10. Angelini C, Peterle E. Old and new therapeutic developments in steroid treatment in duchenne muscular dystrophy. *Acta Myol*. 2012;31(1):9-15.

11. Angus LM, Chakkalakal JV, Mejat A, et al. Calcineurin-NFAT signaling, together with GABP and peroxisome PGC-1{alpha}, drives utrophin gene expression at the neuromuscular junction. *Am J Physiol Cell Physiol*. 2005;289(4):C908-17.

12. Archer JD, Vargas CC, Anderson JE. Persistent and improved functional gain in mdx dystrophic mice after treatment with L-arginine and deflazacort. *FASEB J*. 2006;20(6):738-740.

13. Banks AS, Kon N, Knight C, et al. SirT1 gain of function increases energy efficiency and prevents diabetes in mice. *Cell Metab*. 2008;8(4):333-341.

14. Barger JL, Kayo T, Vann JM, et al. A low dose of dietary resveratrol partially mimics caloric restriction and retards aging parameters in mice. *PLoS One*. 2008;3(6):e2264.

15. Barton ER, Morris L, Musaro A, Rosenthal N, Sweeney HL. Muscle-specific expression of insulin-like growth factor I counters muscle decline in mdx mice. *J Cell Biol*. 2002;157(1):137-148.

16. Barton-Davis ER, Cordier L, Shoturma DI, Leland SE, Sweeney HL. Aminoglycoside antibiotics restore dystrophin function to skeletal muscles of mdx mice. *J Clin Invest*. 1999;104(4):375-381.

17. Baur JA, Pearson KJ, Price NL, et al. Resveratrol improves health and survival of mice on a high-calorie diet. *Nature*. 2006;444(7117):337-342.

18. Blake DJ, Weir A, Newey SE, Davies KE. Function and genetics of dystrophin and dystrophin-related proteins in muscle. *Physiol Rev*. 2002;82(2):291-329.

19. Bogdanovich S, Krag TO, Barton ER, et al. Functional improvement of dystrophic muscle by myostatin blockade. *Nature*. 2002;420(6914):418-421.

20. Bonifati MD, Ruzza G, Bonometto P, et al. A multicenter, double-blind, randomized trial of deflazacort versus prednisone in duchenne muscular dystrophy. *Muscle Nerve*. 2000;23(9):1344-1347.

21. Bordone L, Cohen D, Robinson A, et al. SIRT1 transgenic mice show phenotypes resembling calorie restriction. *Aging Cell*. 2007;6(6):759-767.

22. Bothwell JE, Gordon KE, Dooley JM, MacSween J, Cummings EA, Salisbury S. Vertebral fractures in boys with duchenne muscular dystrophy. *Clin Pediatr (Phila)*. 2003;42(4):353-356.

23. Bowles DE, McPhee SW, Li C, et al. Phase 1 gene therapy for duchenne muscular dystrophy using a translational optimized AAV vector. *Mol Ther*. 2012;20(2):443-455.

24. Brasnyo P, Molnar GA, Mohas M, et al. Resveratrol improves insulin sensitivity, reduces oxidative stress and activates the akt pathway in type 2 diabetic patients. *Br J Nutr*. 2011;106(3):383-389.

25. Bruckbauer A, Zemel MB. Synergistic effects of metformin, resveratrol, and hydroxymethylbutyrate on insulin sensitivity. *Diabetes Metab Syndr Obes*. 2013;6:93-102.

26. Brunetti-Pierri N, Palmer DJ, Beaudet AL, Carey KD, Finegold M, Ng P. Acute toxicity after high-dose systemic injection of helper-dependent adenoviral vectors into nonhuman primates. *Hum Gene Ther*. 2004;15(1):35-46.

27. Bueno Junior CR, Pantaleao LC, Voltarelli VA, Bozi LH, Brum PC, Zatz M. Combined effect of AMPK/PPAR agonists and exercise training in mdx mice functional performance. *PLoS One*. 2012;7(9):e45699.

28. Buitrago CG, Arango NS, Boland RL. 1alpha,25(OH)2D3-dependent modulation of akt in proliferating and differentiating C2C12 skeletal muscle cells. *J Cell Biochem*. 2012;113(4):1170-1181.

29. Bulfield G, Siller WG, Wight PA, Moore KJ. X chromosome-linked muscular dystrophy (mdx) in the mouse. *Proc Natl Acad Sci U S A*. 1984;81(4):1189-1192.

30. Burton EA, Tinsley JM, Holzfeind PJ, Rodrigues NR, Davies KE. A second promoter provides an alternative target for therapeutic up-regulation of utrophin in duchenne muscular dystrophy. *Proc Natl Acad Sci U S A*. 1999;96(24):14025-14030.

31. Bushby K, Finkel R, Birnkrant DJ, et al. Diagnosis and management of duchenne muscular dystrophy, part 1: Diagnosis, and pharmacological and psychosocial management. *Lancet Neurol*. 2010;9(1):77-93.

32. Bushby KM. Recent advances in understanding muscular dystrophy. *Arch Dis Child*. 1992;67(10):1310-1312.

33. Byers TJ, Lidov HG, Kunkel LM. An alternative dystrophin transcript specific to peripheral nerve. *Nat Genet*. 1993;4(1):77-81.

34. Call JA, Ervasti JM, Lowe DA. TAT-muUtrophin mitigates the pathophysiology of dystrophin and utrophin double-knockout mice. *J Appl Physiol*. 2011;111(1):200-205.

35. Canto C, Auwerx J. AMP-activated protein kinase and its downstream transcriptional pathways. *Cell Mol Life Sci*. 2010;67(20):3407-3423.

36. Canto C, Auwerx J. PGC-1alpha, SIRT1 and AMPK, an energy sensing network that controls energy expenditure. *Curr Opin Lipidol*. 2009;20(2):98-105.

37. Canto C, Gerhart-Hines Z, Feige JN, et al. AMPK regulates energy expenditure by modulating NAD+ metabolism and SIRT1 activity. *Nature*. 2009;458(7241):1056-1060.

38. Canto C, Jiang LQ, Deshmukh AS, et al. Interdependence of AMPK and SIRT1 for metabolic adaptation to fasting and exercise in skeletal muscle. *Cell Metab*. 2010;11(3):213-219.

39. Chakkalakal JV, Harrison MA, Carbonetto S, Chin E, Michel RN, Jasmin BJ. Stimulation of calcineurin signaling attenuates the dystrophic pathology in mdx mice. *Hum Mol Genet*. 2004;13(4):379-388.

40. Chakkalakal JV, Michel SA, Chin ER, Michel RN, Jasmin BJ. Targeted inhibition of Ca2+ /calmodulin signaling exacerbates the dystrophic phenotype in mdx mouse muscle. *Hum Mol Genet*. 2006;15(9):1423-1435.

41. Chakkalakal JV, Miura P, Belanger G, Michel RN, Jasmin BJ. Modulation of utrophin A mRNA stability in fast versus slow muscles via an AU-rich element and calcineurin signaling. *Nucleic Acids Res*. 2008;36(3):826-838.

42. Chakkalakal JV, Stocksley MA, Harrison MA, et al. Expression of utrophin A mRNA correlates with the oxidative capacity of skeletal muscle fibre types and is regulated by calcineurin/NFAT signaling. *Proc Natl Acad Sci U S A*. 2003;100(13):7791-7796.

43. Chakkalakal JV, Thompson J, Parks RJ, Jasmin BJ. Molecular, cellular, and pharmacological therapies for Duchenne/Becker muscular dystrophies. *FASEB J*. 2005;19(8):880-891.

44. Chambers SP, Dodd A, Overall R, et al. Dystrophin in adult zebrafish muscle. *Biochem Biophys Res Commun*. 2001;286(3):478-483.

45. Chaubourt E, Fossier P, Baux G, Leprince C, Israel M, De La Porte S. Nitric oxide and l-arginine cause an accumulation of utrophin at the sarcolemma: A possible compensation for dystrophin loss in duchenne muscular dystrophy. *Neurobiol Dis*. 1999;6(6):499-507.

46. Chauhan D, Bandi M, Singh AV, et al. Preclinical evaluation of a novel SIRT1 modulator SRT1720 in multiple myeloma cells. *Br J Haematol*. 2011;155(5):588-598.

47. Chen KH, Cheng ML, Jing YH, Chiu DT, Shiao MS, Chen JK. Resveratrol ameliorates metabolic disorders and muscle wasting in streptozotocin-induced diabetic rats. *Am J Physiol Endocrinol Metab*. 2011;301(5):E853-63.

48. Cheng HL, Mostoslavsky R, Saito S, et al. Developmental defects and p53 hyperacetylation in Sir2 homolog (SIRT1)-deficient mice. *Proc Natl Acad Sci U S A*. 2003;100(19):10794-10799.

49. Chin ER, Olson EN, Richardson JA, et al. A calcineurin-dependent transcriptional pathway controls skeletal muscle fibre type. *Genes Dev*. 1998;12(16):2499-2509.

50. Chung S, Yao H, Caito S, Hwang JW, Arunachalam G, Rahman I. Regulation of SIRT1 in cellular functions: Role of polyphenols. *Arch Biochem Biophys*. 2010;501(1):79-90.

51. Coffey AJ, Roberts RG, Green ED, et al. Construction of a 2.6-mb contig in yeast artificial chromosomes spanning the human dystrophin gene using an STS-based approach. *Genomics*. 1992;12(3):474-484.

52. Cohn RD, Campbell KP. Molecular basis of muscular dystrophies. *Muscle Nerve*. 2000;23(10):1456-1471.

53. Cohn RD, van Erp C, Habashi JP, et al. Angiotensin II type 1 receptor blockade attenuates TGF-beta-induced failure of muscle regeneration in multiple myopathic states. *Nat Med*. 2007;13(2):204-210.

54. Collins CA, Morgan JE. Duchenne's muscular dystrophy: Animal models used to investigate pathogenesis and develop therapeutic strategies. *Int J Exp Pathol*. 2003;84(4):165-172.

55. Crandall JP, Oram V, Trandafirescu G, et al. Pilot study of resveratrol in older adults with impaired glucose tolerance. *J Gerontol A Biol Sci Med Sci*. 2012;67(12):1307-1312.

56. Da Cruz S, Parone PA, Lopes VS, et al. Elevated PGC-1alpha activity sustains mitochondrial biogenesis and muscle function without extending survival in a mouse model of inherited ALS. *Cell Metab*. 2012;15(5):778-786.

57. De la Porte S, Morin S, Koenig J. Characteristics of skeletal muscle in mdx mutant mice. *Int Rev Cytol*. 1999;191:99-148.

58. De Luca A. Pre-clinical drug tests in the mdx mouse as a model of dystrophinopathies: An overview. *Acta Myol*. 2012;31(1):40-47.

59. Delfin DA, Xu Y, Peterson JM, Guttridge DC, Rafael-Fortney JA, Janssen PM. Improvement of cardiac contractile function by peptide-based inhibition of NF-kappaB in the utrophin/dystrophin-deficient murine model of muscular dystrophy. *J Transl Med*. 2011;9:68-5876-9-68.

60. Deol JR, Danialou G, Larochelle N, et al. Successful compensation for dystrophin deficiency by a helper-dependent adenovirus expressing full-length utrophin. *Mol Ther*. 2007;15(10):1767-1774.

61. Do GM, Jung UJ, Park HJ, et al. Resveratrol ameliorates diabetes-related metabolic changes via activation of AMP-activated protein kinase and its downstream targets in db/db mice. *Mol Nutr Food Res*. 2012;56(8):1282-1291.

62. Drachman DB, Toyka KV, Myer E. Prednisone in duchenne muscular dystrophy. *Lancet*. 1974;2(7894):1409-1412.

63. Ehrenborg E, Krook A. Regulation of skeletal muscle physiology and metabolism by peroxisome proliferator-activated receptor delta. *Pharmacol Rev*. 2009;61(3):373-393.

64. Ervasti JM. Dystrophin, its interactions with other proteins, and implications for muscular dystrophy. *Biochim Biophys Acta*. 2007;1772(2):108-117.

65. Ervasti JM, Campbell KP. Membrane organization of the dystrophin-glycoprotein complex. *Cell*. 1991;66(6):1121-1131.

66. Ervasti JM, Ohlendieck K, Kahl SD, Gaver MG, Campbell KP. Deficiency of a glycoprotein component of the dystrophin complex in dystrophic muscle. *Nature*. 1990;345(6273):315-319.

67. Everts ME, Clausen T. Activation of the na-K pump by intracellular na in rat slow- and fast-twitch muscle. *Acta Physiol Scand*. 1992;145(4):353-362.

68. Feener CA, Koenig M, Kunkel LM. Alternative splicing of human dystrophin mRNA generates isoforms at the carboxy terminus. *Nature*. 1989;338(6215):509-511.

69. Fenichel GM, Florence JM, Pestronk A, et al. Long-term benefit from prednisone therapy in duchenne muscular dystrophy. *Neurology*. 1991;41(12):1874-1877.

70. Fisher R, Tinsley JM, Phelps SR, et al. Non-toxic ubiquitous over-expression of utrophin in the mdx mouse. *Neuromuscul Disord*. 2001;11(8):713-721.

71. Foster H, Popplewell L, Dickson G. Genetic therapeutic approaches for duchenne muscular dystrophy. *Hum Gene Ther*. 2012;23(7):676-687.

72. Friedrichsen M, Mortensen B, Pehmoller C, Birk JB, Wojtaszewski JF. Exercise-induced AMPK activity in skeletal muscle: Role in glucose uptake and insulin sensitivity. *Mol Cell Endocrinol*. 2013;366(2):204-214.

73. Fuchtbauer EM, Rowlerson AM, Gotz K, et al. Direct correlation of parvalbumin levels with myosin isoforms and succinate dehydrogenase activity on frozen sections of rodent muscle. *J Histochem Cytochem*. 1991;39(3):355-361.

74. Gan Z, Burkart-Hartman EM, Han DH, et al. The nuclear receptor PPARbeta/delta programs muscle glucose metabolism in cooperation with AMPK and MEF2. *Genes Dev*. 2011;25(24):2619-2630.

75. Gaudel C, Schwartz C, Giordano C, Abumrad NA, Grimaldi PA. Pharmacological activation of PPARbeta promotes rapid and calcineurin-dependent fibre remodeling and

angiogenesis in mouse skeletal muscle. *Am J Physiol Endocrinol Metab*. 2008;295(2):E297-304.

76. Gerhart-Hines Z, Dominy JE,Jr, Blattler SM, et al. The cAMP/PKA pathway rapidly activates SIRT1 to promote fatty acid oxidation independently of changes in NAD(+). *Mol Cell*. 2011;44(6):851-863.

77. Gerhart-Hines Z, Rodgers JT, Bare O, et al. Metabolic control of muscle mitochondrial function and fatty acid oxidation through SIRT1/PGC-1alpha. *EMBO J*. 2007;26(7):1913-1923.

78. Gervois P, Fruchart JC, Staels B. Drug insight: Mechanisms of action and therapeutic applications for agonists of peroxisome proliferator-activated receptors. *Nat Clin Pract Endocrinol Metab*. 2007;3(2):145-156.

79. Gilbert R, Nalbantoglu J, Petrof BJ, et al. Adenovirus-mediated utrophin gene transfer mitigates the dystrophic phenotype of mdx mouse muscles. *Hum Gene Ther*. 1999;10(8):1299-1310.

80. Gordon BS, Delgado Diaz DC, Kostek MC. Resveratrol decreases inflammation and increases utrophin gene expression in the mdx mouse model of duchenne muscular dystrophy. *Clin Nutr*. 2013;32(1):104-111.

81. Gosselin LE, Williams JE, Personius K, Farkas GA. A comparison of factors associated with collagen metabolism in different skeletal muscles from dystrophic (mdx) mice: Impact of pirfenidone. *Muscle Nerve*. 2007;35(2):208-216.

82. Goyenvalle A, Seto JT, Davies KE, Chamberlain J. Therapeutic approaches to muscular dystrophy. *Hum Mol Genet*. 2011;20(R1):R69-78.

83. Gramolini AO, Belanger G, Jasmin BJ. Distinct regions in the 3' untranslated region are responsible for targeting and stabilizing utrophin transcripts in skeletal muscle cells. *J Cell Biol*. 2001a;154(6):1173-1183.

84. Gramolini AO, Belanger G, Thompson JM, Chakkalakal JV, Jasmin BJ. Increased expression of utrophin in a slow vs. a fast muscle involves posttranscriptional events. *Am J Physiol Cell Physiol*. 2001b;281(4):C1300-9.

85. Gramolini AO, Burton EA, Tinsley JM, et al. Muscle and neural isoforms of agrin increase utrophin expression in cultured myotubes via a transcriptional regulatory mechanism. *J Biol Chem*. 1998;273(2):736-743.

86. Gramolini AO, Dennis CL, Tinsley JM, et al. Local transcriptional control of utrophin expression at the neuromuscular synapse. *J Biol Chem*. 1997a;272(13):8117-8120.

87. Gramolini AO, Jasmin BJ. Molecular mechanisms and putative signalling events controlling utrophin expression in mammalian skeletal muscle fibres. *Neuromuscul Disord*. 1998;8(6):351-361.

88. Gramolini AO, Jasmin BJ. Duchenne muscular dystrophy and the neuromuscular junction: The utrophin link. *Bioessays*. 1997b;19(9):747-750.

89. Grounds MD, Davies KE. The allure of stem cell therapy for muscular dystrophy. *Neuromuscul Disord*. 2007;17(3):206-208.

90. Grum VL, Li D, MacDonald RI, Mondragon A. Structures of two repeats of spectrin suggest models of flexibility. *Cell*. 1999;98(4):523-535.

91. Gurd BJ. Deacetylation of PGC-1alpha by SIRT1: Importance for skeletal muscle function and exercise-induced mitochondrial biogenesis. *Appl Physiol Nutr Metab*. 2011;36(5):589-597.

92. Gurd BJ, Yoshida Y, Lally J, Holloway GP, Bonen A. The deacetylase enzyme SIRT1 is not associated with oxidative capacity in rat heart and skeletal muscle and its overexpression reduces mitochondrial biogenesis. *J Physiol*. 2009;587(Pt 8):1817-1828.

93. Gygi SP, Rochon Y, Franza BR, Aebersold R. Correlation between protein and mRNA abundance in yeast. *Mol Cell Biol*. 1999;19(3):1720-1730.

94. Handschin C. The biology of PGC-1alpha and its therapeutic potential. *Trends Pharmacol Sci*. 2009;30(6):322-329.

95. Handschin C, Kobayashi YM, Chin S, Seale P, Campbell KP, Spiegelman BM. PGC-1alpha regulates the neuromuscular junction program and ameliorates duchenne muscular dystrophy. *Genes Dev*. 2007;21(7):770-783.

96. Hawley SA, Ross FA, Chevtzoff C, et al. Use of cells expressing gamma subunit variants to identify diverse mechanisms of AMPK activation. *Cell Metab*. 2010;11(6):554-565.

97. Hnia K, Gayraud J, Hugon G, et al. L-arginine decreases inflammation and modulates the nuclear factor-kappaB/matrix metalloproteinase cascade in mdx muscle fibres. *Am J Pathol*. 2008;172(6):1509-1519.

98. Hoffman EP, Brown RH,Jr, Kunkel LM. Dystrophin: The protein product of the duchenne muscular dystrophy locus. *Cell*. 1987;51(6):919-928.

99. Hoffmann E, Wald J, Lavu S, et al. Pharmacokinetics and tolerability of SRT2104, a first-in-class small molecule activator of SIRT1, after single and repeated oral administration in man. *Br J Clin Pharmacol*. 2013;75(1):186-196.

100. Holmes BF, Kurth-Kraczek EJ, Winder WW. Chronic activation of 5'-AMP-activated protein kinase increases GLUT-4, hexokinase, and glycogen in muscle. *J Appl Physiol*. 1999;87(5):1990-1995.

101. Hong F, Lee J, Song JW, et al. Cyclosporin A blocks muscle differentiation by inducing oxidative stress and inhibiting the peptidyl-prolyl-cis-trans isomerase activity of cyclophilin A: Cyclophilin A protects myoblasts from cyclosporin A-induced cytotoxicity. *FASEB J*. 2002;16(12):1633-1635.

102. Hood DA. Invited review: Contractile activity-induced mitochondrial biogenesis in skeletal muscle. *J Appl Physiol*. 2001;90(3):1137-1157.

103. Hori YS, Kuno A, Hosoda R, et al. Resveratrol ameliorates muscular pathology in the dystrophic mdx mouse, a model for duchenne muscular dystrophy. *J Pharmacol Exp Ther*. 2011;338(3):784-794.

104. Howitz KT, Bitterman KJ, Cohen HY, et al. Small molecule activators of sirtuins extend saccharomyces cerevisiae lifespan. *Nature*. 2003;425(6954):191-196.

105. Hsiao PW, Chang CC, Liu HF, Tsai CM, Chiu TH, Chao JI. Activation of p38 mitogen-activated protein kinase by celecoxib oppositely regulates survivin and gamma-H2AX in human colorectal cancer cells. *Toxicol Appl Pharmacol*. 2007;222(1):97-104.

106. Huang H, Tindall DJ. Dynamic FoxO transcription factors. *J Cell Sci*. 2007;120(Pt 15):2479-2487.

107. Huebner KD, Jassal DS, Halevy O, Pines M, Anderson JE. Functional resolution of fibrosis in mdx mouse dystrophic heart and skeletal muscle by halofuginone. *Am J Physiol Heart Circ Physiol*. 2008;294(4):H1550-61.

108. Imai S, Armstrong CM, Kaeberlein M, Guarente L. Transcriptional silencing and longevity protein Sir2 is an NAD-dependent histone deacetylase. *Nature*. 2000;403(6771):795-800.

109. Jackson JR, Ryan MJ, Hao Y, Alway SE. Mediation of endogenous antioxidant enzymes and apoptotic signaling by resveratrol following muscle disuse in the gastrocnemius muscles of young and old rats. *Am J Physiol Regul Integr Comp Physiol*. 2010;299(6):R1572-81.

110. Jahnke VE, Van Der Meulen JH, Johnston HK, et al. Metabolic remodeling agents show beneficial effects in the dystrophin-deficient mdx mouse model. *Skelet Muscle*. 2012;2(1):16-5040-2-16.

111. Jasmin BJ, Angus LM, Belanger G, et al. Multiple regulatory events controlling the expression and localization of utrophin in skeletal muscle fibres: Insights into a therapeutic strategy for duchenne muscular dystrophy. *J Physiol Paris*. 2002;96(1-2):31-42.

112. Jasmin BJ, Cartaud A, Ludosky MA, Changeux JP, Cartaud J. Asymmetric distribution of dystrophin in developing and adult torpedo marmorata electrocyte: Evidence for its association with the acetylcholine receptor-rich membrane. *Proc Natl Acad Sci U S A*. 1990;87(10):3938-3941.

113. Jennekens FG, ten Kate LP, de Visser M, Wintzen AR. Diagnostic criteria for duchenne and becker muscular dystrophy and myotonic dystrophy. *Neuromuscul Disord*. 1991;1(6):389-391.

114. Johri A, Calingasan NY, Hennessey TM, et al. Pharmacologic activation of mitochondrial biogenesis exerts widespread beneficial effects in a transgenic mouse model of huntington's disease. *Hum Mol Genet*. 2012;21(5):1124-1137.

115. Jorgensen SB, Jensen TE, Richter EA. Role of AMPK in skeletal muscle gene adaptation in relation to exercise. *Appl Physiol Nutr Metab*. 2007;32(5):904-911.

116. Jorgensen SB, Richter EA, Wojtaszewski JF. Role of AMPK in skeletal muscle metabolic regulation and adaptation in relation to exercise. *J Physiol*. 2006;574(Pt 1):17-31.

117. Kafri T, Blomer U, Peterson DA, Gage FH, Verma IM. Sustained expression of genes delivered directly into liver and muscle by lentiviral vectors. *Nat Genet*. 1997;17(3):314-317.

118. Karpati G, Carpenter S, Morris GE, Davies KE, Guerin C, Holland P. Localization and quantitation of the chromosome 6-encoded dystrophin-related protein in normal and pathological human muscle. *J Neuropathol Exp Neurol*. 1993;52(2):119-128.

119. Khurana TS, Hoffman EP, Kunkel LM. Identification of a chromosome 6-encoded dystrophin-related protein. *J Biol Chem*. 1990;265(28):16717-16720.

120. Khurana TS, Rosmarin AG, Shang J, Krag TO, Das S, Gammeltoft S. Activation of utrophin promoter by heregulin via the ets-related transcription factor complex GA-binding protein alpha/beta. *Mol Biol Cell*. 1999;10(6):2075-2086.

121. Kimura E, Li S, Gregorevic P, Fall BM, Chamberlain JS. Dystrophin delivery to muscles of mdx mice using lentiviral vectors leads to myogenic progenitor targeting and stable gene expression. *Mol Ther*. 2010;18(1):206-213.

122. Kinali M, Arechavala-Gomeza V, Feng L, et al. Local restoration of dystrophin expression with the morpholino oligomer AVI-4658 in duchenne muscular dystrophy: A single-blind, placebo-controlled, dose-escalation, proof-of-concept study. *Lancet Neurol*. 2009;8(10):918-928.

123. Kleopa KA, Drousiotou A, Mavrikiou E, Ormiston A, Kyriakides T. Naturally occurring utrophin correlates with disease severity in duchenne muscular dystrophy. *Hum Mol Genet*. 2006;15(10):1623-1628.

124. Koistinen HA, Galuska D, Chibalin AV, et al. 5-amino-imidazole carboxamide riboside increases glucose transport and cell-surface GLUT4 content in skeletal muscle from subjects with type 2 diabetes. *Diabetes*. 2003;52(5):1066-1072.

125. Kong X, Manchester J, Salmons S, Lawrence JC,Jr. Glucose transporters in single skeletal muscle fibres. relationship to hexokinase and regulation by contractile activity. *J Biol Chem*. 1994;269(17):12963-12967.

126. Kornegay JN, Bogan JR, Bogan DJ, et al. Canine models of duchenne muscular dystrophy and their use in therapeutic strategies. *Mamm Genome*. 2012;23(1-2):85-108.

127. Krag TO, Bogdanovich S, Jensen CJ, et al. Heregulin ameliorates the dystrophic phenotype in mdx mice. *Proc Natl Acad Sci U S A*. 2004;101(38):13856-13860.

128. Kramer DK, Al-Khalili L, Perrini S, et al. Direct activation of glucose transport in primary human myotubes after activation of peroxisome proliferator-activated receptor delta. *Diabetes*. 2005;54(4):1157-1163.

129. Lagouge M, Argmann C, Gerhart-Hines Z, et al. Resveratrol improves mitochondrial function and protects against metabolic disease by activating SIRT1 and PGC-1alpha. *Cell*. 2006;127(6):1109-1122.

130. Lan F, Cacicedo JM, Ruderman N, Ido Y. SIRT1 modulation of the acetylation status, cytosolic localization, and activity of LKB1. possible role in AMP-activated protein kinase activation. *J Biol Chem*. 2008;283(41):27628-27635.

131. Lapidos KA, Kakkar R, McNally EM. The dystrophin glycoprotein complex: Signaling strength and integrity for the sarcolemma. *Circ Res*. 2004;94(8):1023-1031.

132. Legardinier S, Legrand B, Raguenes-Nicol C, et al. A two-amino acid mutation encountered in duchenne muscular dystrophy decreases stability of the rod domain 23 (R23) spectrin-like repeat of dystrophin. *J Biol Chem*. 2009;284(13):8822-8832.

133. Leick L, Fentz J, Bienso RS, et al. PGC-1{alpha} is required for AICAR-induced expression of GLUT4 and mitochondrial proteins in mouse skeletal muscle. *Am J Physiol Endocrinol Metab*. 2010;299(3):E456-65.

134. Leng Y, Karlsson HK, Zierath JR. Insulin signaling defects in type 2 diabetes. *Rev Endocr Metab Disord*. 2004;5(2):111-117.

135. Lessa TB, Carvalho RC, Franciolli AL, et al. Muscle reorganisation through local injection of stem cells in the diaphragm of mdx mice. *Acta Vet Scand*. 2012;54:73-0147-54-73.

136. Libri V, Brown AP, Gambarota G, et al. A pilot randomized, placebo controlled, double blind phase I trial of the novel SIRT1 activator SRT2104 in elderly volunteers. *PLoS One*. 2012;7(12):e51395.

137. Lin AY, Prochniewicz E, Henderson DM, Li B, Ervasti JM, Thomas DD. Impacts of dystrophin and utrophin domains on actin structural dynamics: Implications for therapeutic design. *J Mol Biol*. 2012;420(1-2):87-98.

138. Lin J, Wu H, Tarr PT, et al. Transcriptional co-activator PGC-1 alpha drives the formation of slow-twitch muscle fibres. *Nature*. 2002;418(6899):797-801.

139. Ljubicic V, Miura P, Burt M, et al. Chronic AMPK activation evokes the slow, oxidative myogenic program and triggers beneficial adaptations in mdx mouse skeletal muscle. *Hum Mol Genet*. 2011;20(17):3478-3493.

140. Love DR, Hill DF, Dickson G, et al. An autosomal transcript in skeletal muscle with homology to dystrophin. *Nature*. 1989;339(6219):55-58.

141. Luquet S, Lopez-Soriano J, Holst D, et al. Peroxisome proliferator-activated receptor delta controls muscle development and oxidative capability. *FASEB J*. 2003;17(15):2299-2301.

142. Malik V, Rodino-Klapac LR, Mendell JR. Emerging drugs for duchenne muscular dystrophy. *Expert Opin Emerg Drugs*. 2012;17(2):261-277.

143. Malik V, Rodino-Klapac LR, Viollet L, et al. Gentamicin-induced readthrough of stop codons in duchenne muscular dystrophy. *Ann Neurol*. 2010;67(6):771-780.

144. Mallinson J, Meissner J, Chang KC. Chapter 2. calcineurin signaling and the slow oxidative skeletal muscle fibre type. *Int Rev Cell Mol Biol*. 2009;277:67-101.

145. Mann CJ, Honeyman K, McClorey G, Fletcher S, Wilton SD. Improved antisense oligonucleotide induced exon skipping in the mdx mouse model of muscular dystrophy. *J Gene Med*. 2002;4(6):644-654.

146. Matsakas A, Patel K. Skeletal muscle fibre plasticity in response to selected environmental and physiological stimuli. *Histol Histopathol*. 2009;24(5):611-629.

147. Matsumura K, Campbell KP. Dystrophin-glycoprotein complex: Its role in the molecular pathogenesis of muscular dystrophies. *Muscle Nerve*. 1994;17(1):2-15.

148. McClorey G, Moulton HM, Iversen PL, Fletcher S, Wilton SD. Antisense oligonucleotide-induced exon skipping restores dystrophin expression in vitro in a canine model of DMD. *Gene Ther*. 2006;13(19):1373-1381.

149. McMillan HJ, Campbell C, Mah JK, Canadian Paediatric Neuromuscular Group. Duchenne muscular dystrophy: Canadian paediatric neuromuscular physicians survey. *Can J Neurol Sci*. 2010;37(2):195-205.

150. Menzies KJ, Singh K, Saleem A, Hood DA. Sirtuin 1-mediated effects of exercise and resveratrol on mitochondrial biogenesis. *J Biol Chem*. 2013;288(10):6968-6979.

151. Meregalli M, Farini A, Colleoni F, Cassinelli L, Torrente Y. The role of stem cells in muscular dystrophies. *Curr Gene Ther*. 2012;12(3):192-205.

152. Meregalli M, Farini A, Parolini D, Maciotta S, Torrente Y. Stem cell therapies to treat muscular dystrophy: Progress to date. *BioDrugs*. 2010;24(4):237-247.

153. Michel RN, Chin ER, Chakkalakal JV, Eibl JK, Jasmin BJ. Ca2+/calmodulin-based signalling in the regulation of the muscle fibre phenotype and its therapeutic potential via modulation of utrophin A and myostatin expression. *Appl Physiol Nutr Metab*. 2007;32(5):921-929.

154. Millay DP, Sargent MA, Osinska H, et al. Genetic and pharmacologic inhibition of mitochondrial-dependent necrosis attenuates muscular dystrophy. *Nat Med*. 2008;14(4):442-447.

155. Milne JC, Lambert PD, Schenk S, et al. Small molecule activators of SIRT1 as therapeutics for the treatment of type 2 diabetes. *Nature*. 2007;450(7170):712-716.

156. Minor RK, Baur JA, Gomes AP, et al. SRT1720 improves survival and healthspan of obese mice. *Sci Rep*. 2011;1:70.

157. Miura P, Chakkalakal JV, Boudreault L, et al. Pharmacological activation of PPARbeta/delta stimulates utrophin A expression in skeletal muscle fibres and restores sarcolemmal integrity in mature mdx mice. *Hum Mol Genet*. 2009;18(23):4640-4649.

158. Miura P, Jasmin BJ. Utrophin upregulation for treating duchenne or becker muscular dystrophy: How close are we? *Trends Mol Med*. 2006;12(3):122-129.

159. Mizuno Y, Nonaka I, Hirai S, Ozawa E. Reciprocal expression of dystrophin and utrophin in muscles of duchenne muscular dystrophy patients, female DMD-carriers and control subjects. *J Neurol Sci*. 1993;119(1):43-52.

160. Moens P, Baatsen PH, Marechal G. Increased susceptibility of EDL muscles from mdx mice to damage induced by contractions with stretch. *J Muscle Res Cell Motil*. 1993;14(4):446-451.

161. Momken I, Stevens L, Bergouignan A, et al. Resveratrol prevents the wasting disorders of mechanical unloading by acting as a physical exercise mimetic in the rat. *FASEB J*. 2011;25(10):3646-3660.

162. Monaco AP, Bertelson CJ, Liechti-Gallati S, Moser H, Kunkel LM. An explanation for the phenotypic differences between patients bearing partial deletions of the DMD locus. *Genomics*. 1988;2(1):90-95.

163. Moorwood C, Lozynska O, Suri N, Napper AD, Diamond SL, Khurana TS. Drug discovery for duchenne muscular dystrophy via utrophin promoter activation screening. *PLoS One*. 2011;6(10):e26169.

164. Morris GE, Nguyen TM, Nguyen TN, Pereboev A, Kendrick-Jones J, Winder SJ. Disruption of the utrophin-actin interaction by monoclonal antibodies and prediction of an actin-binding surface of utrophin. *Biochem J*. 1999;337 (Pt 1)(Pt 1):119-123.

165. Moser H. Duchenne muscular dystrophy: Pathogenetic aspects and genetic prevention. *Hum Genet*. 1984;66(1):17-40.

166. Mosqueira M, Willmann G, Ruohola-Baker H, Khurana TS. Chronic hypoxia impairs muscle function in the drosophila model of duchenne's muscular dystrophy (DMD). *PLoS One*. 2010;5(10):e13450.

167. Mouly V, Aamiri A, Perie S, et al. Myoblast transfer therapy: Is there any light at the end of the tunnel? *Acta Myol*. 2005;24(2):128-133.

168. Muntoni F, Torelli S, Ferlini A. Dystrophin and mutations: One gene, several proteins, multiple phenotypes. *Lancet Neurol*. 2003;2(12):731-740.

169. Muoio DM, MacLean PS, Lang DB, et al. Fatty acid homeostasis and induction of lipid regulatory genes in skeletal muscles of peroxisome proliferator-activated receptor (PPAR)

alpha knock-out mice. evidence for compensatory regulation by PPAR delta. *J Biol Chem*. 2002;277(29):26089-26097.

170. Muthu M, Richardson KA, Sutherland-Smith AJ. The crystal structures of dystrophin and utrophin spectrin repeats: Implications for domain boundaries. *PLoS One*. 2012;7(7):e40066.

171. Narkar VA, Downes M, Yu RT, et al. AMPK and PPARdelta agonists are exercise mimetics. *Cell*. 2008;134(3):405-415.

172. Odom GL, Gregorevic P, Allen JM, Finn E, Chamberlain JS. Microutrophin delivery through rAAV6 increases lifespan and improves muscle function in dystrophic dystrophin/utrophin-deficient mice. *Mol Ther*. 2008;16(9):1539-1545.

173. Ordway GA, Garry DJ. Myoglobin: An essential hemoprotein in striated muscle. *J Exp Biol*. 2004;207(Pt 20):3441-3446.

174. Palmieri B, Tremblay JP, Daniele L. Past, present and future of myoblast transplantation in the treatment of duchenne muscular dystrophy. *Pediatr Transplant*. 2010;14(7):813-819.

175. Park SJ, Ahmad F, Philp A, et al. Resveratrol ameliorates aging-related metabolic phenotypes by inhibiting cAMP phosphodiesterases. *Cell*. 2012;148(3):421-433.

176. Park SW, Kim HS, Hah JW, Jeong WJ, Kim KH, Sung MW. Celecoxib inhibits cell proliferation through the activation of ERK and p38 MAPK in head and neck squamous cell carcinoma cell lines. *Anticancer Drugs*. 2010;21(9):823-830.

177. Partridge TA, Morgan JE, Coulton GR, Hoffman EP, Kunkel LM. Conversion of mdx myofibres from dystrophin-negative to -positive by injection of normal myoblasts. *Nature*. 1989;337(6203):176-179.

178. Pauly M, Daussin F, Burelle Y, et al. AMPK activation stimulates autophagy and ameliorates muscular dystrophy in the mdx mouse diaphragm. *Am J Pathol*. 2012;181(2):583-592.

179. Pearce M, Blake DJ, Tinsley JM, et al. The utrophin and dystrophin genes share similarities in genomic structure. *Hum Mol Genet*. 1993;2(11):1765-1772.

180. Peault B, Rudnicki M, Torrente Y, et al. Stem and progenitor cells in skeletal muscle development, maintenance, and therapy. *Mol Ther*. 2007;15(5):867-877.

181. Peterson JM, Kline W, Canan BD, et al. Peptide-based inhibition of NF-kappaB rescues diaphragm muscle contractile dysfunction in a murine model of duchenne muscular dystrophy. *Mol Med*. 2011;17(5-6):508-515.

182. Petrof BJ, Shrager JB, Stedman HH, Kelly AM, Sweeney HL. Dystrophin protects the sarcolemma from stresses developed during muscle contraction. *Proc Natl Acad Sci U S A*. 1993;90(8):3710-3714.

183. Pichavant C, Aartsma-Rus A, Clemens PR, et al. Current status of pharmaceutical and genetic therapeutic approaches to treat DMD. *Mol Ther*. 2011;19(5):830-840.

184. Price NL, Gomes AP, Ling AJ, et al. SIRT1 is required for AMPK activation and the beneficial effects of resveratrol on mitochondrial function. *Cell Metab*. 2012;15(5):675-690.

185. Puigserver P, Wu Z, Park CW, Graves R, Wright M, Spiegelman BM. A cold-inducible coactivator of nuclear receptors linked to adaptive thermogenesis. *Cell*. 1998;92(6):829-839.

186. Rando TA. The dystrophin-glycoprotein complex, cellular signaling, and the regulation of cell survival in the muscular dystrophies. *Muscle Nerve*. 2001;24(12):1575-1594.

187. Rasbach KA, Gupta RK, Ruas JL, et al. PGC-1alpha regulates a HIF2alpha-dependent switch in skeletal muscle fibre types. *Proc Natl Acad Sci U S A*. 2010;107(50):21866-21871.

188. Rodgers JT, Lerin C, Haas W, Gygi SP, Spiegelman BM, Puigserver P. Nutrient control of glucose homeostasis through a complex of PGC-1alpha and SIRT1. *Nature*. 2005;434(7029):113-118.

189. Rouger K, Larcher T, Dubreil L, et al. Systemic delivery of allogenic muscle stem cells induces long-term muscle repair and clinical efficacy in duchenne muscular dystrophy dogs. *Am J Pathol*. 2011;179(5):2501-2518.

190. Ruff RL, Whittlesey D. Na+ channel distribution and inactivation properties of human type 1 and 2 muscle fibres. *Ann N Y Acad Sci*. 1993;681:412-414.

191. Ruff RL, Whittlesey D. Na+ current densities and voltage dependence in human intercostal muscle fibres. *J Physiol*. 1992;458:85-97.

192. Ryan MJ, Jackson JR, Hao Y, et al. Suppression of oxidative stress by resveratrol after isometric contractions in gastrocnemius muscles of aged mice. *J Gerontol A Biol Sci Med Sci*. 2010;65(8):815-831.

193. Sakamoto M, Yuasa K, Yoshimura M, et al. Micro-dystrophin cDNA ameliorates dystrophic phenotypes when introduced into mdx mice as a transgene. *Biochem Biophys Res Commun*. 2002;293(4):1265-1272.

194. Salminen A, Kauppinen A, Suuronen T, Kaarniranta K. SIRT1 longevity factor suppresses NF-kappaB -driven immune responses: Regulation of aging via NF-kappaB acetylation? *Bioessays*. 2008;30(10):939-942.

195. Sampaolesi M, Torrente Y, Innocenzi A, et al. Cell therapy of alpha-sarcoglycan null dystrophic mice through intra-arterial delivery of mesoangioblasts. *Science*. 2003;301(5632):487-492.

196. Schiaffino S, Reggiani C. Fibre types in mammalian skeletal muscles. *Physiol Rev*. 2011;91(4):1447-1531.

197. Schiaffino S, Sandri M, Murgia M. Activity-dependent signaling pathways controlling muscle diversity and plasticity. *Physiology (Bethesda)*. 2007;22:269-278.

198. Selsby JT, Morine KJ, Pendrak K, Barton ER, Sweeney HL. Rescue of dystrophic skeletal muscle by PGC-1alpha involves a fast to slow fibre type shift in the mdx mouse. *PLoS One*. 2012;7(1):e30063.

199. Seow Y, Yin H, Wood MJ. Identification of a novel muscle targeting peptide in mdx mice. *Peptides*. 2010;31(10):1873-1877.

200. Shavlakadze T, White J, Hoh JF, Rosenthal N, Grounds MD. Targeted expression of insulin-like growth factor-I reduces early myofibre necrosis in dystrophic mdx mice. *Mol Ther*. 2004;10(5):829-843.

201. Sketelj J, Leisner E, Gohlsch B, Skorjanc D, Pette D. Specific impulse patterns regulate acetylcholinesterase activity in skeletal muscles of rats and rabbits. *J Neurosci Res*. 1997;47(1):49-57.

202. Smith JJ, Kenney RD, Gagne DJ, et al. Small molecule activators of SIRT1 replicate signaling pathways triggered by calorie restriction in vivo. *BMC Syst Biol*. 2009;3:31-0509-3-31.

203. Sonnemann KJ, Heun-Johnson H, Turner AJ, Baltgalvis KA, Lowe DA, Ervasti JM. Functional substitution by TAT-utrophin in dystrophin-deficient mice. *PLoS Med*. 2009;6(5):e1000083.

204. St-Pierre SJ, Chakkalakal JV, Kolodziejczyk SM, Knudson JC, Jasmin BJ, Megeney LA. Glucocorticoid treatment alleviates dystrophic myofibre pathology by activation of the calcineurin/NF-AT pathway. *FASEB J*. 2004;18(15):1937-1939.

205. Straub V, Bittner RE, Leger JJ, Voit T. Direct visualization of the dystrophin network on skeletal muscle fibre membrane. *J Cell Biol*. 1992;119(5):1183-1191.

206. Stuart CA, McCurry MP, Marino A, et al. Slow-twitch fibre proportion in skeletal muscle correlates with insulin responsiveness. *J Clin Endocrinol Metab*. 2013;98(5):2027-2036.

207. Stupka N, Gregorevic P, Plant DR, Lynch GS. The calcineurin signal transduction pathway is essential for successful muscle regeneration in mdx dystrophic mice. *Acta Neuropathol*. 2004;107(4):299-310.

208. Suwa M, Nakano H, Radak Z, Kumagai S. Short-term adenosine monophosphate-activated protein kinase activator 5-aminoimidazole-4-carboxamide-1-beta-D-ribofuranoside treatment increases the sirtuin 1 protein expression in skeletal muscle. *Metabolism*. 2011;60(3):394-403.

209. Suwa M, Nakano H, Radak Z, Kumagai S. Endurance exercise increases the SIRT1 and peroxisome proliferator-activated receptor gamma coactivator-1alpha protein expressions in rat skeletal muscle. *Metabolism*. 2008;57(7):986-998.

210. Tanaka T, Yamamoto J, Iwasaki S, et al. Activation of peroxisome proliferator-activated receptor delta induces fatty acid beta-oxidation in skeletal muscle and attenuates metabolic syndrome. *Proc Natl Acad Sci U S A*. 2003;100(26):15924-15929.

211. Taniguti AP, Pertille A, Matsumura CY, Santo Neto H, Marques MJ. Prevention of muscle fibrosis and myonecrosis in mdx mice by suramin, a TGF-beta1 blocker. *Muscle Nerve*. 2011;43(1):82-87.

212. Tennen RI, Michishita-Kioi E, Chua KF. Finding a target for resveratrol. *Cell*. 2012;148(3):387-389.

213. Terada S, Wicke S, Holloszy JO, Han DH. PPARdelta activator GW-501516 has no acute effect on glucose transport in skeletal muscle. *Am J Physiol Endocrinol Metab*. 2006;290(4):E607-11.

214. Tian Q, Stepaniants SB, Mao M, et al. Integrated genomic and proteomic analyses of gene expression in mammalian cells. *Mol Cell Proteomics*. 2004;3(10):960-969.

215. Timmers S, Konings E, Bilet L, et al. Calorie restriction-like effects of 30 days of resveratrol supplementation on energy metabolism and metabolic profile in obese humans. *Cell Metab*. 2011;14(5):612-622.

216. Tinsley J, Deconinck N, Fisher R, et al. Expression of full-length utrophin prevents muscular dystrophy in mdx mice. *Nat Med*. 1998;4(12):1441-1444.

217. Tinsley JM, Fairclough RJ, Storer R, et al. Daily treatment with SMTC1100, a novel small molecule utrophin upregulator, dramatically reduces the dystrophic symptoms in the mdx mouse. *PLoS One*. 2011;6(5):e19189.

218. Tinsley JM, Potter AC, Phelps SR, Fisher R, Trickett JI, Davies KE. Amelioration of the dystrophic phenotype of mdx mice using a truncated utrophin transgene. *Nature*. 1996;384(6607):349-353.

219. Tremblay JP, Malouin F, Roy R, et al. Results of a triple blind clinical study of myoblast transplantations without immunosuppressive treatment in young boys with duchenne muscular dystrophy. *Cell Transplant*. 1993;2(2):99-112.

220. Um JH, Park SJ, Kang H, et al. AMP-activated protein kinase-deficient mice are resistant to the metabolic effects of resveratrol. *Diabetes*. 2010;59(3):554-563.

221. van Deutekom JC, Janson AA, Ginjaar IB, et al. Local dystrophin restoration with antisense oligonucleotide PRO051. *N Engl J Med*. 2007;357(26):2677-2686.

222. van Leeuwen I, Lain S. Sirtuins and p53. *Adv Cancer Res*. 2009;102:171-195.

223. Voisin V, Sebrie C, Matecki S, et al. L-arginine improves dystrophic phenotype in mdx mice. *Neurobiol Dis*. 2005;20(1):123-130.

224. Wang B, Li J, Xiao X. Adeno-associated virus vector carrying human minidystrophin genes effectively ameliorates muscular dystrophy in mdx mouse model. *Proc Natl Acad Sci U S A*. 2000;97(25):13714-13719.

225. Wang Y, Pessin JE. Mechanisms for fibre-type specificity of skeletal muscle atrophy. *Curr Opin Clin Nutr Metab Care*. 2013;16(3):243-250.

226. Wang YX, Zhang CL, Yu RT, et al. Regulation of muscle fibre type and running endurance by PPARdelta. *PLoS Biol*. 2004;2(10):e294.

227. Webster C, Silberstein L, Hays AP, Blau HM. Fast muscle fibres are preferentially affected in duchenne muscular dystrophy. *Cell*. 1988;52(4):503-513.

228. Welch EM, Barton ER, Zhuo J, et al. PTC124 targets genetic disorders caused by nonsense mutations. *Nature*. 2007;447(7140):87-91.

229. Weller B, Karpati G, Carpenter S. Dystrophin-deficient mdx muscle fibres are preferentially vulnerable to necrosis induced by experimental lengthening contractions. *J Neurol Sci*. 1990;100(1-2):9-13.

230. Wells DJ, Wells KE. What do animal models have to tell us regarding duchenne muscular dystrophy? *Acta Myol*. 2005;24(3):172-180.

231. Wenzel E, Somoza V. Metabolism and bioavailability of trans-resveratrol. *Mol Nutr Food Res*. 2005;49(5):472-481.

232. White JP, Baltgalvis KA, Puppa MJ, Sato S, Baynes JW, Carson JA. Muscle oxidative capacity during IL-6-dependent cancer cachexia. *Am J Physiol Regul Integr Comp Physiol*. 2011;300(2):R201-11.

233. Williams LD, Burdock GA, Edwards JA, Beck M, Bausch J. Safety studies conducted on high-purity trans-resveratrol in experimental animals. *Food Chem Toxicol*. 2009;47(9):2170-2182.

234. Winder SJ, Hemmings L, Maciver SK, et al. Utrophin actin binding domain: Analysis of actin binding and cellular targeting. *J Cell Sci*. 1995;108 (Pt 1)(Pt 1):63-71.

235. Winder WW, Holmes BF, Rubink DS, Jensen EB, Chen M, Holloszy JO. Activation of AMP-activated protein kinase increases mitochondrial enzymes in skeletal muscle. *J Appl Physiol*. 2000;88(6):2219-2226.

236. Witczak CA, Sharoff CG, Goodyear LJ. AMP-activated protein kinase in skeletal muscle: From structure and localization to its role as a master regulator of cellular metabolism. *Cell Mol Life Sci*. 2008;65(23):3737-3755.

237. Xiong F, Xiao S, Yu M, et al. Enhanced effect of microdystrophin gene transfection by HSV-VP22 mediated intercellular protein transport. *BMC Neurosci*. 2007;8:50.

238. Yiu EM, Kornberg AJ. Duchenne muscular dystrophy. *Neurol India*. 2008;56(3):236-247.

239. Zhou G, Myers R, Li Y, et al. Role of AMP-activated protein kinase in mechanism of metformin action. *J Clin Invest*. 2001;108(8):1167-1174.

240. Zierath JR, He L, Guma A, Odegoard Wahlstrom E, Klip A, Wallberg-Henriksson H. Insulin action on glucose transport and plasma membrane GLUT4 content in skeletal muscle from patients with NIDDM. *Diabetologia*. 1996;39(10):1180-1189.